Mechanisms for prevention of recombination at centromeric regions in *Arabidopsis thaliana*

Doctoral thesis

for

the award of the doctoral degree

of the Faculty of Mathematics and Natural Sciences

of the University of Cologne

submitted by

Rigel Salinas Gamboa

Accepted in December 2023

1 CONTENTS

2 ABSTRACT

Most organisms show typically 1 to 3 crossovers (COs) along the chromosome per meiosis; however, in the centromere and pericentromere region COs are strongly repressed by a largely unknown mechanism. Several pathways were shown to negatively regulate CO formation; while the corresponding mutants have a massive CO increase along the chromosome (up to >6 fold), COs are not increased in the peri-centromeric regions. Suggesting the presence of another pathway that specifically restrain CO formation in the centromere region, possibly in a redundant manner with the known anti-CO mechanisms and DNA methylation. This project aims to understand mechanisms that settle the patterns of distribution of COs along the chromosomes by identifying anti-CO factors acting in pericentromeric regions, through a genetic screen. We tested candidate mutants, notably some with modified behaviour of centromere and kinetochore and analysed their recombination frequency through Fluorescent Transgenic Lines (FTLs) expressed in seeds, and genetic markers both flaking centromeric regions. We found 1 to 1,5-fold increase recombination in three mutants: *ARABIDOPSIS SUMO PROTEASE* (*asp2*), *CHROMOSOME TRANSMISSION FIDELITY (ctf18)* and *SHUGOSHIN 2* (*sgo2)*, in comparison to wild type. Double mutants of these genes and with *CHROMOMETHYLASE 3 (cmt3)* were also analysed, finding notable cumulative effects in most of them, except for the *asp2 sgo2* combination, suggesting there are at least three different pathways regulating CO formation in centromeric regions *Asp2/Sgo2*, *Ctf18* and *Cmt3*.

3 LIST OF ABREVIATIONS

AE-axial elements

Cas9-CRISPR-associated protein 9

CCAN-Constitutive Centromere-Associated Network (CCAN)

cM-CentiMorgan

CO-Crossover

Col-0- Columbia-0 (accession)

CPC-chromosomal passenger complex

CRISPR-Clustered Regularly Interspaced Short Palindromic Repeats

DAPI-4',6-diamidino-2-phenylindole (DAPI)

dHJs- double Holliday junctions

DNA- Deoxyribonucleic acid

DSB-Double Strand Break

EMS- Ethyl methane sulfonate

ETSs-Expressed Sequence Tags

FA-Fanconi Complex

FTLs-Fluorescent Transgenic (Traffic) Lines

Gb-Gigabase

GFP-Green Fluorescent Protein

Ler-Landsberg (accession)

LTR-Long Term Repeats

Mb-Megabase

NCO-Noncrossover

PAM-Protospacer Adjacent Motif (DNA sequence targeted by the Cas9 nuclease

PCNA-Proliferating Cell Nuclear Antigen

RdDM-RNA-dependent DNA Methylation

Replication Factor C (RFC)

SAC-Spindle assembly checkpoint

SC-Synaptonemal Complex

SDSA- Synthesis-dependent strand annealing

SMC- Structural Maintenance of Chromosomes

SNP-Single Nucleotide Polymorphism

TE- Transversal Element

TF- transverse filaments

Ws-Wassilewskija (accession)

ZMMs- referred to a group of proteins important for Class I CO formation including Zip1, Zip2, Zip3 and Zip4, Mer3 and Msh4–Msh5

5 INTRODUCTION

5.1 MEIOSIS IN SEXUAL REPRODUCTION

Meiosis is a specialized form of cell division that holds crucial importance in the context of sexual reproduction, ensuring the production of genetically diverse gametes. It stands as a fundamental process within the life cycle of eukaryotes. Through its facilitation of genetic material exchange between homologous chromosomes, meiosis generates novel combinations of alleles, thereby augmenting genetic variation within populations and facilitating the adaptability and survival of species amidst changing environments. Existing hypotheses propose that meiosis serves not only as a means to generate genetic diversity for adaptation but also functions in the repair of DNA damage resulting from point mutations or accumulated mutations, as well as the restoration of methylation patterns (Hörandl, 2009; Lenormand et al., 2016).

The genetic determinism of meiosis and process conservation has been established through the extensive study of meiotic mutants in various species. These include meiotic mutants of *D. melanogaster* (Sandler ef al., 1968;Baker and Carpenter, 1972; Boyd et al., 1976a; Smith, 1976), *Pisum sativum* (Gottschalk and Jahn, 1964; Gottschalk and Klein, 1976), *Vicia faba* (Sjodin, 1970), *Zea mays* (Grishaeva & Bogdanov, 2000), *Arabidopsis thaliana* (Armstrong, Caryl, Jones, & Franklin, 2002; Cai, Dong, Edelmann, & Makaroff, 2003; De Muyt et al., 2009; Higgins, Sanchez-Moran, Armstrong, Jones, & Franklin, 2005), *Saccaromyces cerevisae* (Agnès Bergerat et al., 1997; Börner, Kleckner, & Hunter, 2004; Scott Keeney, Giroux, & Kleckner, 1997) (Reviewed in (R. Mercier & Grelon, 2008; Y. Wang & Copenhaver, 2018)), gives us many clues of the regulation of meiotic cells.

Meiosis follows essential steps for shuffling genetic information (Fig.1), including one round of DNA replication (Fig.1-a), Double Strand Break (DSB) formation with a repairing step usually involving homologous recombination during Leptotene to Diplotene from Meiosis I (Fig.1-b. Fig.2-A-D) and two rounds of segregation during Anaphase I (Fig.2-G) and Anaphase II(Fig.2-K). The initial round of segregation split up homologous chromosomes (Fig.1-c. Fig. 2-F-G), while the subsequent round separates sister chromatids (Fig.1-d. Fig. 2-K-L), ultimately resulting in the formation of four distinct haploid cells (Fig.1-e. Fig. 2-L).

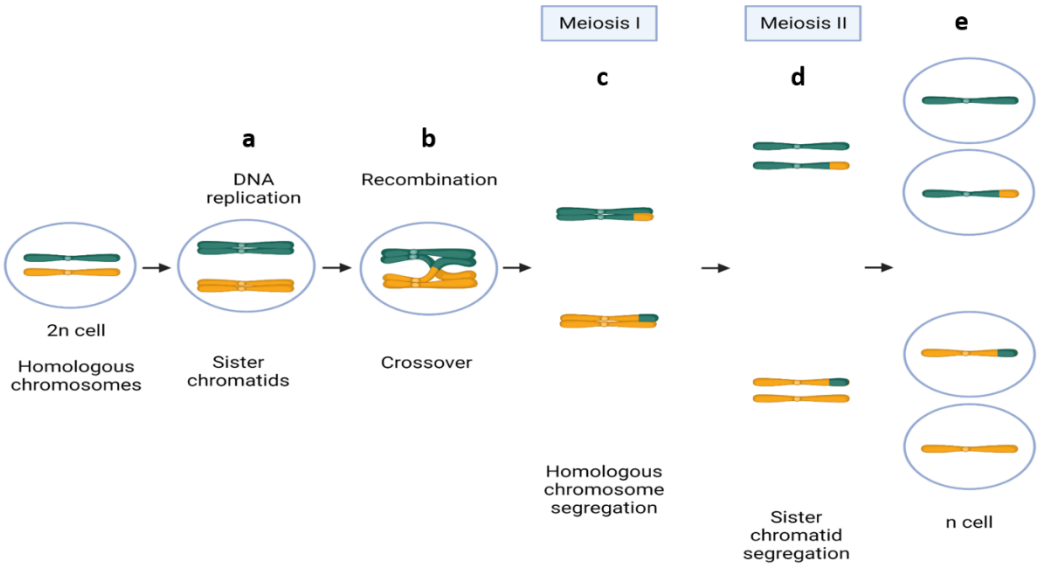

Figure 1 Meiotic division process. a) DNA replication. b) Recombination, homologous chromosomes form Crossovers (COs) between them, c) Anaphase I is the first segregation round, d) Anaphase II is the second segregation round e) 4 haploid products with recombined DNA content. Homologous chromosomes are depicted in different colours.

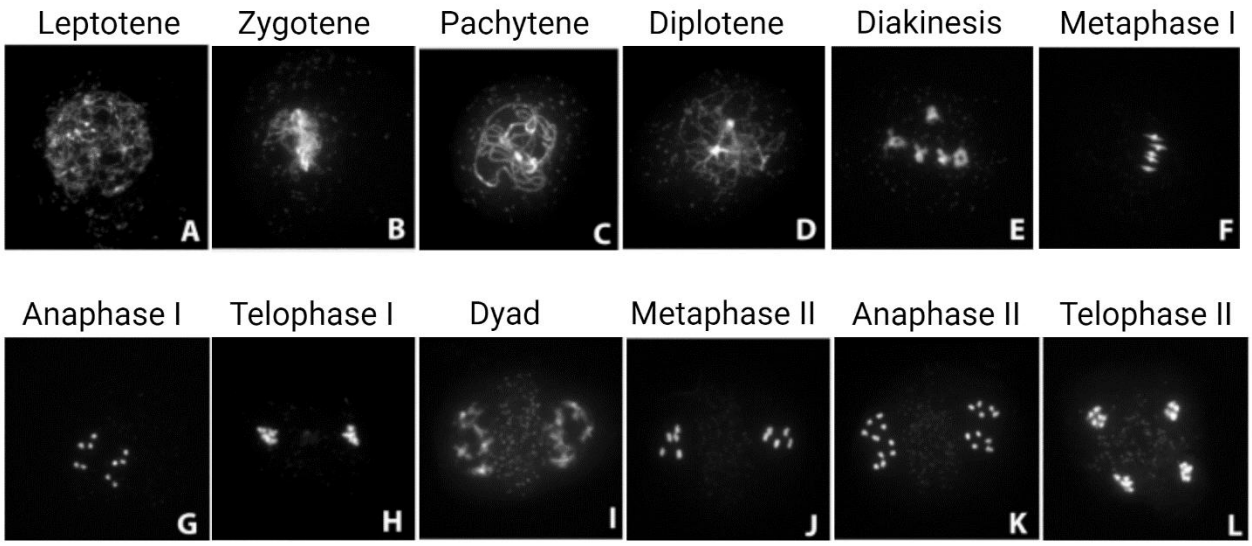

Figure 2 Male Chromosome spreads (DAPI) ***Modified*** *from* (Sims, Schlögelhofer, & Kurzbauer, 2021) *. Created with BioRender.com*

5.2 FROM DSBS TO CROSSOVER FORMATION

Recombination, together with mutation, is the primary source of genetic diversity among eukaryotes. Crossover (CO) formation, where genetic information is exchanged between homologous chromosomes, is the primary process. This process is quite conserved among all eukaryotes. The specific names of the involved factors in this section is referred to *Arabidopsis thaliana*.

The process starts with replication which involves the synthesis of leading and lagging strands, through the coordinated action of polymerase pairs that employ homologous chromosomes as templates for the replication process (Haber, 2014). During the beginning of Prophase-I in meiosis, it is crucial to have proper pairing to ensure correct segregation and recombination which initiates by the Double Strand Breaks (DSBs) formation, initiated by the topoisomerases-like SPO11-1 and SPO11-2 during Prophase I (Fig.4) (Agnès Bergerat et al., 1997; Grelon, Vezon, Gendrot, & Pelletier, 2001; Scott Keeney et al., 1997). Invasion of a non-sister chromatid is crucial for the crossover formation -which dictates the difference to a simple break repair-. This happens when the 3´ paternal ssDNA invades and pairs with the maternal complementary strand, mediated by DMC1 and RAD51 recombinases (S. Keeney & Neale, 2006) to form a joint molecule. Some of the molecules would form double Holliday junctions (dHJs) which can be resolved as COs, by resolvases in asymmetric manner. However, the presence of mismatches during strand invasion leads to noncrossover (NCO) repair (Petronczki, Siomos, Maria, & Nasmyth, 2003).

The close association between maternal and paternal axes along the length of bivalents (synapsis) is achieved by the Synaptonemal Complex (SC) for the duration of zygotene and until early diplotene when the SC disassembles and the chiasmata are possible to observe cytologically (Fig. 2-A-D.) (Petronczki et al., 2003). The initial linear protein axis, during Prophase I, known as synapsis forms the SC associating with the paired sister chromatids increasingly juxtaposed (Higgins et al., 2005). The structure of the SC is tripartite fromed by two paralel axial elements (AE) (lateral elements after synapsis) and several transverse filaments (TF) (Fig. 3-A). AE are driven mostly by the ASY1 protein, which are expressed with Rec8 during zygotene, span the central region and attach the lateral elements together in a zipper-like structure, driven by ZYP1 (Capilla-Pérez et al., 2021). By pachytene the chromosomes are completely synapsed and linked by the SC. From diplotene and later, the SC disassembles, so homologous chromosomes remain associated only by chiasmata, the cytologically visible structure corresponding to COs (Higgins et al., 2005) (Fig. 3-B).

Notably, the SC is not essential for all types of COs, observed in *Schizosaccharomyces pombe* where there is neither SC formation nor Class I COs (Cromie & Smith, 2007). However, in yeast and animals, the SC is needed to make CO and the SC and Zyp1 have been proven to be key for interference and heterochiasmy signals (Capilla-Pérez et al., 2021). Recently it has been hypothesized that is likely that the SC is also responsible for the HEI10 diffusion coarsening

signal that drives interference (Girard, Zwicker, & Mercier, 2023; Morgan et al., 2021; L. Zhang, Stauffer, Zwicker, & Dernburg, 2021).

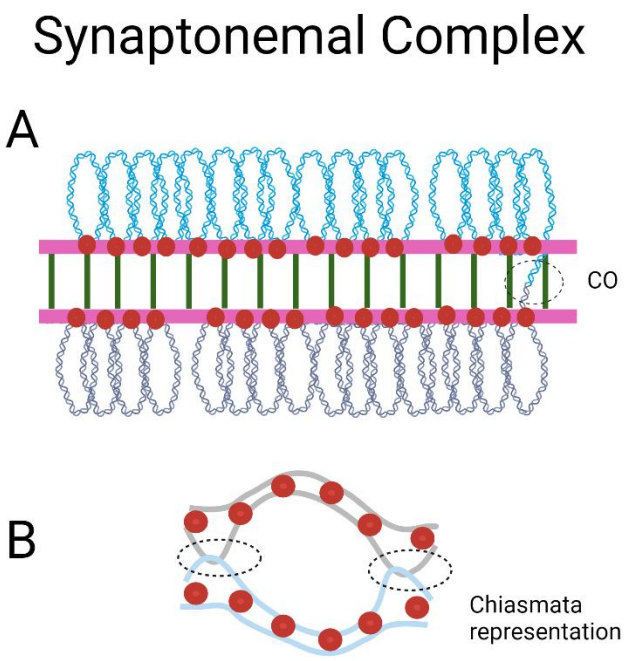

Figure 3 Synaptonemal Complex and Chiasma. Created by BioRender.com

5.2.1 Class I and Class II CO formation

The repair of DSBs into crossovers (COs) are mediated through two different pathways (Class I or Class II), or as noncrossovers (NCOs), facilitated by the recombinases DMC1 and RAD51, which facilitate the search for homologous sequences (Fig.4) (Kurzbaue et al., 2012; Mercier et al., 2015). In Arabidopsis, on average around 100 to 200 DSB are formed and only around 10 are repaired as COS by two different mechanisms.

The Class I pathway accounts for approximately 90% of CO formation, while the rest occurs through the Class II pathway (Fig. 4). Within the Class I CO formation process, a group of proteins found in S. *cerevisiae* known as ZMMs (Zip1, Zip2, Zip3, Zip4, Mer3, Msh4, and Msh5) are essential (Börner et al., 2004). Mutations in this pathway lead to a significant reduction in CO formation and subsequent fertility issues in organisms. Additionally, MLH1 and MLH3, although not classified as ZMM proteins, play crucial roles in CO formation within the same pathway. Mutations in these proteins result in a 50% decrease in CO formation. Notably, MLH1 serves as a specific marker for ZMM COs during late prophase. During early prophase, other ZMM proteins (MSH5, ZIP4, MER3, and HEI10) form multiple foci, but the remaining proteins disappear during pachytene. Among the various intermediates, only a few successfully mature into COs, which are colocalized by HEI10 and MLH1 (Grelon et al., 2001; Raphaël Mercier et al., 2015).

HEI10, similar to a described protein in mammals as the Enhancer of Cell Invasion N°10, it is related to the yeast Zip3 and identified in Arabidopsis as a ZMM protein. HEI10 is necessary for class I CO formation, loaded early during prophase I and while recombination progresses, HEI10 is observed in defined loci, colocalizing with MLH1 until the end of recombination process (Chelysheva et al., 2012). HEI10 is highly dosage-sensitive, therefore transformation of additional HEI10 copies is sufficient to increase CO formation, demonstrating that it acts as a limiting factor for COs formation, sensitive to interference (Ziolkowski et al., 2017). Aditionally, it has been proposed the HEI10 diffusion signal along the SC axis as the main regulator of interference and CO designation of Class I COs (Coarsening Model) (Morgan et al., 2021; L. Zhang et al., 2021).

In plants, the factors involved in Class II CO formation (Fig. 4-G) are less thoroughly characterized, with MUS81 being the sole known participant. MUS81 contributes to a minority of COs in most organisms, but its activity is generally critical for the efficient resolution of joint molecules (Hunter, 2015).

In contrast of COs which exchange large fragments of DNA, Noncrossovers (NCO) copy a small patch of homologous chromosome to the broken chromosome, modifying only one chromatid, instead of both of them (Fig. 4-H) (Raphaël Mercier et al., 2015).

COs are crucial for meiosis not only to create genetic diversity but also, to work as a physical link necessary for proper segregation during meiosis; mutants affected in the CO formation are also showing a big percentage of sterility and embryo lethality due to aneuploidy (Giraut et al., 2011; Lynn, Soucek, & Börner, 2007). Therefore, COs are highly regulated. It is known that there should be formation of at least 1 CO per bivalent for a successful meiosis. Typically, Class I CO formation is regulated through interference -which refers to the formation of COs at greater distances along the chromosome than would be expected by chance-. Class II CO formation is regulated by anti-CO factors (Joiselle B. Fernandes, Wlodzimierz, & Henderson, 2019a; Giraut et al., 2011).

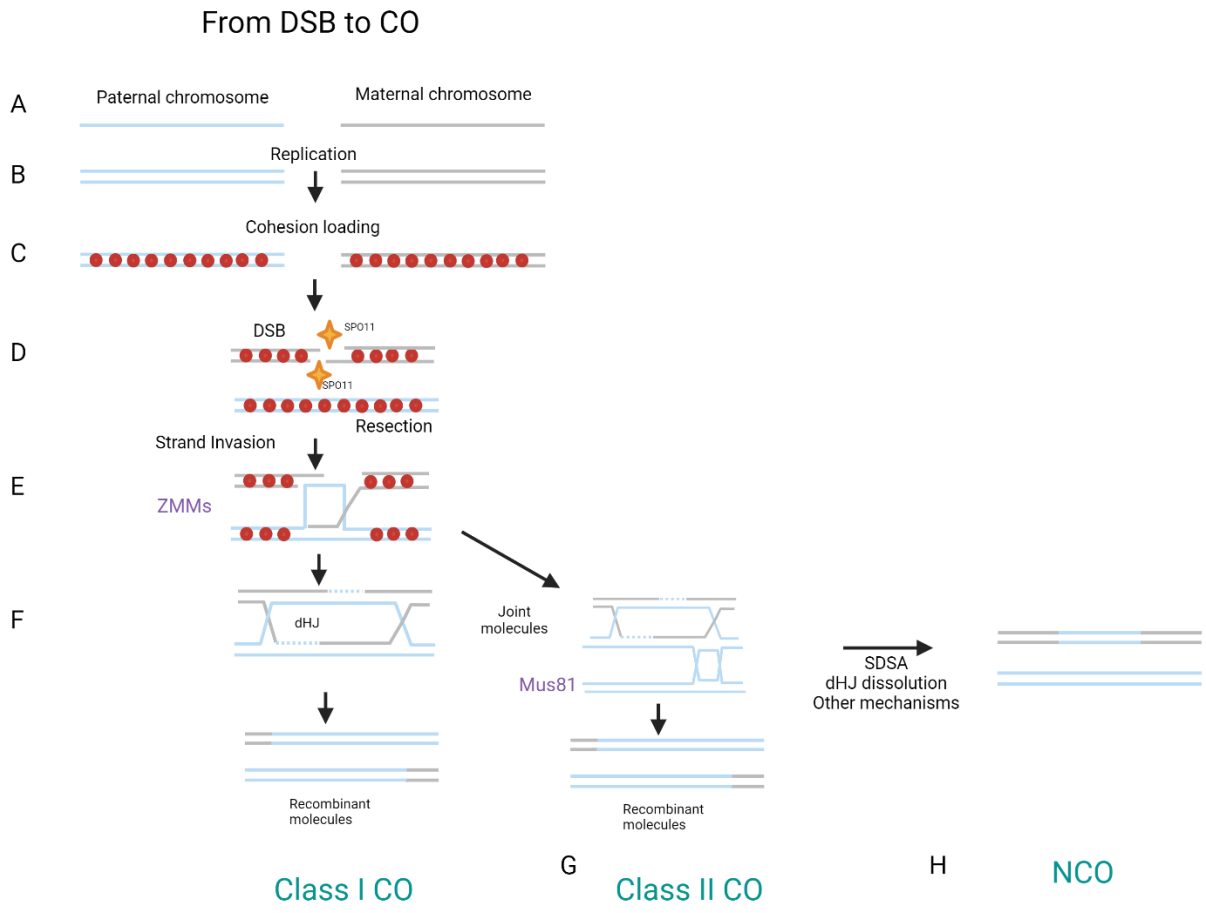

Figure 4 From DSB to CO. Created by BioRender.com (Raphaël Mercier et al., 2015; Petronczki et al., 2003)

5.3 CROSSOVER DISTRIBUTION

The distribution of COs along the chromosome is non-homogeneous, with higher frequencies observed in regions known as hotspots, primarily located in the chromosome arms. Two main types of hotspots have been identified. The first type, likely ancestral, is found in fungi, plants, birds, and some mammals. These hotspots exhibit temporal stability over extended periods (up to millions of years) and are concentrated near gene promoter regions and terminators and transcription start sites (Sen, Dodamani, & Nambiar, 2022; Underwood et al., 2018). The second type which is believed to have evolved later, is observed in mice and humans. In these species, the positioning of hotspots is governed by the zinc-finger protein PRDM9 which catalyzes trimethylation of Histone 3 at lysine 4 and lysine 36 (H3K4m3 and H3K36m3), although is still unclear how the chromatin mark is recognized by the DSB machinery. However, in *S. cerevisiae* the Set1 protein complex is in charge to deposit the H3K4me3 mark to delimit DSB. In contrast, in plants PRDM9 subfamily is not present either because it has been lost in plants lineage or gained in the vertebrate one, but there is still an observed link between chromatin and/or DNA features and DSB localization (Lenormand et al., 2016; Raphaël Mercier et al., 2015).

As mentioned before, Class I CO formation is regulated by interference. Recent studies by Morgan et al., 2021 and Zhang et al., 2021 have proposed the Coarsening Model to be the

primary driver of CO interference where the HEI10 protein diffuses along the chromosome, likely through the SC, forming larger foci that restrict the growth of nearby foci. These larger foci serve as the primary determinants for ZMM-mediated COs (Class I). In contrast, Class II COs have been shown to be distributed independently from one another. While Class II COs cannot interact with other Class II events, studies conducted in tomato have demonstrated that the two different types of COs can influence each other. Further, the anti-CO pathways including I) FANCM/MHF1 and MHF2 II) FIDGETIN-LIKE-1 (FIGL1) and III) RECQ4AB are also regulating the CO formation by disassembling joint molecules or by regulating strand invasion (Anderson et al., 2014; Joiselle B. Fernandes et al., 2019a; Raphaël Mercier et al., 2015)

Inhibition of recombination is observed in the heterochromatin regions usually in centromeres and pericentromeres, known as the "centromere effect", which will be discuss further. Despite extensive research performed in this field in several species, the mechanisms underlying the distribution of COs along the chromosome are not yet fully understood (Choi & Henderson, 2015; Copenhaver et al., 1999; Nambiar & Smith, 2016).

In some plants with large genomes like maize (2.5Gb), barley (5 Gb), and wheat (17 Gb), recombination show to gradually increase from centromeres to telomeres (Saintenac et al., 2009). The recombination rate in wheat's chromosome arms averages between 0.60 to 0.96 cM/Mb, while spanning the centromere shows an average of 0.05 cM/Mb. Wheat and maize both have an average of 2.6 CO forms per chromosome. Depending on the window size, these rates can vary. With a 1 Mb window, the rates are more similar to those observed in maize (0.8 to 11.5 cM/Mb) and sorghum (0 to 10 cM/Mb). (Choulet, et al., 2014).

Recombination in maize has been shown to be localized to the distal part of the chromosomes and is correlated to the Expressed Sequence Tags (ESTs), sequences used to identify transcripts during sequencing (Saintenac et al., 2009). In Arabidopsis, potato and maize, recombination tends to be associated to open chromatin hallmarks, including low levels of DNA methylation, high levels of H3K4me3 and low nucleosome density (Choi et al., 2018; S. Liu et al., 2009; Marand et al., 2017; Rowan et al., 2019; Nataliya E. Yelina et al., 2012)

In Arabidopsis a mean of CO rate of 7,8 CO per F2 individual -meaning that each gamete contributes with overall half of the total recombination, in this case 3,9 CO- in Col/Ler hybrids. The general distribution of COs rates show a mean of 1,3-1,9 COs per chromosomes positively corelating with the chromosome length (Choi et al., 2016; Rowan et al., 2019; N E Yelina et al., 2015). However, it was observed that recombination is higher in male (11,15 CO) than in female meiocytes (6,6 COs); it was found that the mean number of COs per male cell varied between 1,7 to 3,2 CO per bivalent, in contrast to female meiosis where only 1,1 and 1,6 COs per bivalent, this is due to the SC length that has shown to correlate with CO numbers (Capilla-Pérez et al., 2021; Girard et al., 2023; Giraut et al., 2011).

In plants, has been hypothesized that recombination hotspots are favouring diversity by forming COs within genes that play an important role in the immune system. And it was observed that a subset of pathogen-resistance genes are overlapping with a strong crossover hotspot. However, this is not the only selection pressure because a coldspot is also observed in resistance genes, which correlates with the chromosomal rearrangements observed in

hybrid contexts, between different ecotypes. Concluding that there is a complex variation in the CO patterns of the resistance genes, which can be related to coevolutionary pressures (plant-pathogen) at different loci and also can be due to effects of structural genetic diversity (Choi et al., 2016).

5.4 ANTI-CO FACTORS

Many eukaryotic species have conserved anti-CO pathways that oppose the pro-CO factors. In humans, the FANCM complex and its ATPase activity have been implicated in Fanconi anemia, a syndrome characterized by an increased risk of cancer, developmental abnormalities, and bone marrow failure. Furthermore, this protein complex has been demonstrated to prevent replication forks from causing damage (Xue, Sung, & Zhao, 2015). In yeast, an orthologue of FANCM has been shown to actively participate in the mechanisms that protect against double-strand breaks (DSBs) becoming crossovers (COs) (Lorenz et al., 2012).

Likewise, in Arabidopsis, the anti-CO helicase FANCM was the first protein discovered to exhibit an anti-CO role (Crismani et al., 2012). FANCM was identified through a Forward genetic screen in a partially infertile *zip4* mutant background lacking meiotic COs, causing missegregation of homologs and reduced fertility leading to shorter fruits. Subsequently, two additional pathways were identified as having anti-CO functions, involving the AAAATPase FIDGETIN-LIKE-1 (FIGL1) and the BLM/Sgs1 helicase (Girard et al., 2015; Hartung et al., 2007) both homologs of RECQ4A and RECQ4B (Joiselle Blanche Fernandes, Séguéla-Arnaud, Larchevêque, Lloyd, & Mercier, 2018).

Several Arabidopsis anti-CO factors and other related interactors such as FIDGETIN-LIKE-1 INTERACTING PROTEIN (FLIP1) (Joiselle Blanche Fernandes, Duhamel, et al., 2018) and regulators BRCA (Kumar, Duhamel, Coutant, Ben-Nahia, & Mercier, 2019) were identified from the same genetic forward screen.

Additional regulators have been recently identified: HIGH CROSSOVER RATE 1 (HCR1) (Nageswaran et al., 2021) and SUPPRESSOR OF NPR1-1 INSUCIBLE (SNI1) (Zhu et al., 2021).

Interestingly, the double mutant *recq4a*b shows CO increase of 4,1-fold in the arms of the chromosomes (Serra et al., 2018a), single *figl1* showed around half of the increase observed in *recq4a,* but still a significant increase in comparison to wild type and *fancm* had no detectable effect on recombination (Joiselle Blanche Fernandes, Séguéla-Arnaud, et al., 2018). When all these three mutants were combined with each other it was found that the biggest increase was the double mutant *fancm* when combined with *figl1* or *recq4* (until 30cM/Mb) but there was no further increase with the triple mutant, suggesting these three genes work in different pathways and that some upper limit was reached (Joiselle Blanche Fernandes, Séguéla-Arnaud, et al., 2018). To enhance the recombination increase in Class II factors, *recq4ab* double mutant was combined to the Class I ZMM pro-crossover factor HEI10 overexpressed, the increment in recombination was 5-fold higher than wild type (Serra et al., 2018a). In all the previous cases, pericentromeres recombination was never significantly increased, in the champion of recombination *recq4ab HEI10* the maximum increase in pericentromeres was only 1,5-fold, compared to Wild Type (Serra et al., 2018a). Since the

recombination in centromeric regions is never significantly increased, it suggests that there might be a specific pathway for these regions that are limiting the CO formation (Fig. 5).

Similarly, *hcr1* and *sni1* mutants showed increasing crossovers in distal chromosome arms, a drop in interference and partial restoration in Class I COs, indicating these two factors are involved in Class II CO repair. The centromeric region did not display any increased recombination in either of them (Nageswaran et al., 2021; Zhu et al., 2021).

The main objectives for this project is to find specific genetic factors that are restricting recombination in the chromosome centromeric region.

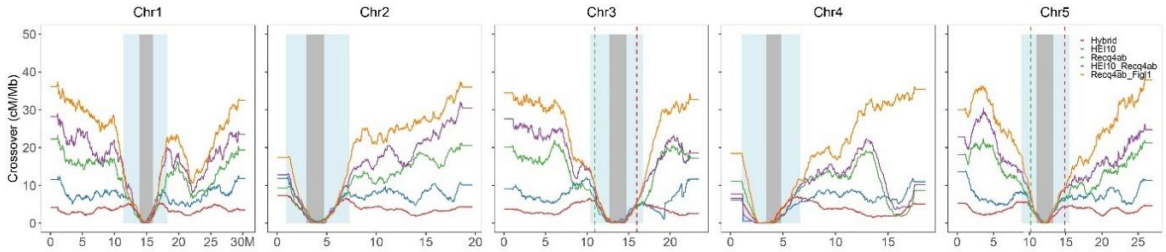

Figure 5 Recombination rates in mutant anti-CO factors. Each plot represent each chromosome of Arabidopsis, where they are depicted in 5Mb windows in the X axis and the Y axis depicts the number of CO formed per Mb. Grey vertical column represents the centromeres, flancked by the light blue vertical columns representing pericentromeric regions. They are compared with the hybrid (Col/Ler) wild-type sequence (red), HEI10 overexpressor (blue), recq4ab (green), double mutant HEI10 OE and recq4ab (purple) and the one showing the highest recombination is the double mutant recq4ab figl1. The dotted lines in the pericentromeric regions in chromosome 1 and 5, depict the location of the FTLs.
Picture credits Dr. Qichao Lian with data from: Joiselle Blanche Fernandes, Séguéla-Arnaud, et al., 2018; Rowan et al., 2019; Serra et al., 2018

5.5 CENTROMERES, PERICENTROMERES AND KINETOCHORES

Centromeres are the primary constriction on condensed mitotic and meiotic chromosomes. They were first observed in salamander cells in 1882 by light microscopy as the chromosomal attachment site for spindle microtubules in dividing cells. Their primary function is to assemble the kinetochore for the spindle to attach and allow proper chromosome segregation (McKinley & Cheeseman, 2016). Among the eukaryotic tree, chromosomes with one constriction (monocentric) is highly widespread, although organisms with chromosomes with several CENP-C/CENH3 proteins, or holocentric show a sporadic distribution (e.g. C. elegans, *Rynchospora pubera*).

The centromere is specified epigenetically, usually defined by the presence of the centromeric nucleosome CENH3 which is a component of chromatin with biochemical similarity to histone and that its shared homology with histone H3. Usually the signal is expressed together with CENP-C and KNL2; CENP-C works as a bridge that binds to CENH3 (CENP-A in humans), to its chaperone and to DNA, in addition to bind to outer kinetochore proteins (MIS12) in order to

ensure a proper segregation. KNL2 and CENP-C have an important role in female gametogenesis and zygote formation positioning the centromere (N. Wang & Dawe, 2018) .

Specific DNA sequences are neither necessary nor sufficient for centromere function, especially in regional centromeres. However, in Drosophila has been proved that artificial targeting of CENP-A to an ectopic chromosomal locus is sufficient to generate structures that are capable of directing microtubule attachment and chromosome segregation. Additionally, epigenetic factors have been demonstrated to be essential for *de novo* kinetochore assembly in budding yeast (Joiselle B. Fernandes, Wlodzimierz, & Henderson, 2019b; McKinley & Cheeseman, 2016).

In eukaryotes there are two types of centromeres: point centromeres and regional centromeres. Point centromeres are primarily determined by specific centromeric DNA sequences, which in turn recruit centromeric DNA-binding proteins. They are assembled on a single CENPA/CENP-C/CENH3 and are flanked by nucleosomes. Point centromeres in budding yeast are relatively small, spanning approximately 125 base pairs. However, the majority of organisms including humans, mice, flies, and fission yeast have monocentric regional centromeres which is built on nucleosomes containing centromeric-specific histone H3 variant, CENPA that interspace with H3-containing nucleosomes, flanked by the pericentric heterochromatin and a central kinetochore assembly. They can extend over several megabases (Ling & Yuen, 2019; Sen et al., 2022).

Sequencing technologies (Nanopore and PacBio Hig-fidelity (HiFi)) have recently allowed to sequence the repetitive centromeric sequences of humans, maize and Arabidopsis. The centromeres of human chromosomes are almost entirely made up of repetitive sequences; alpha-satellites, being the most common (Altemose et al., 2022). Similarly, maize centromeres which were detected by the enrichment of the centromeric histone H3 (CENH3), they are 2.22 Mb long and also contain repetitive sequences including retrotransposons from the *Gypsy* family and also non-*Gypsy* family, both were showing different proportions but the most abundant is the CentC retrotransposon which was forming clear patterns of highly and low abundance of CentC (Chen et al., 2023).

In Arabidopsis, centromeres exhibit a unique chromatin state that combines features of both euchromatin and heterochromatin; they are characterized by tandemly repeated satellite arrays that contain a high abundance of the CENH3-specific histone variant and are densely DNA methylated. The satellite repeats, known as CEN180 satellites, are approximately 178 base pairs in length. Additionally, Arabidopsis centromeres are susceptible to invasion by long-terminal retrotransposons known as ATHILA. The presence of these retrotransposons disrupts the genetic and epigenetic organization of the centromeres. Each chromosome have different proportion of repeats satellites and retrotransposons, proposing that each chromosome represent a different stage in cycles of satellite homogenization and transposon diversification (Naish et al., 2021a).

The pericentromeres are flanking the centromeres. They are heterochromatin regions, highly DNA methylated that show more regular nucleosome spacing than euchromatin. The pericentromeres have a major role during chromosomal segregation because of the enriched

deposition of cohesins, which are critical to maintain sister-chromatid cohesion. In budding yeast the pericentromeric region is not defined by specific sequences. Particularly in Arabidopsis, pericentromeric regions are overlooked by transposable elements and are also enriched for heterochromatic chromatin marks including H3K9me2, H3K27me1, H2A.W6, H2A.W7 and the meiotic cohesin REC8 (Joiselle B Fernandes et al., 2023; Sen et al., 2022; Simon, Voisin, Tatout, & Probst, 2015). Pericentromeres have relativelly high SNP and CO density in hybrid (Col/Ler), despite of higher levels of heterochromain (Rowan et al., 2019). Specifically the mark H3K9me2 has been proved to be a good pericentromeric marker in both whole genome sequencing and cytologically (Naish et al., 2021a).

Kinetochores are big protein complexes in charge to specify and bind centromeres, interact with microtubules and their companion proteins and to regulate chromosome movement during segregation of both mitosis and meiosis. Its presence is essential for accurate chromosomes segregation, when the kinetochore is defective, it can be reflected in aneuploidy which can lead to diseases complex diseases (Chan, Liu, & Yen, 2005; Yu, Dawe, Hiatt, & Dawe, 2000). The function and the overall structure of this complex is conserved among species, but the molecular level the subunits and their disposition tend to differ, supposedly because the kinetochores of metazoans are assembled from repeated subunits where each repeat might reflect the unit module of the yeast kinetochore (Chan et al., 2005). There have been identified more than 14 proteins involved in this structure and they are disposed into two main domains: inner and outer kinetochore. The outer kinetochore proteins are transient and only necessary during chromosome segregation, whereas the inner kinetochore proteins recognize centromeric DNA and establish a specialized chromatin environment. A specialized histone H3 variant, centromeric histone CENH3, is a fundamental feature of the inner kinetochore. CENP-A, the first CENH3, was identified in humans, and homologous proteins have been found in all studied eukaryotes, including Arabidopsis and maize (Jiang, Birchler, Parrott, & Dawe, 2003). It has been shown recently in *S. cerevisae* that the kinetochore proteins are also involved in the recombination regulation near the pericentromeres (Vincenten et al., 2015).

Together, centromeres, pericentromeres and kinetochores are critical in chromosome segregation. Defects in their function can lead to segregation problems, resulting in developmental defects or diseases both in mitosis and meiosis (McKinley & Cheeseman, 2016).

5.6 CENTROMERE EFFECT

The concept of the centromere effect was first reported in 1932 in *Drosophila*, referring to a reduction in CO near centromeres. The centromere effect has been observed in unicellular eukaryotes, multicellular invertebrates, plants, and mammals. In yeast, limitation of formation of both CO and NCO spanning around 10kb flanking the centromere, can be remarkably around 50 times the length of the centromere (Sen et al., 2022).

The surrounding heterochromatin of centromeric regions is believed to contribute to their genetic scarcity (Sen et al., 2022). However, it has been observed the presence of genes in centromeric and pericentromeric regions of wheat (Ahmed et al., 2023; Choulet et al., 2014), maize (Chen et al., 2023) and even humans (Altemose et al., 2022) and the repression is still present, they didn´t show COs formation in the most proximal centromeric regions in wheat (Saintenac et al., 2009; Tock et al., 2021), rice (Si et al., 2015), tomato (Sherman & Stack, 1995; X. Su et al., 2021) and maize (Kianian et al., 2018).

In 1988, in *S. cerevisae* centromere 3 (CEN3) interval reported around 5-fold reduction in CO frequency but after introducing a mutation in a centromere element CDEIII, the repression was lost. Contemporarily, in *S. pombe* it was observed that the reduction of recombination level in the CEN3 interval was around 200-fold lower than the genome-mean. However, it was observed that heterochromatin away from the centromere could still exhibit distance-dependent COs, suggesting that the proximity to centromeric regions themselves inhibits recombination (Sen et al., 2022).

Despite a tight control in repressing COs at centromeres, other recombination events such as gene conversions are found to be prevalent in several species such as maize (Shi et al., 2010), rice and mouse(Sen et al., 2022; Talbert & Henikoff, 2010). This process is not enough to trigger chromosomal mis-segregation errors, so there are no deleterious phenotypes. The presence of pericentromeric regions flanking the centromeres have been a possible factor to limit COs in pericentromeric regions; however, in *S. cerevisiae* pericentromeric regions are absent, leaving other factors to limit them (Sen et al., 2022).

Zyp1 is one of the main players of the Synaptonemal Complex structure and synapsis establishing, it also plays an important role in heterochiasmy and promotes class I COs independent from SC (Capilla-Pérez et al., 2021; Girard et al., 2023). The *zyp1* mutant was analysed in budding yeast and they indeed found more recombination in pericentromeric regions (Vincenten et al., 2015) and it was even hypothesized for Zyp1 to play a role also in pericentromeric regions modifying CO formation in Arabidopsis. However, in Arabidopsis, *zyp1* showed to have even less recombination in pericentromeres, compared to wild type, while there are more COs than in the rest of the chromosome, suggesting Zyp1 is not responsible for limitating COs in pericentromeres (Capilla-Pérez et al., 2021), something confirmed in this project.

In Arabidopsis, crossover were suppressed in proximity to the centromeres but SPO11-1-oligonucleotids (likely reflecting DSB formation) are low, although increase relative in pericentromeres (Naish et al., 2021b). In maize, the mapping of DSB hotspot showed that recombination starts along the whole chromosome; however, the COs are limited only in pericentromeric regions, suggesting that the mechanisms that are regulating the CO formation here are at the level of repair (He et al., 2017). This fact coincides with the results from Yelina et al., 2015 where they show that the *Methyltransferase (met1)* mutant shows decrease in COs formation specially in pericentromeres, probably by changing the proportion of euchromatic and heterochromatic. Additionally, when combined with *zyp1* or *fancm* they also show less recombination comparing with the single mutants, suggesting that the methylation pathways can affect recombination and a negative interaction occurs when combining genetic

and epigenetic pathways. This is supported by the *cmt3* mutant that shows more recombination in centromeric regions (Underwood et al., 2018), suggesting that *cmt3* has a role in limiting CO formation and that epigenetic marks can contribute to limit recombination, probably by silencing specially *Gypsy* retroelements (rich in CG content). However, the epigenetic marks are not the only contributors to limit the CO formation.

The molecular mechanisms for the recombination repression are still not completely understood, although it has been shown that the kinetochore assembly on the centromeres and the pericentromeric cohesins and heterochromatin have a key role in the regulation. As observed in *S. cerevisae,* where they establish the kinetochore as a major responsible factor for repressing crossover in the pericentromeres during meiosis (Vincenten et al., 2015).

5.7 MAIN OBJECTIVES

Centromeric region and kinetochores are essential structures important for properly oriented segregation of homologous chromosomes and sister chromatids. Recombination in these regions is hardly present among eukaryotes.

Mutants in anti-CO factors (RECQ4, FIGL1, FANCM) can significantly increase recombination only in the chromosome arms, never in centromeric regions. However, in *C. serevisae* the *zyp1* mutant, in charge of the SC formation, could also unblock centromeric recombination. These main two evidence suggest that there could be a pathway that limits recombination specific in centromeric regions. Additionally, in Arabidopsis, the *cmt3* mutant showed increased recombination, suggesting that DNA methylation in CG and non-CG contexts are contributing to recombination limitation in centromeric regions.

The main goal of this project is to find specific genetic factors that contribute to the understanding of the CO repression in centromeric regions.

5.8 GENE AND TRANSPOSABLE ELEMENTS DISTRIBUTION ALONG THE GENOME

Genes, like COs, are not evenly distributed along the chromosomes. Overall, eukaryotes show a higher gene density in the arms of the chromosomes and tend to have less genes in the centromeric regions (Cheng et al., 2017; Arabidopsis Initiative, 2000). Wheat (*Triticum aestivum* L) is not the exception, where its genes are not evenly distributed, and gene density is increasing on both arms along the centromere-telomere axis. The average gene density is around 9 genes/Mb. Variation of gene density in wheat is higher than the chromosomes of rice that are more compact and lower than in sorghum that have a more dense in the telomeric regions but in the same range as maize (Choulet et al., 2014). In Einkorn wheat (*Triticum monococcum*) accessions TA299 and TA10622, 1 to 9 genes were found within the CENH3-enriched domains, except of chromosome 7A of accession TA299 which contained 39 annotated genes, most of them were not expressed (Ahmed et al., 2023) and many of those were described as "housekeeping" genes (Tock et al., 2021). The outside-genes of CENH3-enriched domains showed varying expression levels.

Similarly, in maize around 82 genes were identified within centromeres, 52 of those genes shared homology with sorghum. Around 46 of the present genes in centromere were expressed slightly lower than the rest of the annotated genes and many of them seem to be tissue specific (Chen et al., 2023). Even in the centromeric region of the human 13th chromosome, annotation revealed 676 genes and pseudogenes embedded between their large satellites, 23 of them were coding for proteins (Altemose et al., 2022).

As gene density decreases in centromeric regions, the transposon density increases. Transposon Elements (TEs) are highly repetitive sequences that are mobile along the genome. They constitute until 60% of wheat genome (Choulet et al., 2014), 65% of tomato genome (X. Su et al., 2021) and around 15% in Arabidopsis (Joly-Lopez & Bureau, 2014). TEs can be autonomous, encode the necessary genes to propagate and transpose themselves; alternatively, they can be non-autonomous and use the transposition machinery of other families. Depending on how they transpose, there are two types of TEs: the DNA transposons and retrotransposons. The first, transpose via a "cut and paste" mechanism with the help of a transposase. While retrotransposons, need to transcribe to RNA, reverse transcribed and the new complementary DNA reinserts in other location of the genome, "copy and paste" mechanism. By transposition, TEs can affect gene structures, gene copy number or even induce deleterious insertions. To avoid important defects the genomes have evolved to silence TEs firstly by the RNA dependent DNA Methylation (RdDM) pathway and perpetuated them through generations of cell divisions through histones modifications (Joly-Lopez & Bureau, 2014).

The input that TEs can give to the genomes such as genome organization (Polyploidization, genome size), genome variation (chromosomal rearrangements), genome innovation (gene duplication rearrangements), response to stress, speciation, domestication, among others. Notably, telomeres and centromeres contain big numbers of TEs (Joly-Lopez & Bureau, 2014). It has been observed that in maize, the centromere contains 75.52% retrotransposons and 9.78% DNA transposons. The genome is formed by essentially 3 types of satellite repeats (90% genome): Knob180, CentC and TR-1, being CentC the only one exclusively found in

centromeric and pericentromeric regions, in addition to the *Ty3/Gypsy* retrotransposon CRM (chromodomain) (Chen et al., 2023). Arabidopsis centromeres are invaded with *ATHILA* retrotransposons -of the *GYPSY* superfamily- targeting the satellite arrays, interrupting the genetic and epigenetic organization of the centromeres, with centromeres 4 and 5 being the most invaded. The *ATHILA* long term repeats (LTR) retrotransposons have a mean length of 11kbp, they are young retrotransposons as they share 98.7% of LTR sequence identity, higher than the *ATHILA,* located outside the centromeres. Sometimes, as observed in chromosome 5, the retrotransposons are duplicated within a CEN180 satellite repeat, suggesting they share target site duplications (Naish et al., 2021b). *ATHILA* shows greater histone H3 lysine 9 dimethylation (H3K9m2) enrichment, mostly in pericentromeric regions in comparison to the centromeric CEN180 satellite repeats mostly enriched with H3K4me3; therefore, the *CEN180* satellites show divergence in the flanking regions, suggesting *ATHILA´*s insertion is influencing either the surrounding satellites or the subsequent divergence of the adjacent *CEN180.* It is thought that there is a balance within the opposing forces of whether *ATHILA* inhibiting *CEN180* homogenization, or that the loss of homogenization facilitates ATHILA insertion, that keeps the centromere integrity (Naish et al., 2021b).

5.9 DNA METHYLATION

H3K9me2 mark is in charge of silencing plant transposable elements and DNA cytosine methylation by the chromodomain cytosine methyltransferases CHROMOMETHYLASE2 (CMT2) and CHROMOMETHYLASE3 (CMT3) which recognize heterochromatic H3K9me2 via Bromo Adjacent Homology (BAH) and chromodomains in CG and non-CG contexts (CHG and CHH, where H= A, C, or T). Histone H3K9 methylation is mediated by the SET domain methyltransferases KRYPTONITE/SUPPRESSOR OF VARIEGATION HOMOLOG4 (KYP/SUVH4), SUPPRESSOR OF VARIEGATION HOMOLOG5 (SUVH5), and SUPPRESSOR OF VARIEGATION HOMOLOG6 (SUVH6). The maintenance of non-CG DNA methylation and its effect on H3K9me2 are dependent on the de novo DNA methyltransferase DOMAINS REARRANGED METHYLTRANSFERASE2 (DRM2). To silence euchromatic crossover hotspots, the DNA and H3K9me2 methylation through the RNA-directed DNA methylation (RdDM) pathway, is enough.

Mutants in Arabidopsis affecting CG methylation (*met1* and *ddm1*) increase crossovers in chromosome arms and decreased them in pericentromeres (Underwood et al., 2018; Nataliya E. Yelina et al., 2012). The *cmt3* mutant which affects non-CG DNA methylation in pericentromeric was analysed and after measuring recombination by the Fluorescent Transgenic Lines (FTLs) in the CEN3 interval, it showed to increase CO formation close to the centromere but specially in the pericentromeres of Col-0, Ler accessions and hybrid mutants. However, they also showed a slight decrease in CO formation in the vicinity of these regions, as if they were compensating the CO formed in centromeric regions (Underwood et al., 2018). Additionally, *met1* showed higher DSB formation in pericentromeres but not CO formation (Choi et al., 2018). In addition, the double mutant of *cmt3zip4* is able to restore fertility from the single *zip4* mutant, indicating that the class II pathway is contributing to increased COs in the *cmt3* mutant; in contrast to the suggestion that mutations in the H3K9me2/non-CG

pathway activate crossover frequency in proximity to the centromeres (Underwood et al., 2018; Nataliya E. Yelina et al., 2012).

5.10 Structural Maintenance of chromosomes (SMC) proteins

SMC (structural maintenance of chromosomes) proteins are vital for the regulation of chromosome dynamics during both mitosis and meiosis. These proteins are present in prokaryotes and eukaryotes and possess five conserved structural domains: an N-terminal NTP-binding motif, a C-terminal DA box, and two central coiled-coil domains. Based on their functions, SMC proteins can be classified into three categories: condensins (SMC2 and SMC4) involved in chromosome condensation and compaction, cohesin complexes (SMC1 and SMC3) responsible for maintaining the cohesion of sister chromatids, and DNA recombination/repair complexes (SMC5 and SMC6) involved in DNA lesion and double-strand break (DSB) repair. Cohesin complexes play a crucial role in holding sister chromatids together during DNA replication until chromosome segregation. During meiosis, sister chromatid cohesion is mediated by the cohesion complex, formed by Scc3, Smc1, Smc3, Scc1 (also called Mdc1) and Rec8, the last one being specific to meioisis while the rest acting also during mitosis (Klein et al., 1999). The cohesin complex consists of a tripartite ring, with the SMC heterodimer forming a V-structure. The N- and C-terminal regions of SCC1 bind to the head domains of SMC3 and SMC1, respectively, to close the ring. Cohesins are loaded onto chromatin before replication in an ATP-dependent reaction by the SMC heads and the cohesin-loading complex SCC2/SCC4. At the end of meiotic prophase, homologous chromosomes are linked through chiasmata (Gloria A. Brar, Ly-sha S. Ee, & David, 2009; Lam, Yang, & Makaroff, 2005).

5.11 Cohesion loading

Cohesion is deposited in unreplicated chromatin in a ATP-dependent reaction by the SMC heads and the cohesion-loading complex SCC2/SCC4. Cohesion loading starts before S phase, and is connected to DNA replication. In budding yeast cohesion depends on an acetyltransferase Eco1/Ctf7 that acetylates head domain of SMC3. Both in budding yeast and humans Chromosome Transmission Fidelity 18 (Ctf18) is part of the complex Replication Factor C (RFC), together with the theoredoxin Dcc1, creating a heptameric complex with the Proliferating Cell Nuclear Antigen (PCNA) that has a loading and unloading activity and plays a role in sister chromatid cohesion. In yeast, the knockout mutation of Arabidopsis CTF18 homolog shows impaired sister chromatid cohesion (Takahashi et al., 2010).

5.12 Protection of Centromeric Cohesins by Shugoshin proteins (SGOs)

To enable the segregation of homologs during meiosis I, cohesins must be removed from chromosome arms by the cleavage of Rec8 by the separase, which releases the cohesion of chromosomes at anaphase I. However, centromeric Rec8 is protected from cleavage by Shugoshin 2 (SGO2) at the anaphase I to maintain a physical connection between sister

chromatids, and is released at onset of anaphase II. SGOs are crucial for the proper segregation of homologous chromosomes, by monopolar attachment to the meiosis II spindle microtubules. SGO is a specific protein responsible for protecting centromeric cohesion during both meiosis and mitosis. It also plays additional roles in regulating kinetochore-microtubule attachment and sensing kinetochore tension by interacting with members of the chromosomal passenger complex (CPC) and the spindle assembly checkpoint (SAC). SGOs are highly conserved among eukaryotes including *Schizosaccharomyces pombe*, plants, and vertebrates; notably, the progressive process of discovery of SGOs in different organisms didn´t allow to homogenise the names, meaning that SGO1 from plants does not necessarily correspond to the same protein in other organisms. In Drosophila and *Saccharomyces cerevisiae*, SGO1 is responsible for protecting centromeric-specific sister chromatid cohesion in meiosis I. In fission yeast, SGO2 is involved in chromosome segregation and controlling the localization of the CPC. In Arabidopsis, SGO1 is required for maintaining centromeric cohesion of sister chromatids in meiosis I but is not essential for the establishment and maintenance of the synaptonemal complex. Disruption of SGO1 leads to premature separation of sister chromatids before telophase I, but its loss in the *sgo2-1* mutant can be compensated by overexpressing Sgo1 (Gloria A. Brar et al., 2009; Zamariola et al., 2013).

5.13 MONOPOLAR ORIENTATION AND SEGREGATION

The monopolar attachment or monopolar orientation allows kinetochores of the sister chromatids to attached to the same pole (monopolar). This innovative mechanism enables the cohesion between chromatid arms to counteract the tendency of microtubules to separate homologous chromosomes during metaphase I and ensure that sister centromeres are pulled to the same pole during anaphase I, in contrast to the separation of sister centromeres observed during mitosis anaphase (Fig. 6). The poleward segregation of chromosomes during meiosis I is shown to be triggered by destruction of cohesion along chromatid arms; this occurs due to the cleavage of a meiosis-specific variant of the separase Scc1, known as Rec8 (Buonomo et al., 2000). During this process, between sister chromatids, cohesion in the vicinity of centromeres survives until the onset of the second division.

Mam1 in *Saccharomyces cerevisiae* is the first example of a new identified class of proteins (monopolins) whose role is to ensure that sister kinetochores do not form bipolar attachments during meiosis I, independently from the protection of sister centromere cohesion (Tóth et al., 2000). A homolog protein was found in mouse, MEIKIN that is required for mono-orientation, while in *S. pombe* the homolog is Moa1. Both of them are targeting to kinetochore through CENP-C (Katis et al., 2004) (Galander & Marston, 2020). In Drosophila (Lee et al., 2005)(Kerrebrock et al., 1995) and plants (Chelysheva et al., 2005; Cromer et al., 2019) homologs are not found yet. As mentioned before, mouse and fission yeast use a monopolar dependent mechanism, in comparison to budding yeast that the mechanism is dependent on cohesins (Rec8). The mechanisms are still not fully deciphered but the cohesion complex play an important role. In Arabidopsis, it was found that the disruption in REC8 (meiotic specific) and SCC3 induces to monopolar orientation (Chelysheva et al., 2005). In Arabidopsis involving

REC8/SCC3 and the securins PATRONUS play an important role (Chelysheva et al., 2005; Cromer et al., 2019; Eijpe, Heyting, Gross, & Jessberger, 2000) single mutants of *rec8* and *scc3* present univalent and chromosome fragmentation during metaphase I as well as chromatin bridges at anaphase I, single *spo11-1* shows univalent formation during metaphase I, as well as random segregation in the majority of the cells. When *rec8* or *scc3* were combined with *spo11-1* they showed ten univalents aligning at metaphase I and the sister chromatids are separated at anaphase I (Fig. 7) no more fragmentation or separation of the sister chromatids at anaphase I. Suggesting that SCC3 and REC8 are required for kinetochore orientation (Chelysheva et al., 2005). More efforts have been made to decipher the mechanisms of monopolin orientation.

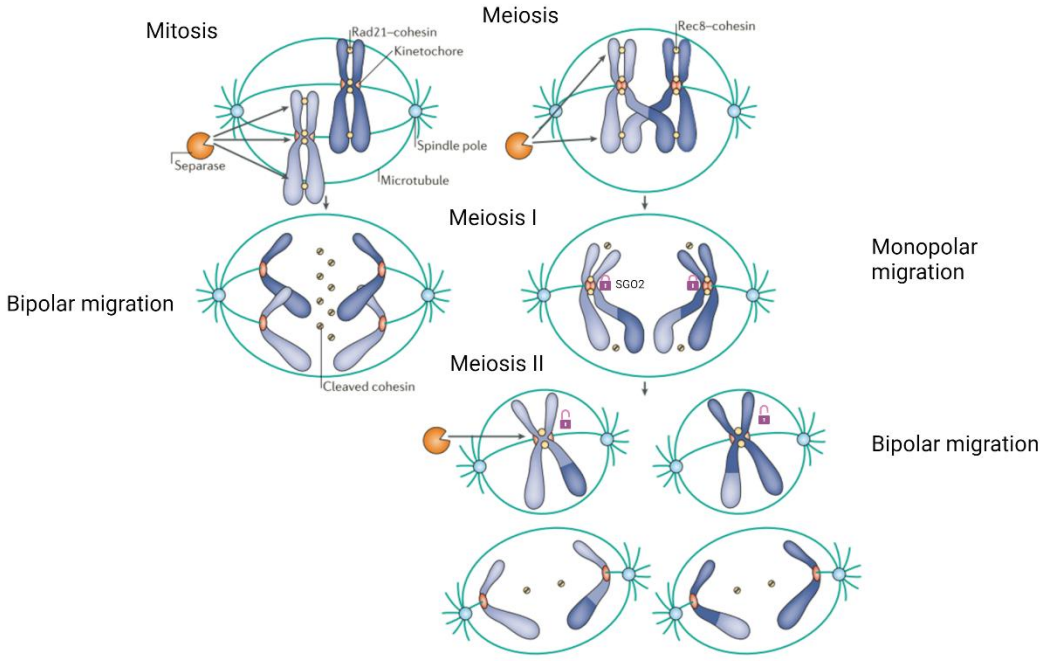

*Figure 6 Kinetochore orientation during mitosis and meiosis. (**Modified** from* (Watanabe, 2012)*) BioRender.com*

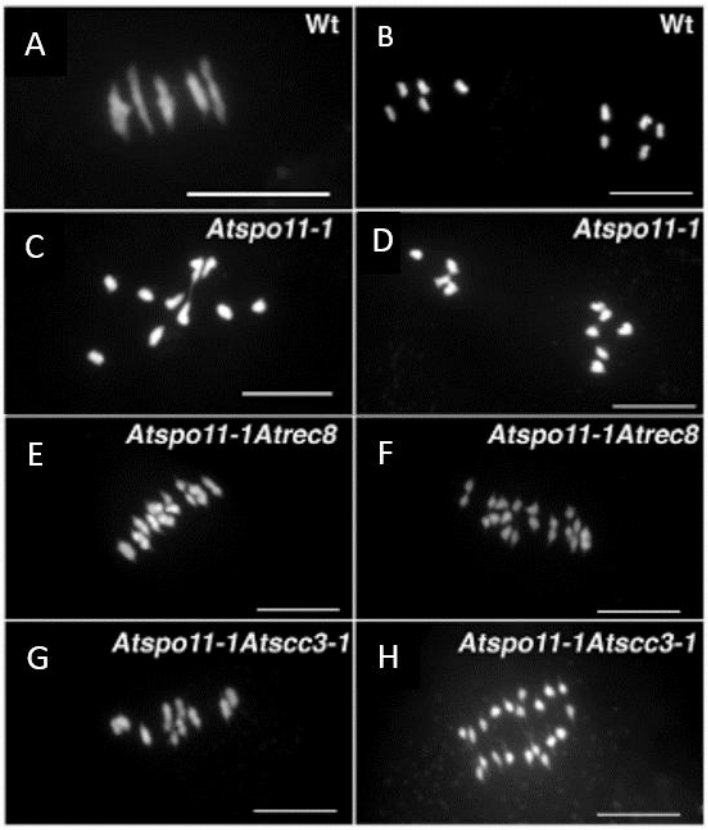

Figure 7 DAPI male meiocytes spreads at metaphase-anaphase transition (left column) and anaphase I (right column). Wild type (A-B), spo11-1 *(C-D)* , spo11-1rec8 *(E-F),* aspo11-1scc3-1 *(G-H). (**Modified** from Chelysheva et al., 2005)*

The Forward screen a mutant background was built in the double mutant *spo11-1 osd1*, and the potential monopolin candidates were distinguished by the fertility recovery. The screen revealed the mutants of the following genes: *Structural Maintenance of Chromosomes 1 and 3 (Smc1, Smc3), Centromere protein C (Cenp-c), Shugoshin 1 and 2 (Sgo1 and Sgo2), Arabidopsis Sumo Protease (Asp2) and Chromosome Transmission Fidelity (Ctf18)*. All the mutants found, with the double mutant *spo11osd1* background showed a significant increase in seed set, suggesting all the mutants were involved in monopolar orientation of kinetochores (Dipesh Singh et al, unpublished).

5.14 Reverse Screen: Candidate Mutants With Monopolar Orientation Defects

The mutants recovered from the Monopolin screen performed mainly by Dr. Dipesh Singh have a modification of the kinetochore/centromere organisation with a potential modified centromere (or its chromatin), therefore, we hypothesized that recombination could also be affected, then we proceed to measured recombination to test this possibility. The chosen mutants with modified kinetochore behavior were also related to cohesion (*sgo2, smc1, smc3),* to centromere identity (*cenpc*), to cohesion loading (*ctf18*) and in to deSUMOylation (*asp2).* Last two with unknown role within meiosis.

5.14.1 Centromere Protein C (CENP-C)

CENP-C is a kinetochore protein, been described previously as the bridge that binds to CENH3 and colocalize with it, in addition to bind to outer kinetochore proteins (MIS12) in order to ensure a proper segregation. (N. Wang & Dawe, 2018).

5.14.2 Structural Maintenance of Chromosomes (SMC1 and SMC3)

To maintain the integrity of the Structural Maintenance of the Chromosome (SMC), the proteins SMC1 and SMC3 part of the cohesin complex is essential. These proteins ensure the cohesion of sister chromatids during meiosis, and their absence can negatively impact fertility.

5.14.3 Shugoshin 2 (SGO2)

Sgo2 plays a crucial role in maintaining cohesion dynamics during meiosis by protecting centromeric cleavage from Rec8 in prophase I. Moreover, Sgo2 regulates kinetochore-microtubule attachment and kinetochore tension. Proper removal of Sgo2 is essential for the correct segregation of sister chromatids during the second meiotic division.

5.14.4 Arabidopsis SUMO Protease (ASP2)

SUMOylation regulates various nuclear processes, including transcription, DNA repair, chromatin remodeling, precursor mRNA splicing and ribosome. Similar to ubiquitination that usually marks target proteins for degradation proteasome-dependent, SUMOylation is in intimate relation with the ubiquitination process. SUMO proteases usually work as priming to thereby inducing ubiquitination and then protein degradation. Both process are highly important in determining protein fate; in humans, deregulation of these processes can lead to trigger cancer processes (Wei & Lin, 2012). When SUMO proteases are conjugated, they form an isopeptide bond between the SUMO-C terminus and a lysine e-amino group within the target protein (Mukhopadhyay & Dasso, 2007).

Interestingly, it has been observed that SUMO proteases are involved in chromosome organization and segregation, although the molecular processes are unknown. In *S.pombe* strains lacking SUMO proteases have high frequencies of chromosome loss and viability problems. Same deleterious phenotypes have been observed in *D. melanogaster (dpias)* and *S. cerevisae (ulp2Δ)* mutants. In mammalian cells SUMO proteases localize in close proximity to kinetochores (Johnson, 2004) and the SENP6 SUMO-protease was found to be required to stabilize CENP-A chromatin throughout the cell cycle (Mitra et al., 2020).

In Arabidopsis, the Arabidopsis SUMO protease 2 (Asp2) together with its partner, Asp1 have been described previously as SUMO PROTEASE RELATED TO FERTILITY1 and 2 (SPF1,2) and were suggested to act redundantly as SUMO proteases important for microgametogenesis, megagametogenesis, and embryo development, were the mutants show varies defects in ovules and pollen formation, and embryo viability, especially in single *spf1-1* and *spf1-1 spf2-*

1 double mutants (L. Liu et al., 2017) (Kong, Luo, Qu, Liu, & Jin, 2017). Asp2 was also recently shown to be an integral part of far-red light singling pathways for hypocotyl growth (Srivastava et al., 2022).

5.14.5 Chromosome Transmission Fidelity 18 (CTF18)

In budding yeast and humans, Chromosome Transmission Fidelity (CTF18) localizes at the replication fork and is crucial for cohesion establishment, it has been suggested to be coupled with fork progression which associates with Replication Factor 2 (Rfc2), Rfc3, Rfc4, and Rfc5 to form the RFCCtf18 complex, that has a loading and unloading activity and plays a role in sister chromatid cohesion. Putative orthologous proteins were found in human, mouse, Arabidopsis, rice, fruit fly worm, and fission yeast. In Arabidopsis, its expression was found at the shoot apical and root meristems in 7-day-old seedlings, corresponding with an anticipated role for CTF18 during cell cycle progression. The loss of function (*ctf18-2* in Nossen-0 accession*)* showed sister chromatid separation in 40,5% of homologous chromosomes, in contrast to wild type (28,1%) in vegetative leaf cells demonstrating that CTF18 contributes to sister chromatid cohesion. During mitosis in *ctf18-2* cohesion was observed to be lost at mid-arm positions but not at centromeres, only when it was introduced to the replisome factor *E2F TARGET GENE 1* (*etg1)* mutant, it was observed additional loss of sister centromere cohesion, leaves and roots development had strong defects, suggesting that DNA repair by homologous recombination is less efficient because of the reduced sister arm cohesion. (Takahashi et al., 2010). In Arabidopsis, during the monopolar screen on gametic cells, it was observed that *ctf18* doesn´t show any defects in fertility*. Ctf18* when is combined to *spo11-1-3,* the double mutant recovers the bipolar orientation and unbalanced segregation, observed in the single *spo11.*

5.15 METHODOLOGY USED TO MEASURE RECOMBINATION

The two more common tools to measure recombination are cytogenetic analysis of meiocytes and segregation assays of heterozygous genetic markers through meiosis. Cytogenetic methods rely on microscopy to analyse meiotic chromosomes with immunodetection methods or by interpretating bivalent and chiasmata morphology, which can be advantageous to use because it could also be correlated to other proteins involved in the process. However, since this method takes long time and can be challenging we used the segregation assays. The segregation assays detect COs by measuring CO-inheritance of the genetic markers. These markers can be single-nucleotide polymorphisms, simple sequence length polymorphisms or transfer DNA (T-DNA) insertions (Nataliya E. Yelina et al., 2013). T-DNA visible markers (GFP, dsRed, etc) expressed in pollen (Francis et al., 2007) and in seeds (Melamed-Bessudo, Yehuda, Stuitje, & Levy, 2005; Nataliya E. Yelina et al., 2013; Ziolkowski et al., 2015a), with seed-specific reporters (NAP) (Stuitje et al., 2003). The T-DNA fluorescent markers in seeds, known as Fluorescent Transgenic Lines (FTLs) expressed in seeds were the tools used in this project for being highly powerful because they are easy to select under the microscope and is not necessary to genotype by DNA extraction, is possible to obtain many data points (until 3000 seeds) per picture from a single recombinant population with accurate measurements. The

location of the selected FTLs are useful to locate recombination in specific intervals of the chromosomes

In this project we measure recombination by measuring the segregation of a pair of fluorescent transgenic lines (FTLs), markers flanking the centromeric regions, around 200Mb apart in both Columbia-0 (CTL3.437.55) and Landsberg (LTL5.43.179). These intervals are closer together than the CEN3 interval (Nataliya E. Yelina et al., 2012) although other intervals in the arms of the chromosomes were also used (Melamed-Bessudo et al., 2005). (Fig. 8).

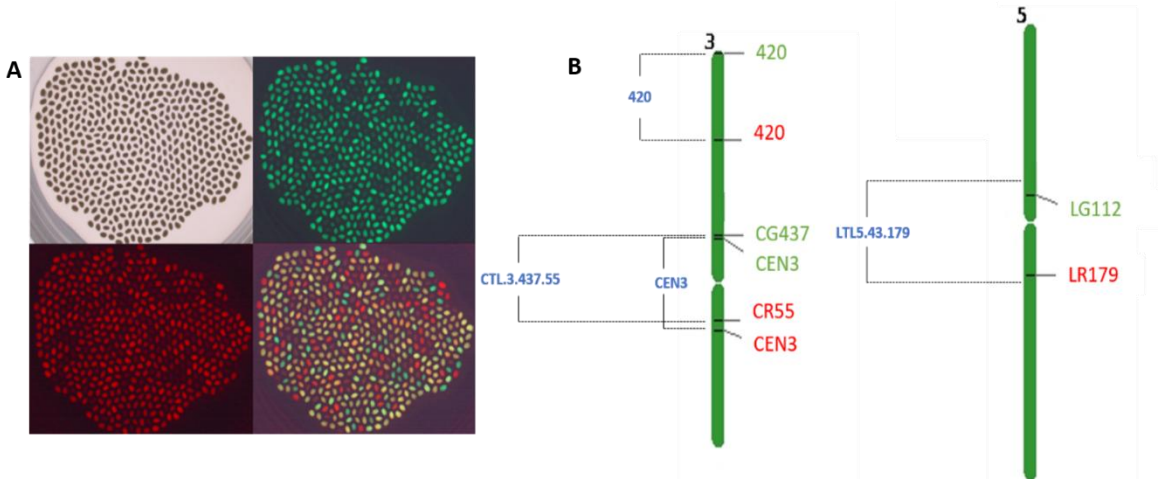

Figure 8 FTLs in seeds with each of the colours and merged. Representation of FTLs location in the chromosomes in chromosomes 3 for Col-0 accessions and in chromosome 5 for Ler accession.

6 MATERIALS AND METHODS

6.1 GENETIC MATERIAL AND GROWTH CONDITIONS

Most of the Arabidopsis plants were grown in a greenhouse under controlled long-day conditions. The double mutant plants used for measuring recombination with Fluorescent Traffic Lines (FTLs) were grown in growth chambers under long-day conditions (16 h day/8 h night, 20 °C), and the seeds were dried and harvested under the same conditions.

The Arabidopsis seeds used in this study were as follows:

Fluorescent traffic lines tested in Col-0: CG531 (CS71084), CR1047 (CS71086), CR909 (CS71202), CG350 (CS71203), CG15 (CS71204).

Fluorescent lines tested in Ler: LG267 (CS71337), LR133 (CS71339), LG274 (CS71341), LG225 (CS71342), LR225 (CS71338), LR358 (CS71448), LG112 (CS71447)

Fluorescent lines used to measure recombination: CG437 (CS71169), CR55 (CS71173) and LG43 (CS71446), LR179 (CS71449).

For the forward genetic screen: *recqA* in Col (GABI_203C07 (N419423)), *recq4B* (N511330), *fancm* Col (ROCO1-/), *recq4* Ler (msh4(S)84), *fancm* Ler (fancm-10 qrt -/-).

For the reverse genetic screen: *asp2* (salk_140824), *asp2* (MP150), *cenpc* (monopolin 221), *ctf18* (*ctf18*-MP193), *ctf18* (salk_043339), *smc1* (MP172), *smc1* (SALK017437/N517437), *smc3* (MP226), *zyp1 (zyp1-1), sgo2* (*sgo2-1* (Zamariola et al., 2013)), *cmt3* (*cmt3-11*. SALK_148381).

For ZMM suppressor: *hei10* (N514624) and the mutant H342 (resulting from the same EMS screen for new anti-CO factors, in which other anti-CO factors like *recq4* were identified).

Before any recombination analysis, all plants were always genotyped by PCR with an annealing temperature of 58 °C (corresponding primers in Table 2).

6.2 FTL SELECTION

FTLs were selected by analysing their segregation and fluorescence intensity under a stereomicroscope (Leica M205 Fluo) with green (GFP) and red filters (N2.1). The seeds used were the most suitable for correlating fluorescence intensity with genotype (more intensity for homozygous, less intensity for heterozygous and no intensity for WT) and the ones showing a Mendelian segregation.

6.3 EMS MUTAGENESIS

The ethylating agent ethyl methanesulfonate (EMS) was used at a final concentration of 0.30% and was neutralized with 1 M sodium thiosulphate ($Na_2S_20_3$) after 17 hours of constant agitation and rinsed with water for 20 min, three times. The seeds were rinsed for two days in water and resuspended in 0.1% agarose before sowing.

6.4 RECOMBINATION ANALYSIS WITH FTLS

To measure recombination, we used fluorescent transgenic lines (FTLs) (420) generated in Col and Ler backgrounds. Seed coats in FTLs express GFP (Chr 3:256,516-GFP) and dsRed (Chr 3:5,361,637-dsRed2) fluorescent protein markers in the cis position. For quantification of the fluorescence of the seeds, two different approaches were used: the Fiji image analysis software, which was used together with a pipeline to analyse the data (Perl and R) and the Cell Profiler software (the output differences are explained in the Results section).
Both approaches detect each seed individually and quantify fluorescence intensity for each seed in all pictures. With Cell Profiler, the output was analysed automatically and only recombination was calculated separately with the formula below; in contrast, the Fiji method was analysed separately using a pipeline that was created to automatically normalize data, plot the frequency of objects with each fluorescent colour, plot the fluorescence intensity and

quantify the number of seeds with only one fluorescent colour, select the number of recombinant seeds, and finally to calculate recombination with the following formula:

$$cM = 100 * (1 - [1 - \frac{2(N_G + N_R)}{N_T}]^{1/2}$$

Where N_G is the number of green-only fluorescent seeds, N_R is the number of red-only fluorescent seeds and N_T is the total number of seeds counted.

Recombination was measured in the F3 segregating populations, coming from crosses with the mutants and FTLs. We preselected F2 seeds by fluorescence to be heterozygous for the markers; sister wild-type plants were used as a control. For each genotype at least three biological replicates (independent plants) were used with at least three technical replicates (three seed different batches), each of them containing a minimum of 400 seeds in the first round of measurements and at least 4,000 in the second round. Differences between genotypes where tested by one-way ANOVA without correcting for multiple comparison

6.4.1 The plate Method

The script in Fiji extracts three different pictures (bright field, red and green) from their different folders and checks that each image is present in the three corresponding folders; it then creates three new folders where the output will be saved after the processing. Pictures taken by the microscope were saved in *.TIFF format and were given specific names without special characters.

A binary mask is generated to highlight and separate each of the seeds, in addition to filtering out smaller or bigger particles that could also be found in the picture. Then, the fluorescence intensity is measured in each colour. The output files per picture are: 1) list of red fluorescence intensity for each seed (*.CSV), 2) list of green fluorescence intensity for each seed (*.CSV) and 3) a list of the regions of interest (ROIs); in this case, the seeds are associated with their location and numbered (*.ZIP).

In the main controller script (Bash), the following scripts were executed one after the other (./Main_Fluor_V4.sh). The first step was to double check that the same number of seeds are present in each of the fluorescence files, and both lists were then merged (Merge_channels_V1.pl), creating a new file (files.lst) that allows creation of a histogram for each colour and a scatter plot combining both colours from the same picture (R); then it normalizes the fluorescence data (norm2class.pl) and uses the same threshold for all the measurements. Finally, it counts the number of only red and only green fluorescence and measures recombination with the formula already described (METRICS2recomb.pl).

6.4.2 The slide Method

This method was developed by Ziolkowski et al., 2015 and modified by Joiselle Fernandes. To take the pictures the seeds were placed in a mate black base (usually used for stereomicroscopes) and flattened by a glass slide to leave all the seeds visible and captured with the stereomicroscope with the mentioned green and red filters. The pictures were saved in a *.JPG format. For analysis, the pictures should be in the same folder together with the following files: 1. SeedsMeta.csv, which takes the name of the picture which needs to be manually written and 2. SeedsScoring11.cpproj, which runs the program that detects and counts seeds and measures fluorescence intensity of each seed. It is important to note that when this CellProfiler file is used, the input has to be carefully selected; the program is then run, the threshold value which needs to be changed in the menu "Classify objects" is manually identified for each colour, and the program is run a second time with the new threshold value. If the plots are needed, they need to be saved separately. Finally, the automatic spreadsheet output with the fluorescence intensity will be placed in the same folder (FilteredSeeds.csv).

The results are manually copied to another file (SeedScoringTemplate.xlsx) where the number of seeds with only one colour, with both colours or with none is automatically calculated, and the total amount of seeds is counted; it also calculates the green+red ratio, the recombination (with the same formula mentioned before) and the ratios of each colour vs. the non-coloured seeds, the total number of seeds and the ratio of the colours themselves. These last ratios are important as a quality control for the segregation of the colours.

The statistical analysis used was Ordinary one-way ANOVA without correcting for multiple comparisons. Both statistical analysis and final plots were made with Prism software.

6.5 GENERATION OF MUTANTS

asp2, ctf18, and *sgo2* mutants were generated in the Ler background with the high-efficiency Crispr/Cas9 system with multiple introns (Grützner et al., 2020, 2021) with two guides in exons from the 5' end and two more in the 3' end of each gene.

6.5.1 Guide RNA design and plasmid construction

All the guide RNAs were designed based on the genome of the Arabidopsis Columbia-0 accession of (public data) and their specificity was confirmed in the genome of the Landsberg accession (Lab resources), using the CRISPR-P 2.0 website with U6 promotor. Two suggested guides were selected at the 3' end and two more at the 5' end without considering the UTRs (Table1, Figure 9). The guides selected were rich in GC content, without repetitions, 19 bp long and with the PAM region in the reverse complementary version. The distances between the guides were around 40–50 bp and, very importantly, the guides did not have restriction sites

for the restriction enzymes used in the plasmid construction process (BbsI and BsaI, in this case); however, the guides should have a BsaI restriction site 4 bp after the complete guide.

Table 1. Sequences of designed guide RNAs for knockout mutants

	asp2 guides		*sgo2* guides		*ctf18* guides	
3‘	A1	CCGTCAAGATGTGAACTCAG	S1	GTATTGAGATTCAGAAACTG	C1	CCTCTTCATCTCCCAAAGCC
	A2	AATCCTTCTATGGGAGCCAT	S2	TCTTGCAGCCAAGTTCATGC	C2	TGCTGCAAAAGAACACTGAT
5‘	A3	TTGGAAACTCCACAATGAGG	S3	GTTTCATGCCTGCTTTCGGA	C3	GCAGTCCCAACTGAAACCGA
	A4	CGTTTGGGAAATGTCTGTAA	S4	ACGAGAAGACAATCAACAAA	C4	TCGTTAAACTTGAAGAGAAG

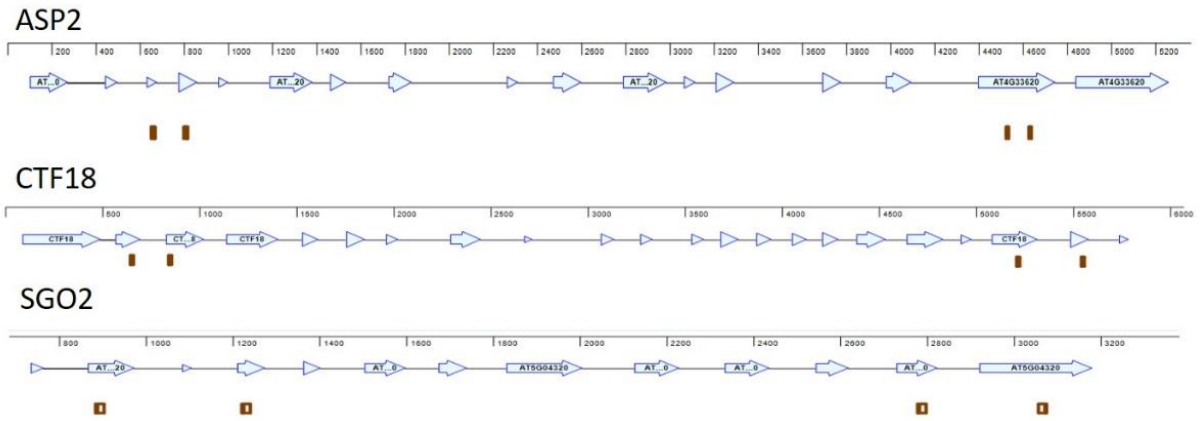

Figure 9. Location of designed guide RNAs for knockout mutants. For each of the asp2, sgo2, and ctf18 genes two guides were designed within the exons at both ends of the genes.

The guides were cloned by CloneAmp into the plCH86966 plasmid with an annealing temperature of 65 °C. Subsequently, a purification step of the guides with PCRquik Qiagen kit and adjustment of the concentration to 150 ng, was done. The final plasmid was constructed as described in the supplementary material of Grützner et al., 2020, were each of the constructs have a specific order (Details of vectors used in Table 2).

In the first reaction, each guide was cloned into level 1 vectors according to their position; then, they were transformed into *Escherichia coli*: in the first position the plasmid pClCH47751(#48002), second pClCH47761(#48003) , third pClCH47772 (#48004), and fourth pClCH47781 (#48005). Each colony selected by carboxiciline resistance was purified with Spin Plasmid kit and Sanger-sequenced (Eurofins night kit) with primers corresponding to plasmid fragments (L142 or L143) to confirm the presence of 1) restriction sites for BpiI, 2) the anchor site of each plasmid (reverse complementary) and 3) the guide.

In the second reaction, all four plasmids – each containing a guide – were subcloned into the final vector. It is necessary to assemble the Cas9 expression cassette (pAGM51323 (90 ng/µl), the binary vector (pAGM4723), Fast-Red expression cassette (pICSL11015), the linker (plCH50927) plus the four guides for each gene. These assembled vectors were transformed into competent cells (TopTen) and selected by kanamycin treatment (white colonies). To confirm the presence of the four guides, their promotors and overhangs, each vector was digested by HindIII or EcoRv (Thermo) and purified by NucleoSpin Plasmid, followed by sequencing as described above (L142 primer). In addition, the complete plasmid was sequenced by Nanopore (ONT) to confirm all their structural components together with the guides' positions; this sequencing confirmed that the plasmids were complete. For sample preparation an amplification-free long-read sequencing library using v14 library prep chemistry was applied, which included linearization of the circular input DNA in a sequence-independent manner by the Plasmidsaururs company (https://www.plasmidsaurus.com/index/).

These final plasmids were transformed into electro-competent Agrobacterium cells (GV3101) and selected for in LB media with gentamycin, kanamycin and rifampicine. The selected colonies were diluted in water and the presence of the final plasmid was confirmed by PCR, using as primers L142 and any of the corresponding guides.

6.5.2 Plant transformation, growth and selection

Transformed bacteria were selected from a preculture in LB media with gentamycin, kanamycin and rifampicine grown overnight and incubated in a new culture for approximately 5 hours, until the optical density had reached 0.5 A. Bacteria were recovered by centrifugation (4000 g for 10 min), resuspended in freshly made 5% sucrose solution with 20 µl of silwett L-77. Around 16 plants of both Columbia and Landsberg accessions were transformed for each batch by dipping young flowerbuds for about 15 seconds. Plants were covered with dark plastic bags overnight.

Transformed seeds (T1) were selected by fluorescence expressed in the seed coat, under a stereomicroscope (Leica M205 Fluo) with red filter (N2.1) and after sowing, with the amplification of Cas9 by PCR (Primers L368+L369, ~870 bp). In addition, a set of primers was used for each gene (Table 2). To confirm the mutation, the PCR products were purified and sequenced (Sanger) both with forward and reverse primers, together with the WT sequence.

6.5.3 Primers used for transformants detection

To detect the presence of mutations in each of the mutants, the activity of all four guides and to detect small and big deletions, two primers amplifying the 3' end were used, a further two primers were used to amplify the 5' end. Using a mix of the primers, we could detect bigger deletions (Table 2).

6.6 RECOMBINATION ANALYSIS IN COL/LER HYBRID BACKGROUND

6.6.1 Hybrid background building

Once the T1 *asp2, sgo2* and *ctf18* plants were positive for Cas9 activity and for the gene editing, their seeds were harvested. Seeds without fluorescence were selected and confirmed in the plant for the editing of the gene, as well as for the absence of Cas9. If the mutation was homozygous we added a backcross step; otherwise, the heterozygous plants for Ler were crossed with *asp2, sgo2* and *ctf18* heterozygous plants in Col-0, the same alleles used for all the previously mentioned recombination measurements. In the next generation, we selected at least four plants with two main genotypes, wild type and homozygous mutants, and grew their progeny, which was the population used to sequence whole genomes and for measuring recombination with genetic markers. Then, 95 wild-type plants and 190 homozygous mutant plants were grown and after confirming their genotypes, the tissue was collected twice and sequenced with the NextSeq 2000 sequencer with 700,000 reads at the Max Planck-Genome-centre Cologne.

Genetic markers were used as primers for the PCR amplification; the design was based on characteristic SNPs that can differentiate Landsberg (Ler) and Wassilewskija (Ws) from Columbia-0 (Col-0), flanking the pericentromeric regions.

For the Col/Ler background in the *zyp1* mutant we used one pair of markers in chromosome 1 (ind1.12909 and ind1.17153), five markers in chromosome 2 (ind2.01940, K2-1 MCW2.3, ind2.05645, ind2.06168, ind2.06392) and another pair of markers in chromosome 3 (ind3.10747 and ind3.15966), for a population of around 180 plants.

For the *smc1* mutant in the Col/Ws background, we used one pair of markers in chromosome 1 (MSAT1.4 and ind1.17153), four markers for chromosome 2 (ind2.02286, K2-1 MCW2.3, K2-2 MCW2.1, ind2.05544, ind2.06168) and one pair of markers in chromosome 5 (ind5.10447 and ind5.14566) for a population of around 170 plants.

To calculate the recombination rate, we divided the number of recombinants by the total number of plants multiplied by 2, as Arabidopsis is a diploid plant; the number of plants were adjusted to each population accordingly.

Results were analysed with Fisher Test with Prism Software.

6.6.2 *ctf18* and *asp2* whole genome analysis in hybrid background

The data from the sequencing was analysed by Dr. Qichao Lian from our Lab, following the same method as used in Capilla-Pérez et al., 2021. The sequences used as references to compare recombination data were the wild type data from the *ctf18* sister plant; however, to validate the control sequence. Also previous data was used generated by Serra et al., 2018 and by Rowan et al., 2019.

6.6.3 Shore mapping

After selecting for the plants with recovered fertility, 51 plants were sequenced with Ilumina HiSeq3000 with 50,000,000 reads with 85% coverage.

Results were analysed with the CLC Workbench, where the input was compared to the reference public genome of Arabidopsis, annotated and mapped to the reference. Variant detection was used with a coverage of 500 and frequency of 50.

6.7 CYTOLOGICAL TECHNIQUES

Spreads were performed as described in Cromer et al., 2019, except that the buds were digested for 1 h instead of 3 h.

Alexander staining (Alexander, 1969) was done in one or two plants (depending on the genotype), using 3 different stamens from 3 different buds.

7 RESULTS

7.1 TOOLS TO MEASURE RECOMBINATION

7.1.1 Conditions and selection of Fluorescent Traffic Lines (FTLs)

An important part of the project relies on the Fluorescent Traffic Lines (FTLs) which are fluorescent markers that are useful to measure recombination, involving two different fluorescent markers, green (GFP) and red (dsRed) to spot a chromosome interval. The collection of the T-DNA lines are located in specific sites of the chromosomes and can be expressed either in pollen *LAT52* or in seeds *NAP*, depending on the promoter (Wu, Rossidivito, Hu, Berlyand, & Poethig, 2015; N E Yelina et al., 2015; Ziolkowski et al., 2015b) (Melamed-Bessudo et al., 2005). Selected ones for this project are spanning the pericentromeres and are expressed specifically on seeds (Fig.10A, 1B) which were captured with a microscope with fluorescent filters and the pictures were processed with image analysis. The selection of the proper pair is of major importance. The FTLs were selected based on the fluorescence intensity, the capacity to link it to the number of present allele copies and their Mendelian segregation.

The fluorescence intensity can vary depending on the FTLs pairs and most of the times linking their fluorescence with their genotype is possible: the most intense fluorescence for the homozygous state, lesser fluorescence for the heterozygous state and no fluorescence for the wild type. Relying on this principle, the FTL segregation is possible to observe by plotting fluorescence intensity of their offspring like depicted in Fig. 10 D. Because seeds are diploid, the ideal outcome is nine populations reflecting all the possible allele combinations but as observed previously by Ziolkowski et al., 2015, having at least four populations that define the fluorescent seeds from the non-fluorescent ones is enough to measure recombination.

As observed in Fig. 10 A, recombination would separate the FTLs in the spanning regions, the recombined alleles are transmitted into their offspring and we would detect them as either red or green heterozygous seeds which would be embedded in the four populations defined by the histogram (Fig. 10D).

To accurately measure recombination, we carefully selected the most suitable FTL pair. We analysed their segregation by plotting fluorescence intensity and were able to identify those closest to the expected 3:1 ratio per colour. We then identified nine distinct populations to prevent any overestimation or underestimation of categories during subsequent recombination analysis. We used four marker combinations in Columbia-0 (Col-0) accession and six in Ler (Table 2), to test the segregation. We took pictures of around 200 seeds per genotype (with a defined FTL pair), analysed them, measured fluorescence and counted the number of seeds with the different possible genotype combinations and plot the fluorescence intensity (generated by heterozygous parental plants). Figure 11-A illustrates the expected

outcome if the plant would follow 3:1 recombination: nine different populations. This plot has the fluorescence intensity as the axes genotypes distinguished by colours, and the size of circles representing the corresponding seed proportion. Therefore, the ideal recombination would present the majority of seeds as double heterozygous, indicated by the black circle. There should be a symmetrical and lesser amount of seeds homozygous for one colour and heterozygous for the other (blue circles). Additionally, fewer seeds, in a mirror-symmetrical manner, should be homozygous for one colour and wild type for the other (parental genotype) (pink circles). Finally, the smallest quantity of seeds should have the same symmetry, with wild type and homozygous for both colours (purple circles). In this context, asymmetry refers to the preference of one allele over the other. This preference could be due to poor transmission or lethality of a certain genotype. Such a result would have an impact on recombination results.

The lines that were showing closest to Mendelian segregation (Fig. 11-B-F) were the following intervals in Col-0 accession: in chromosome 2 CTL2.531.1047 (CG531 X CR1047), chromosome 3 CTL3.437.55 (CG437 X CR55) and chromosome 4 CTL4.350.909 (CG350 X CR909) and in Ler, the following intervals: in chromosome 1 LTL1.274.225 (LG274 X LR225) and chromosome 5 LTL5.43.179 (LG43 X LR179). Notably, these lines are in *trans* position because they were F1 of the crosses between the colours, however, to be able to detect recombination, FTLs in parental seeds need to be positioned in *cis* which was the case for the rest of the analysis. The *cis* position allows to account for the recombination happening only in the same chromosome

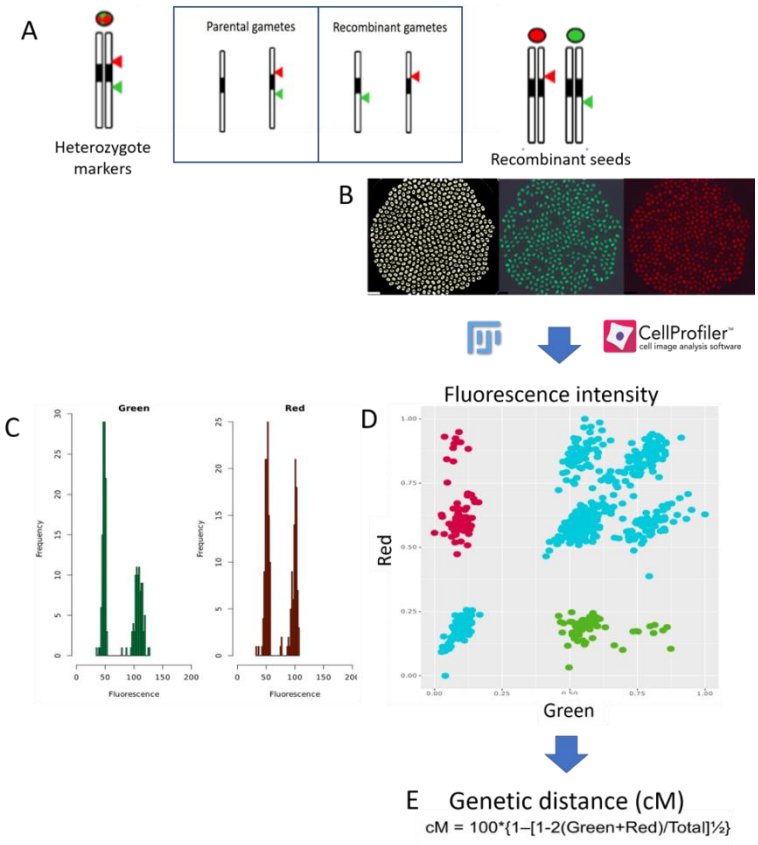

Figure10. Recombination measurements with FTLs. A) FTLs in heterozygous manner in parental gametes and separated by recombination in the recombinant offspring. B) Pictures of FTLs, visible in the seeds (NAP promoter); the correct flattening of seeds was necessary to observe the different fluorescence intensity of each seed. C) Histograms in each colour to confirm at least two populations: non-fluorescent and fluorescent seeds. D) Fluorescence intensity plot of both green and red colours. Green and red dots represent the individuals to be used for recombination measurements, blue dots represent the individuals that are not considered for recombination. E) Genetic distance formula.

Table 2. FTLs tested for mendelian segregation

Accession	Chromosome	Markers	Interval name
Col	2	CG531 X CR1047	CTL2.531.1047
	3	CG437 X CR55	CTL3.437.55
	4	CG350 X CR909	CTL4.350.909
	4	CG15 X CR909	CTL4.15.909
Ler	1	LG267 X LR133	LTL1.267.133
	1	LG274 X LR225	LTL1.274.225
	1	LG225 X LR225	LTL1.225.225
	5	LG43 X LR179	LTL5.43.179
	5	LG43 X LR358	LTL5.43.358
	5	LG112 X LR358	LTL5.112.358

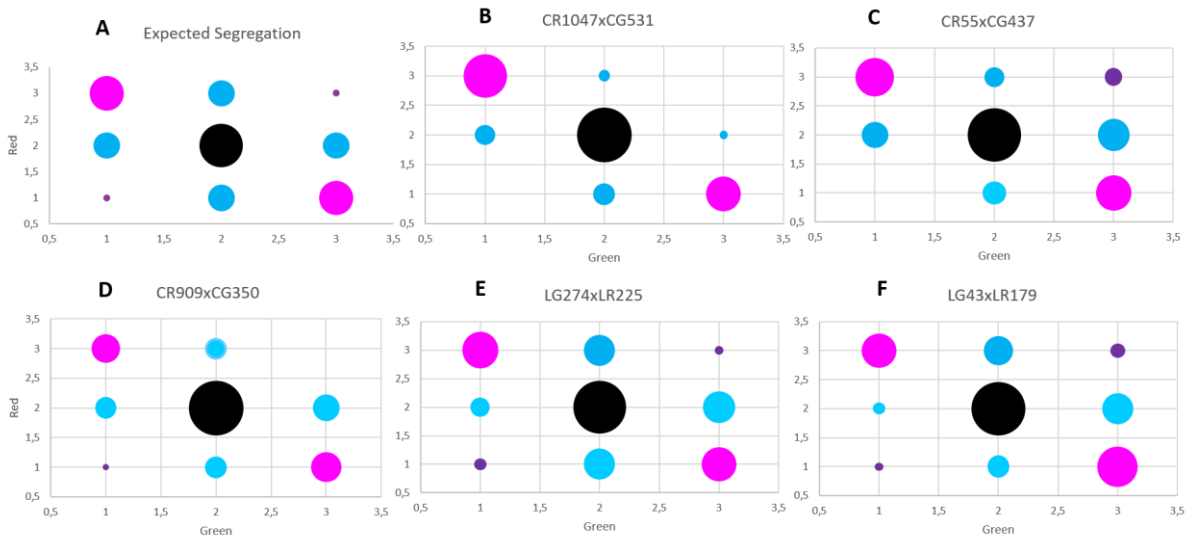

*Figure 11. **A**. Schematic representation of categories and its respective size population for the expected segregation of FTLs. Black-Heterozygotes for both colours, Blue- Homozygotes for one colour, heterozygote for the other, Pink- parental genotype, Purple-double crossover. Segregation of Markers in Col-0 **B**. CTL2.531.1047 line C. CTL3.437.55 D. CTL4.350.909 and in Ler E. LTL1.274.225 and F. LTL5.43.179.*

Additionally, it was observed that the fluorescence intensity can vary due to 1) Transgene expression is likely due to the chromosome position (e. g. 420 a distal line, shows more intensity) and by number of insertion sites in accordance to Wu et al., 2015. 2) plant growth conditions and 3) seed drying conditions; the last two were challenging to detect however, we found that a constant temperature of 20°C with a cycle of 16h days/8h night from the growth chambers and to leave to dry the seeds in the same conditions (without changing the plants to a drying area) were the most suitable conditions for the plants and the seeds. To avoid a big loss of seeds between the drying and harvesting processes, we carefully threaded the plants to their sticks while still young and directly harvested the dried seeds without needing the whole plant to dry.

7.1.2 Recombination measurement methods

To measure recombination with the FTLs we used two different approaches, the first one, the Slide Method works by placing the seeds in a base, flattening them with a slide and analysed with the program CellProfiler already settled and published (Ziolkowski et al., 2015b) but that

was not working properly on our hands at first, that is why a second method was developed the second one, the Plate method, a method that places the seeds in an agar plate and analyse the seeds with Fiji (ImageJ) and a program in Perl, R and Bash, which also helped us to automatize the analysis and to measure recombination more efficiently.

It was necessary to find the best set-up for taking pictures for each of the methods. For both methods, it involved to have completely clean seeds (without dirt, dry petals, leaves or stems) and to have a flat base where all the seeds can be evenly separated (Fig. 10-B). For the Slide method, a mate black background to flat the seeds with a glass slide was enough; for the Plate method, we took the pictures placing the seeds on small plates with Agar and left them overnight before taking pictures, leaving them to soak, which allows the seed mucilage formation which separates the seeds to a certain extent (Fig. 10 B).

Both methods are powerful tools to measure recombination but have differences in terms of their efficiency and reliability (Table 2). With the Plate method, it needs to build a set-up at least 24 hours in advance for the seeds to be available, these seeds will be no longer useful for more experiments (because they will be exposed to an important amount of water), unless they are sawn right after; while with the Slide setup is to flatten dry seeds with a glass slide, therefore the seeds could be used later. The number of seeds used in each picture is slightly reduced (100-300) in the Plate Method, in comparison to the Slide method, where we can take 10 times more seeds at once; however, the time that the analysis takes per batch (around 10 pictures) is faster with the Second method (30 min) rather than with the second one (5 hours). The disadvantage of the Plate method is that the threshold used for every picture is the same, therefore the number of colour seeds can be under or overestimated if the fluorescence of the seeds is not intense enough. This was a problem with the pericentromeric FTLs but not for the telomeric ones (T420) (Fig. 11 and Fig. 14 from *fancc* section) used for measuring recombination of the *fancc, fance* and *fancf* mutants, recognized to be interacting in the Fanconi Complex (FA), published in 2023 (Singh et al., 2023) (discussed at the end of this chapter).

To ensure accurate recombination measurements and maximize the number of individuals with reliable results, the most frequently utilized method was the Slide Method.

Table 3. Comparison of methods to measure recombination

Method	Seed treatment	Number of seeds per batch	Time analysis per batch	Specific constraints	Advantages	Disadvantages
Plate	Agar 0.3% (at least 3 days in advance)	100-300	30min	-Picture labelling - Homogenous threshold	Speed	-Seed destruction Thresholding might sub-represent coloured seeds -Seed maintenance in the greenhouse
Slide	Dry	1000-3000	5hrs	-Specific threshold for each picture	More accurate number of coloured and non-coloured seeds	-Speed -Seed maintenance in the greenhouse

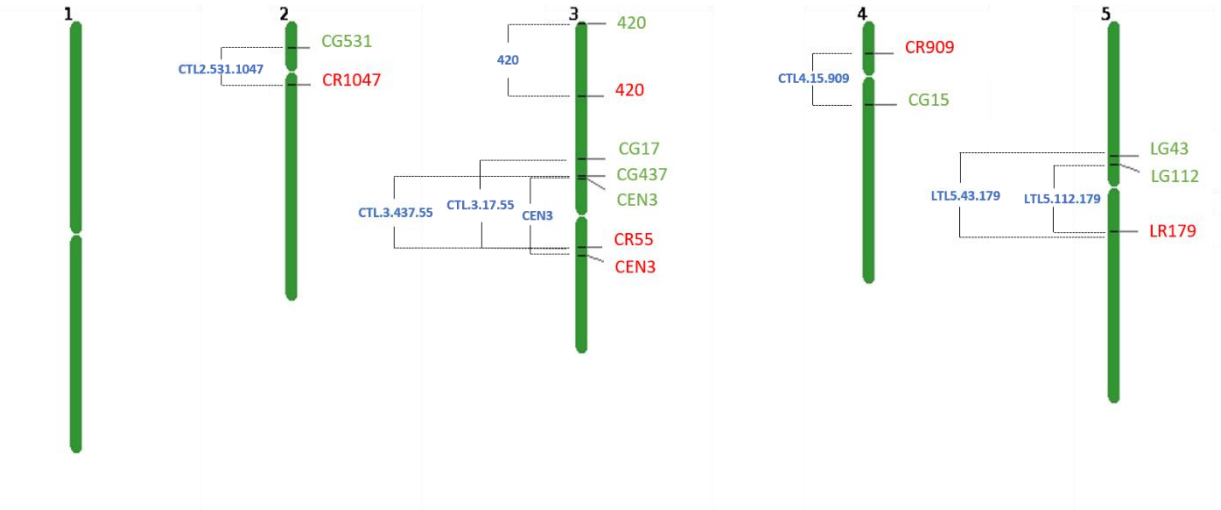

Figure12. Representation of location of FTLs used, in chromosomes 2, 3 and 4 in Coulmbia and in chromosome 5 in Ler. In addition, the markers used as reference: Telomeric 420 and Centromeric CEN3.

7.2 NOVEL CENTROMERIC-SPECIFIC ANTI-CO FACTORS

Historically, genetic screens have been the principal tool for finding new factors in charge of meiotic processes. Forward genetic screens have been performed before to identify important genes such as the anti-CO factors FANCM (Crismani et al., 2012), RECQ4A and RECQ4B (Séguéla-Arnaud et al., 2015) and FIGL1 (Girard et al., 2015). Specifically, we set up the bases for a Forward screen directed to find new meiotic factors that modify the pericentromeres regions, developed in a *recq4* background with the intention to amplify the effect of the anti-CO factor found.

Further, another forward genetic screen was performed previously to find new factors involved in the Monopolar orientation of kinetochores during segregation (Not published). The candidate genes found with modified kinetochore dynamics were used to develop a Reverse screen to find new pericentromeric anti-CO factors, by measuring recombination with the FTLs. Three important genes were found to be importantly involved in this process: *ctf18, asp2 and sgo2.*

Finally, other novel analysis was performed in a *hei10 background* that was inconclusive and another one in *msh-4* background to find more general anti-CO factors, where three genes were identified to be involved in limiting CO by a protein complex: FANCC, FANCE and FANCF.

7.2.1 Forward genetic screen

For this screen a level of complexity is added as the screen is built in a mutant *reqc4* or *fancm* background because these mutants have been shown to increase recombination along the *Arabidopsis* genome until 4.1 fold times in the arms of the chromosomes; however, only 1.1 fold in the pericentromeric regions (Serra et al., 2018a); therefore with this mutant background we can amplify the effect of the CO factor limiting at pericentromeres and increase the sensitivity of the screen.

To further investigate the suppression of crossover formation in pericentromeric regions, a forward genetic screen was set up using seeds treated with ethyl methanesulfonate (EMS) and self-fertilized plants with *recq4ab* or *fancm* and the FTLs background. The goal was to identify new genes related to the suppression of CO formation in pericentromeric regions by measuring increased recombination in the offspring. The screen overview (Fig.13) involves building the anti-CO with the FTLs background, applying EMS, sowing the seeds, and measuring recombination in the offspring to identify plants with increased recombination for further study. While the final output was not achieved, valuable knowledge was gained in the process, and further details will be described in the following sections.

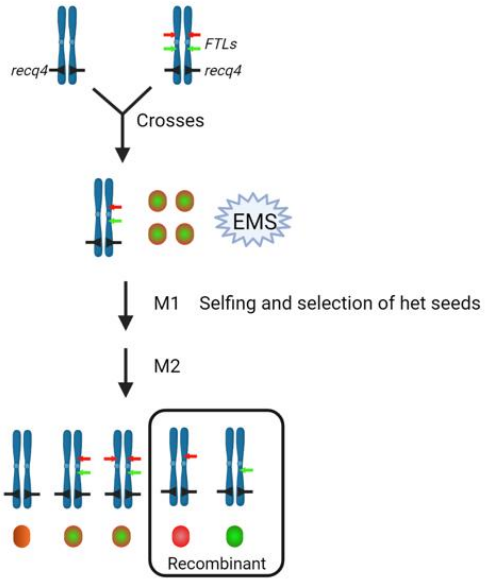

Figure13 Forward screen set up with mutant and FTL background

7.2.1.1 Skewed segregation in recq4ab mutants, in Col-0 background

During the construction of the mutant background, in Col-0 accession we observed that the segregation specifically of the mutant *recq4b* when combined with the FTLs was not Mendelian. We observed that after selecting homozygous seeds for the colours (under the microscope) it was not possible to recover the expected quarter of quadruple homozygous in the *recq4b* background in both intervals CTL3.437.55 and CTL4.15.909. Interestingly, we observed the same pattern with the *fancm* mutation where is not possible to recover triple homozygous in the same intervals (Table 3), suggesting that the presence of FTLs affects the segregation of both *recq4ab* and *fancm* and when we pre-selected homozygous seeds for the colours, we were counterselecting for *recq4b* mutant. The reason for this skewed segregation is not clear but since this problem was found at different times independently by different members of the lab, it is suggesting that probably there is an additional T-DNA insertion not detected in this FTLs that is adding a chromosome rearrangement, or probably the chromosome rearrangement is even related to an inversion in the *recq4ab* mutants located previously (Serra et al., 2018a). Since the FTLs recombination measurements are relying only on the segregation of the genes, this skewed segregation is a source of artefact for the screen, therefore we decided not to use the markers in Col-0 background in our screen; instead, we decided to test the segregation of *recq4, fancm* and FTLs (chromosome 5) in Landsberg background; notably, Ler accession lacks Recq4b gene, simplifying the segregation analysis.

In Landsberg accession, we observed normal segregation for the *recq4* and the FTLs (Table 5) and when we preselect FTLs homozygous under the microscope, we recover the expected quarter of homozygous and wild-type, and half of heterozygous for *recq4* (Table 6); however,

for *fancm* we recovered a smaller population (only 13, in total) (Table 6). Is still unclear the reason for the small amount of recovered *fancm* mutants, but the *recq4* line was enough to apply EMS mutagen for the screen.

Table 4. Skewed segregation in Col-0, after preselecting FTLs double homozygous

	CTL3.437.55		CTL4.15.909	
	rec4a	*recq4b*	*rec4a*	*recq4b*
Homo	13	2	19	2
Het	16	17	19	17
WT	13	18	8	23
Total	42	37	46	42

Table 5. Normal segregation of recq4 and LTL5.43.179 in Ler

	recq4	LG43	LR179
Homozygous	47	54	47
Heterozygous	84	79	73
WT	37	40	51
Total	168	173	171
Expected			
Homozygous	42	43,25	42,75
Heterozygous	84	86,5	85,5
WT	42	43,25	42,75

Table 6. Segregation of reqc4 and fancm in Ler after pre-selecting LTL5.43.179 double homozygous

	recq4	*fancm*
Homozygous	10	3
Heterozygous	16	4
WT	9	6
Total	35	13

7.2.1.2 EMS mutagenesis in Landsberg background

We applied ethyl methyl sulfonate (EMS) agent for mutagenesis to F2 seeds, crosses from LTL5.43.179 and *recq4* in Ler background, however, the fluorescence of these seeds was not intense because they were under extreme conditions in the greenhouse, so it was difficult to preselect for the colours.

We divided the plants into two different batches. In the first batch, we used plants coming from three different crosses with two different EMS concentrations: 0,3% and 0,4% to ensure we would have enough mutant seeds. Unfortunately, these seeds were subjected to unexpected extremely warm conditions in the greenhouse and out of 576 seeds sown, only 359 germinated; several of these plants were showing the characteristic white pattern in the leaves confirming the success of the EMS exposition with both tested concentrations but had notably less fertility. All these plants were genotyped and confirmed for the *recq4* background.

Since the fertility of the first batch was impaired, a second batch of EMS mutagenesis was performed. The background of the second batch was *recq4* and LTL5.112.179 (Fig. 12). We added EMS agent to 1490 seeds with 0,3% concentration. The plants were growing in expected conditions, they also showed the white characteristic pattern for a successful mutagenesis and had the *recq4* background.

This Forward screen had to be put aside because of time constrains of the PhD program; however, the necessary material was generated, properly collected and stored to use it in the near future which will hopefully lead to the discovery of new anti-CO factors specific for the pericentromeres regions.

7.3 REVERSE SCREEN

7.3.1 Increased recombination in pericentromeric regions

One of the most intriguing processes during meiosis is the monopolar orientation of segregation in the first round of division where the homologous chromosomes migrate to the same pole, in contrast to the second round of division (and to mitosis) where the sister chromatids are segregating to different poles of the cell. This phenomenon is called monopolar orientation and is conserved among species; however, the mechanism of how this process is working is still unclear. In comparison to *Saccharomyces cerevisae* where the Monopolin protein complex is essential to control the monopolar orientation (Tóth et al., 2000), other species like *S. pombe* (Katis et al., 2004), Drosophila (Lee et al., 2005)(Kerrebrock et al., 1995), mammals (Watanabe, 2004) and plants (Chelysheva et al., 2005; Cromer et al., 2019) are lacking this protein complex. The mechanism is still not fully deciphered butn it is clear that the cohesion complex play an important role, involving cohesin REC8 (meiotic specific), SMC1 and SMC3 and the centromeric cohesion protector SGO1/SGO2/MEI-S332. Specifically, in Arabidopsis involving REC8/SCC3 and the securins PATRONUS play an important role. REC8 and SCC3 are essential for monopolar orientation of kinetochores. They were possible to be detected when combined to *spo11-1* and showed a bipolar orientation instead of a monopolar, like in mitosis (Chelysheva et al., 2005).

SGO1 and SGO2 are essential proteins to ensure the monorientation during meiosis I in *S. cerevisiae, S. pombe,* mouse and humans, a similar protein is substituting its function (MEI-S332) (Watanabe, 2004). So, they were both introduced to a *spo11-1* mutant and both *sgo1* and *sgo2* had defects in monopolar orientation during segregation and also had a reduced seed set; however, *sgo1spo11-1* had milder defects in comparison to *sgo2spo11-1,* which showed to have a stronger defect in monopolar orientation.

With the same principle, using a forward genetic screen in a *spo11-1 -/- osd1 +/-* background, plants that recovered fertility were selected to be mapped. Several interesting candidates were found, some cohesion subunits: *scc3, smc1* and *smc3,* cohesion protectors: *sgo1* and *sgo2,* a cohesion loader: *ctf18*, a kinetochore protein: *cenpc* and a sumo protease: *asp2*. An important feature of these mutants is that they are essential genes and their null alleles can be completely sterile like *cenpc, scc3, smc1* and *smc3*; however, these alleles were leaky and further analysis of their progeny was possible.

These mutants thus have some kind of modification of the kinetochore/centromere organisation and we wondered if the recombination in pericentromeric regions could be also affected. To test if pericentromeric recombination is impacted in mutants with altered kinetochore dynamics, we introduced the FTL lines to the mutants: *smc3, sgo2, ctf18, cenpc* and *asp2* to measure recombination in their F2 progeny and identify the mutants with increased recombination in pericentromeric regions. *Smc1* was analysed by PCR genetic markers in hybrid (Columbia-0 / Wassilewskija) context (Fig.14. Table 7).

Zyp1 is a transverse filament protein essential for the formation of the Synaptonemal Complex (SC) during zygotene, to stablish synapsis. z*yp1* mutation in Arabidopsis has shown to overall slightly affect recombination (chiasma formation) (Higgins et al., 2005). In budding yeast *zyp1* has shown to increase recombination in pericentromeric regions, suggesting that Zyp1 have an important role in CO formation in pericentromeric regions (Vincenten et al., 2015); therefore, it was included in the study to test if in Arabidopsis had a similar role. The *zyp1* mutant is not coming from the Monopolin screen and it was evaluated with PCR genetic markers (Fig.14. Table 7).

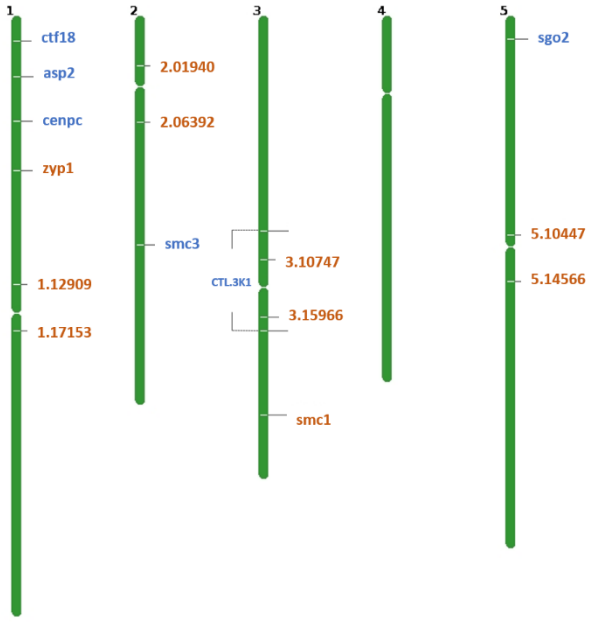

Figure14. Mutants with modified kinetochore/centromere behaviour. In orange are the genes measured with PCR genetic markers. In blue the genes measured with FTLs CTL.3.437.55 interval.

Table 7. Candidate genes to measure recombination in pericentromeric regions

Gene	Gene ID	Role	Nature of mutation
Ctf18	AT1G04730	Cohesion loader	Null
Cenpc	AT1G15660	Centromeric protein	Point
Smc1	AT3G54670	Sister chromatid cohesion	Point
Smc3	AT2G27170		Point
Sgo2	AT5G04320	Protection of centromeric chromosome cohesion	Null
Asp2 MP	AT1G09730	SUMOylation protein	Point
asp2-2 TDNA			Null
Zyp1	AT1G22260	ZMM SC protein	Null

We conducted a study using PCR genetic markers to evaluate recombination in pericentromeric regions of various chromosomes in hybrid mutants *smc1+/-* (Col-0/Ws) and *zyp1 -/-* (Col-0/Ler) (Fig. 14). Our findings indicate that SMC1 plays a role in promoting CO in

pericentromeres, as the mutant *smc1* showed 1,94-fold decreased recombination in chromosome 1, almost significant (P=0,0537). In chromosome 2, significant decrease of 2,3-fold (P=0,0242) and 1,5-fold in chromosome 5, respectively. Suggesting *smc1* having a role in CO promotion in centromeric regions. We are not ruling out the possibility of SMC1 having a role in the chromosome arms as well.

Similarly, in the mutant *zyp1* we observed a significant decreased recombination by 2,2-fold in chromosome 1 (P=0,0121), 3,5-fold decreased in chromosome 2 (P=0,0012) and non-significant 1,48-fold in chromosome 3 (P=0,276)(Fig. 15), suggesting ZYP1 has a role promoting CO as well. In this case it has been confirmed by sequencing (Capilla-Pérez et al., 2021) that ZYP1 has an effect specifically in the pericentromeric regions as they observed that pericentromeres had slightly less recombination than the arms in every chromosome. Suggesting that ZYP1 has an effect favouring the CO formation in the pericentromeric regions.

Table 8 Frequency of recombination in smc1 and zyp1 mutants

		Number of recombinants	Total plants	cM	Number of recombinants	Total plants	cM	Number of recombinants	Total plants	cM
smc1	Chromosome	1			2			5		
WT-col/ws		25	169	7,4	23	165	7	18	153	5,9
smc1-col/ws		12	158	3,8	9	151	3	12	166	3,6
zyp1	Chromosome	1			2			3		
WT-col/ler		28	169	8,3	24	173	6,9	20	181	5,5
zyp1-col/ler		13	173	3,8	7	175	2	13	174	3,7

Independently, we analysed the recombination of mutants from the Monopolin screen using the FTLs through image analysis in two biological replicates (two plants) and at least three technical replicates (different set of seeds from the same plant). The results showed that the recombination of *cenpc* (8.9cM ±1.6) and *smc3* (10.55cM ±1.1) did not significantly differ from the wild-type (11.1 cM ±1.6), suggesting that these mutants are not affected in pericentromeric recombination. However, we found significantly higher recombination in

ctf18 (14.6 cM ±2.4), *sgo2* (15.9cM ± 1.4), and a*sp2*TDNA (19.1cM ± 3) compared to the wild-type (Fig. 16). Suggesting that CTF18, SGO2 and ASP2 have a role in crossover control.

To confirm the recombination measurements done by fluorescence, we selected the three mutants with higher recombination. Since the FTLs, under the microscope and image analysis, tend to be difficult to distinguish between homozygous and heterozygous, we decided to confirm with a highly reliable method: PCR amplification of the transgenes, using as primers the same FTLs markers, in around 170 plants. We confirmed higher recombination for *sgo2-1* (14.4 cM ±2), *ctf18* (12.9cM ± 2.8) and the null mutation of *asp2* (16.1cM ± 2.7), in comparison to WT (9.3cM ± 2.3) (Fig. 16), suggesting that these three genes are implicated in limiting CO formation and it is observed in pericentromeric regions.

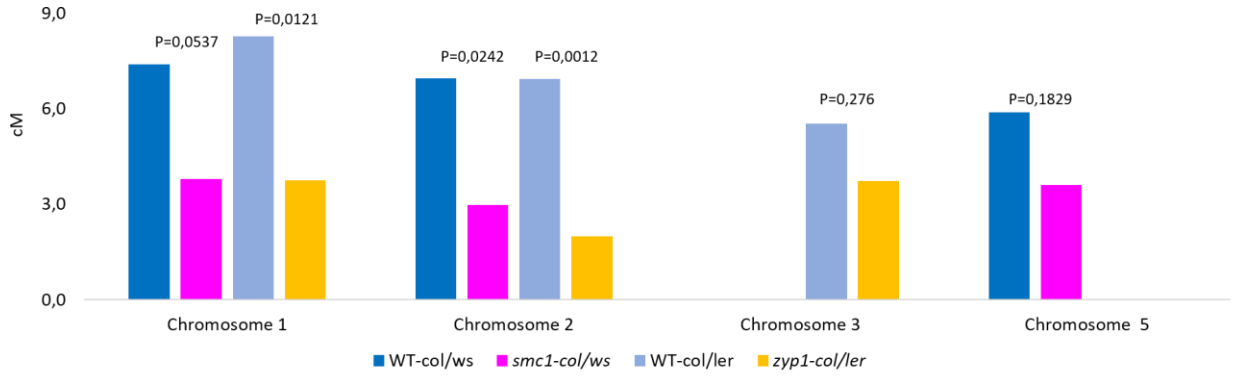

Figure15. Recombination frequency in zyp1 and smc1 mutants in hybrid backgrounds. Fisher Test

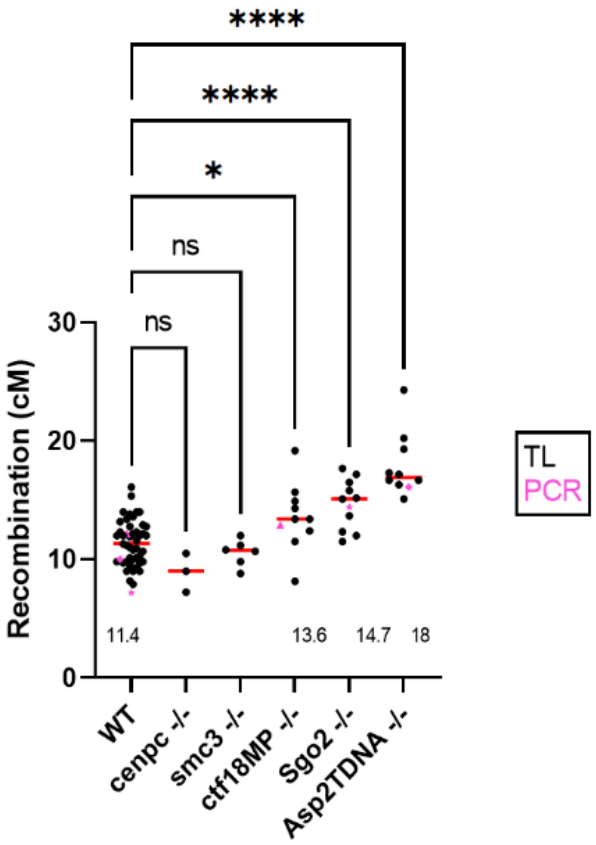

Figure 16 Recombination measurements in mutants with modified behaviour at centromere and kinetochore with TL set up (black points) and confirmed by PCR (pink shapes), showing the highest recombination in ctf18, sgo2 and asp2. Ordinary one-way ANOVA test.

7.3.2 Genetic interactions within genes with higher recombination

To understand if these genes with higher recombination are acting in the same pathway to regulate CO formation in pericentromeres, we crossed the mutants with higher recombination *ctf18, sgo2* and *asp2,* between each other. We also incorporated the *cmt3* mutant, a chromodomain cytosine methyltransferase that has been previously demonstrated to exhibit increased recombination in pericentromeric areas (Underwood et al., 2018). In total, we had six different combinations of double mutants: *ctf18cmt3, cmt3sgo2, ct18sgo2, asp2sgo2, asp2cmt3* and *asp2ctf18.*

After doing the needed crosses, we preselected heterozygous F1 seeds for FTLs under the microscope, the plants were genotyped and we kept the F2 seeds coming from segregant genotypes: Wild type, homozygous for single mutants for each of the genes and homozygous for double mutants. These seeds were carefully harvested immediately after the seeds turned brown, as described before in the Conditions and Selection of Fluorescent Lines (FTLs) Section. We observed that this way, the fluorescence of the seeds was more consistent throughout the different individuals, therefore the recombination measurements as well. Different to the recombination measurements done in Fig. 17-A where we used the Plate Method, for the

double mutants we used the program CellProfiler to measure recombination with a larger amount of dry seeds, described before as the Slide Method.

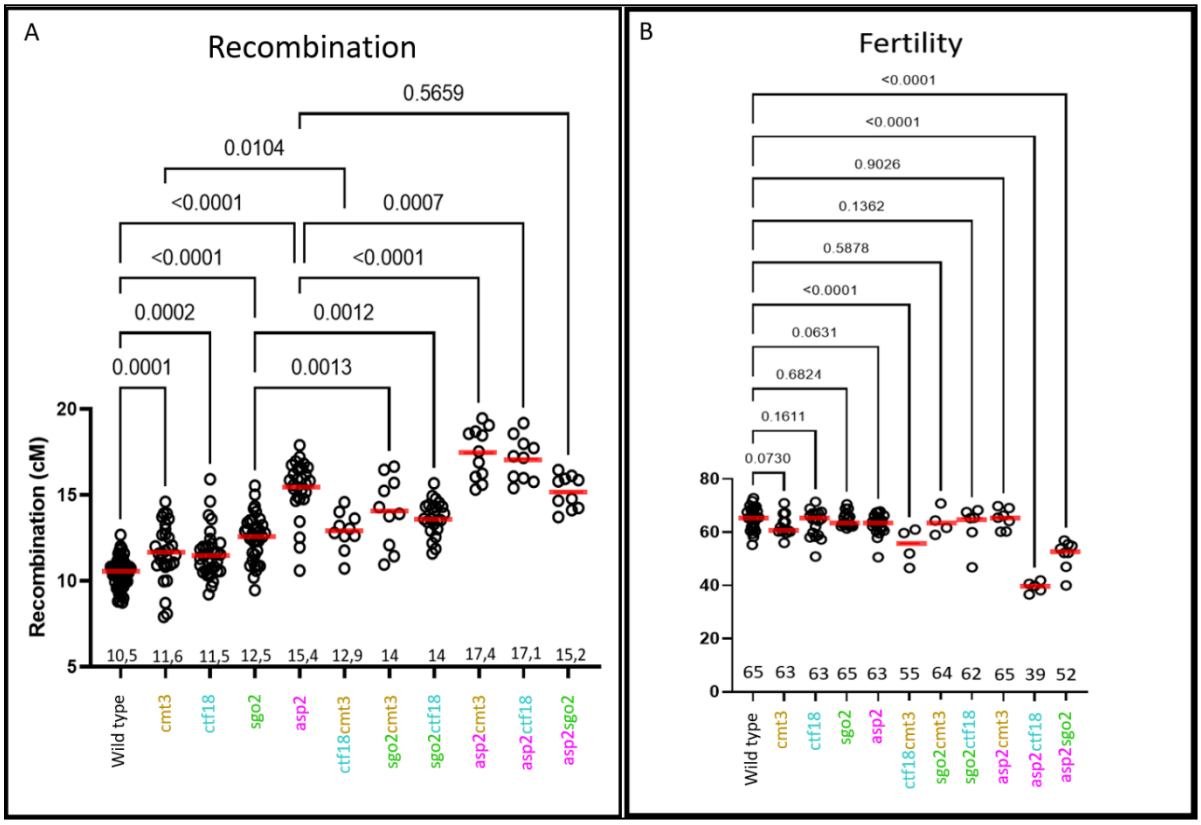

Figure17. Genetic Interaction Analysis. Recombination measurements in double mutants. Each point represents an independent recombination measurement of around 2500 seeds coming from both different plants and from the same plant. Numbers below represent the mean recombination distance for a given genotype. Ordinary one-way ANOVA test.

We confirmed higher recombination in the three single selected genes *ct18, sgo2* and *asp2* with again the same order of increasing recombination in the same order. We also noticed that the *cmt3* mutant has significantly higher recombination than wild type, confirming previous reports (Underwood et al., 2018). The *asp2* mutant consistently displays the highest levels of recombination of all tested mutant (Figure 17-A-B). These findings confirm the robustness of our recombination measurement tools and highlight the significance of these four genes in the CO formation in the pericentromeric region.

The results of the double mutants suggested the existence of three different pathways: CMT3, CTF18 and ASP2/SGO2. The first two pathways CMT3 and CTF18 are revealed with the double mutant *ctf18 cmt3* (12.9 cM, p=0.0104) which showed a cumulative effect when compared to *ctf18* (11.5 cM) and every time any of these two mutants *cmt3* or *ctf18* are combined with *sgo2, sgo2cmt3* (14 cM, p=0.0013) and s*go2ctf18* (14 cM, p=0.0012) are compared to single

sgo2 (12.5 cM) they show a cumulative effect. The same is observed when they are combined with *asp2*, *asp2cmt3* (17.4 cM, p<0.0001) and *asp2ctf18* (17.1 cM, p=0.0007) compared to single *asp2* (15.4 cM), again showed a cumulative effect, suggesting two independent pathways: CTF18 and CMT3. The last pathway ASP2/SGO2 was revealed by the double mutant *asp2sgo2* (15.2 cM, p=0.5659) which showed no significant difference compared to single *asp2,* indicating they are indeed acting in three different pathways. Altogether the results indicate that the control of pericentromeric recombination is very well regulated by kinetochore assembly and by the dynamics within the cohesion loading and the centromeric cohesion protection complex.

To assess the impact of increased recombination on fertility, we counted the number of seeds produced per silique for every genotype (Figure 17-B). We found that fertility is unaffected in single mutants, with a mean of 63 seeds per silique when compared to the *wild type*; however, in all the double mutants, we see a slight decrease in fertility in comparison to *wild type*, on average, 55 seeds per silique. Specifically, in *asp2ctf18* and *asp2sgo2* we observed the lowest amount of seeds with 39 and 52 seeds per silique, respectively.

Based on our observations, the mutant *asp2ctf18* has the highest recombination rate according to Figure 7 but it also has the lowest fertility (Figure 17-B). This leads us to hypothesize that recombination may have an impact on fertility. However, our findings also indicate that *asp2sgo2* also has a decrease in fertility but does not exhibit significantly higher recombination rates. Similarly, *asp2cmt3* has one of the highest recombination rates yet the fertility is not affected. This suggests that other factors may be playing a role in the decrease of fertility, such as the dynamic on the centromeric cohesion loading and cohesion protection.

To test the possibility that modified cohesion is the cause of the fertility loss, we observed under the microscope chromosome spreads of *asp2ctf18* and *asp2cmt3* male meiocytes, focusing on Meiosis II, after segregation. As expected, for none of the mutants a defect in Meiosis I was found, as segregation has not taken place. However, for Meiosis II some defects were found likely in cohesion for both double mutants. For *asp2ctf18* which was one of the mutants with the highest recombination and highest fertility loss, we found that from 12 cells in Metaphase II, 8 of them (67%) showed at least 1 chromatid lagging behind the rest of the chromosomes (Fig. 18-G) and the rest of the chromatids showed a very subtle difference in cohesion in comparison to the wild type chromatids in the same stage (Fig. 18-C). For *asp2cmt3* which also showed a higher recombination rate but without fertility loss, all the four cells observed in late stages showed a defect in the Metaphase II-Anaphase II transition (Fig. 18-J), where we observe the sister chromatids quite apart from each other. The defect doesn´t allow to distinguish clearly which stage it is. In the tetrad stage non-clear differences were found for any of the mutants (Fig.18-H, K). To make a more convincing conclusion, more cells should be analysed.

To distinguish if the fertility problem is related specifically to male gametes, we performed pollen viability essays with Alexander staining, on both mutants. We observed in three

different anthers of 3 different buds of an *asp2ctf18* plant and on average we only found a 1,9% of dead pollen grains, in comparison to Wild type where we found only 0,01% of dead pollen grains (Fig. 19-A,B and E). However, in *asp2cmt3* we see that overall there is only 0,7% of dead pollen (Fig. 19-E); intriguingly, we see some anthers with only 3-6 viable pollen grains (Fig. 19-D) but in the same plant we see other anthers with only 2 unviable pollen grains (Fig.19-C). All these results are suggesting that the fertility issues are indeed coming from a subtle defect in chromosome cohesion. In *asp2ctf18* that is more affected in fertility but not in pollen viability, suggests that it is likely that the female side is also affected in cohesion. To discard completely that the defect in fertility is coming from the female side, it would be necessary to perform similar analysis. In *asp2cmt3* that the fertility is not affected, but the pollen viability is, suggests that the female fertility is not affected and even though the male fertility is affected, the amount of pollen is enough to keep producing a normal amount of seeds.

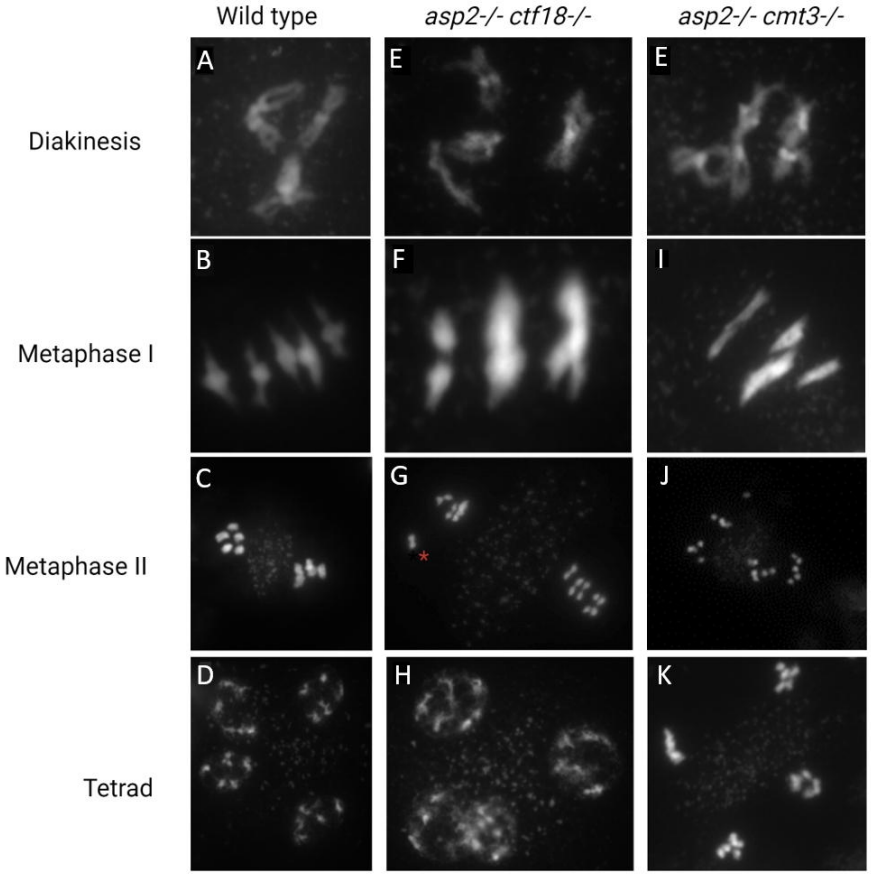

Figure 18 Meiotic spreads in double mutants with higher recombination asp2ctf18 and asp2cmt3

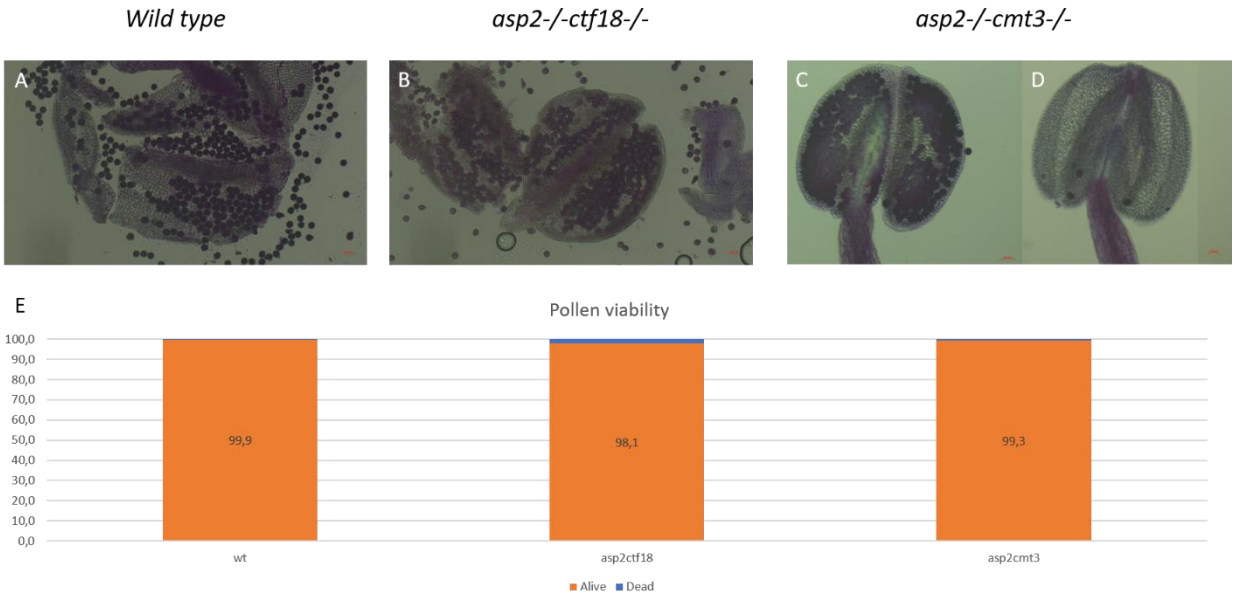

Figure 19 Pollen viability. Alexander staining of double mutants asp2ctf18 and asp2cmt3

7.3.3 Whole genome recombination analysis in Crispr mutants

We observed that the mutants exhibited greater recombination in pericentromeric regions with the FTLs. Now, we wondered how is the recombination distributed in the remaining regions of the genome. To solve this question, we measured CO frequency by genome wide analysis in the F2 progeny of Col/Ler hybrid carrying the mutations *ctf18, sgo2* and *asp2*.

To obtain the single mutant in Ler, we used CRISPR Cas9 technology with guides designed with the Columbia-0 genome as a reference but comparing always with the Landsberg genome, to make sure that they were specific to each gene (Ctf18, Sgo2, Asp2) and they were functional in both accessions. The final plasmids were sequenced by Nanopore (Figure 20) and transformed in Ler.

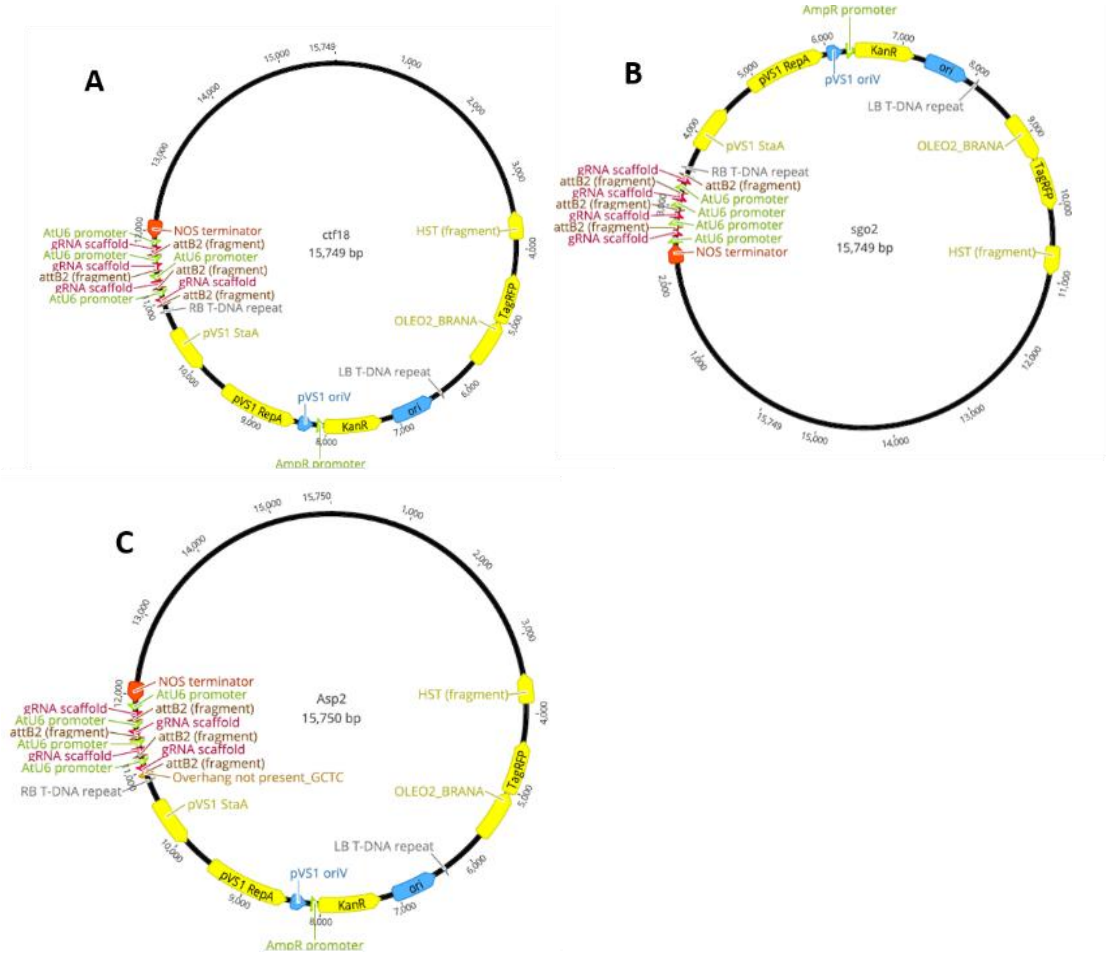

Figure 20. Sequenced plasmids used for mutant building in Ler background

To select the transformed seeds in the T1, each seed was picked under the microscope with a Red filter (N2.1). To select the seeds without the Cas9 activity, we looked at the next generation (T2) of the seeds without the fluorescence and we also confirmed it by amplifying the Cas9 protein. In these plants we also detected and selected the different alleles recovered for each gene (Figure 21) but only one was chosen to use for whole-genome recombination measuring. In the case of the mutant *ctf18*, five alleles were recovered, out of which two had a large deletion of 4583bp (*ctf18-1*), resulting in a frameshift, while the remaining three had small deletions of 10bp (*ctf18-2, ctf18-3, ctf18-4*), leading to truncated proteins in the N-terminus. For *sgo2*, only one allele was identified, with a 323bp deletion, causing a frameshift mutation. Lastly, *asp2* had two alleles, but only one of them had a large deletion of 3861bp (*asp2-1*), and even though the other allele had a smaller deletion of 142bp (*asp2-2*), both had frameshifts. We selected the largest deletions with frameshifts for both *ctf18* and *asp2.*

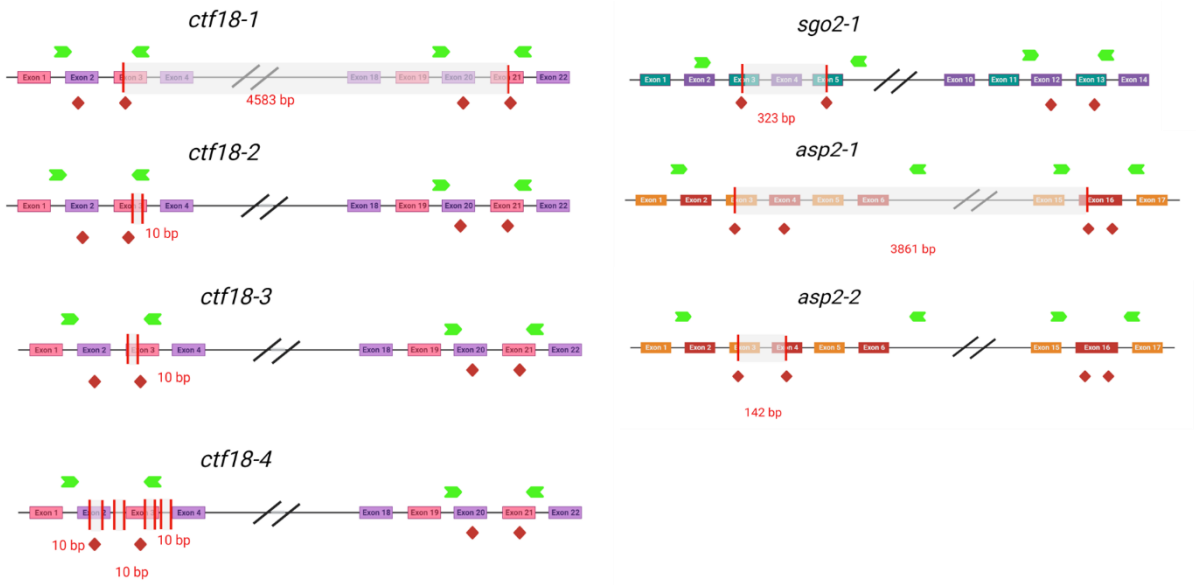

Figure 21. ctf18, sgo2 and asp2 mutant alleles identified in Ler, using Crispr-Cas9. Each line represents a gene, the colourful rectangules represent the exons (different colour per gene), the red diamonds are the guides used for Crispr-Cas9 and the green arrowheads are the primers used to detect mutations. The transparent rectangle with red bars represent the deletions, in red is written the size of each deletion (Figure made with BioRender.com)

To obtain the hybrid background, we crossed the plant heterozygous for the selected mutation in Ler, to the heterozygous plants in Col-0 (asp2-2(salk_140824)), same allele as used for the previous recombination measurements). In the F1 of this cross, we selected both genotypes important for CO analysis: wild type and mutant for both mutant alleles in a hybrid context. Once we found the suiting genotype, we selfed these plants and grew their seeds: 400 plants of the F2 population per genotype.

We used two methods to measure the recombination of hybrid plants: molecular markers and whole genome sequencing. The molecular markers were located in pericentromeric regions, around 2,500kbp apart from each other in chromosomes 1, 2 and 3 (Figure 22). They helped us confirm that there was higher recombination in pericentromeric regions of other chromosomes and we were able to eliminate the possibility that the increased recombination was only due to bias in the FTLs or sampling on chromosome 3. By conducting whole genome sequencing, additional insights were obtained regarding recombination not only in pericentromeres of some chromosomes, but in all the genome.

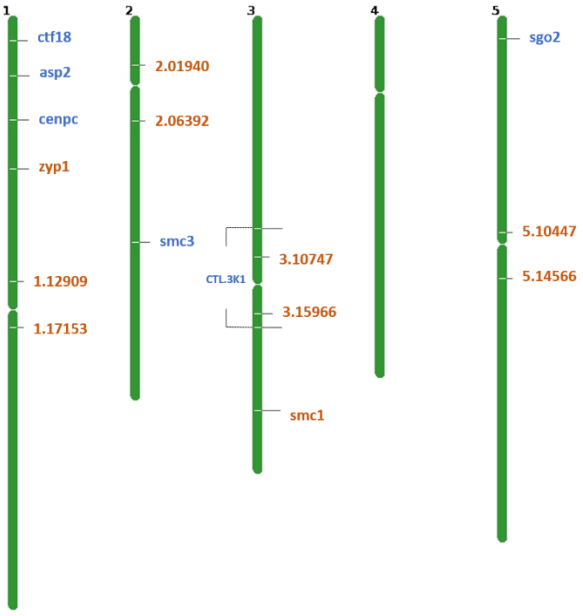

Figure 22. Molecular markers used for measuring recombination in a hybrid context. The gene IDS are the genes closer to the markers used.

Based on our examination of nearly 300 plants and utilizing molecular markers on chromosomes 1, 2, and 3, we have established that there is not significantly higher occurrence of recombination in the pericentromeric regions detected (as shown in Table 8 and Figure 23). In chromosome 1, the *ctf18* mutant exhibits 1,2-fold more recombination (9,5 cM) compared to the wild type (8,1 cM) (P=0,3982). In chromosome 2, *ctf18* displays 1,2-fold more recombination (9,3 cM) in comparison to the wild type (11,2 cM) (P=0,2736). Finally, chromosome 3, the *ctf18* mutant shows only 1-fold more recombination (12,8 cM) than the wild type (12,1 cM) (P=0,7102). No chromosome showed significantly higher recombination, in contrast to the FTLs measurements; likely because of the mild effect that *ctf18* presents, that it might be necessary to analyse a bigger number to detect, as we did with the FTLs (at least 900 seeds).

In contrast to the recombination measurements obtained using FTLs as shown in Figures 16 and 17-A, *ctf18* showed 11 and 13 cM, respectively; the recombination rates detected with molecular markers in Chromosome 3 are similar, confirming the similar location of molecular markers in chromosome 3 are spaced approximately 2,800 kbp, whereas the FTLs are separated by approximately 5,000 kbp.

Table 8. Recombination in ctf18 hybrid

Chromosome	1			2			3		
	Number of recombinants	Total plants	cM	Number of recombinants	Total plants	cM	Number of recombinants	Total plants	cM
WT-col/ler	45	277	8,1	52	279	9,3	68	280	12,1
ctf18-col/ler	65	341	9,5	76	340	11,2	87	341	12,8

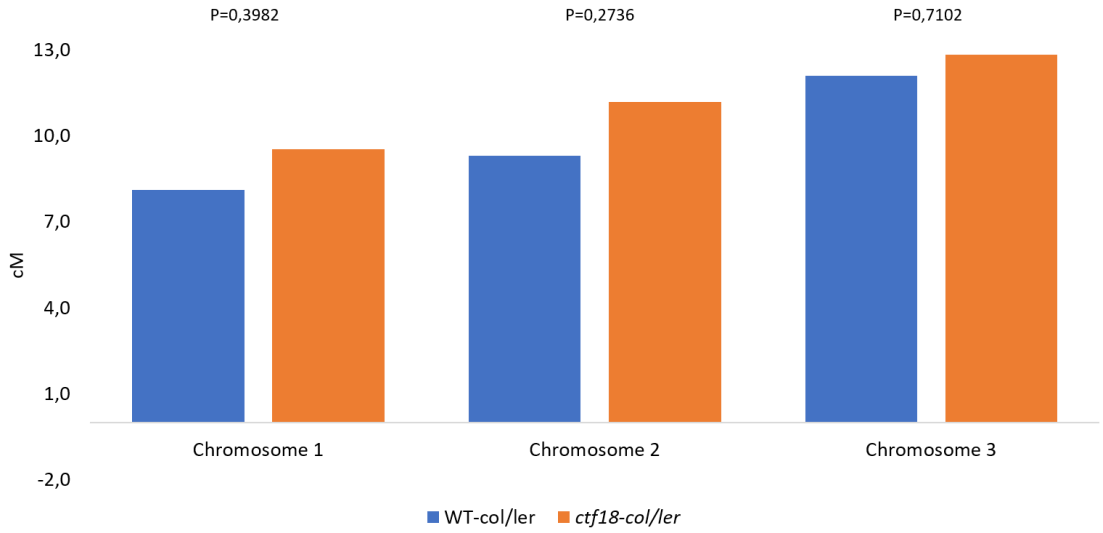

Figure 23. Recombination in ctf18 hybrid

To observe recombination in the rest of the genome, we analysed whole-genome sequencing data in wild type and mutant for both mutant alleles in hybrid Col/Ler context (Bioinformatic analysis done by Dr. Qichao Lian) (Fig. 25). The populations used for this analysis are the same as the ones that we used to measure the pericentromeric regions with molecular markers in chromosomes 1, 2 and 3.

Notably, the wild type crossover landscape was showing very drastic peaks; the wild type data was compared to wild-type results from other data sets generated by this and other labs as well (Capilla-Pérez et al., 2021; Joiselle Blanche Fernandes, Séguéla-Arnaud, et al., 2018; Rowan et al., 2019; Serra et al., 2018a) to see if the patterns remain and it showed that this result was most likely not showing the real CO landscape probably because the amount of samples was not big enough, therefore, a new batch of recombination will be performed. With the current preliminary data, the findings reveal a predominantly similar recombination landscape between the *ctf18* mutant and wild type, along the chromosomes without showing any difference between the arms and the centromeric regions . Figure 24 illustrates that the overall difference in crossover (CO) numbers is only marginal, with a slight non-significant

increase of 0.03. In the *ctf18* mutant (7.87) compared to the wild type (7.84). Additionally, Figure 25 shows that the overall patterns of recombination landscape closely resemble those observed in the wild-type.

In the pericentromeric regions, noticeable peaks of increased recombination are observed, particularly in chromosomes 1, 2, and 4. In chromosomes 3 and 5, the increase is subtler and more confined to shorter regions. To compare the results obtained from genetic markers and sequencing data, we counted the recombinant numbers in the same interval and we observed that with the sequencing data the non-significant fold-increase in chromosome 1 was 2,4-fold (P=0,6305), in chromosome 2 2,7-fold (P=0,4009) and 2,25-fold increase (P=0,6555), suggesting *ctf18* is having a very mild effect in recombination and it was not easy to detect,

It should be noted that *ctf18* was the mutant with the milder effect according to the FTL data. It would be of the greatest interest to observe recombination genome wide in the other mutants.

It was observed in the met1 mutant that when more recombination was found in the pericentromeric regions, in the neighbouring areas, there was a drop in recombination, suggesting a "compensating" pattern (Choi et al., 2018). In our data, we don´t see that described pattern overall, although we do see it in the arms of the chromosomes where some peaks show a much higher recombination and much lower drop next to it, more or less every 2-4 Mb.

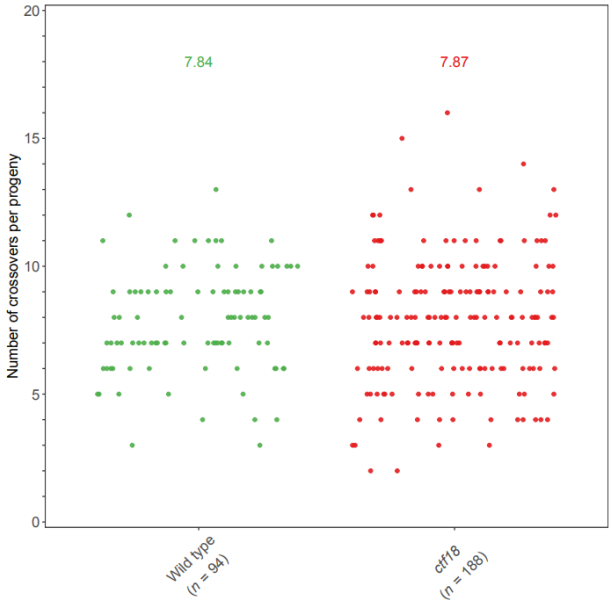

Figure 24 Overall recombination in ctf18 hybrid mutant and its wild-type counterpart

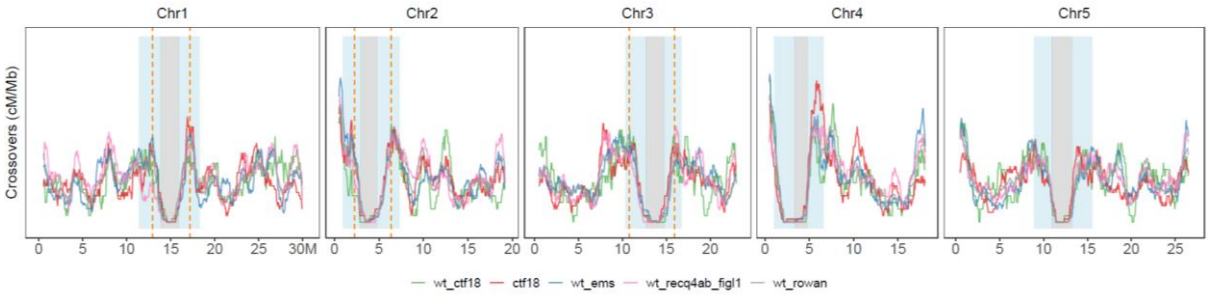

Figure 25. Recombination landscape in ctf18 hybrid mutant and its wild-type counterpart and CO frequency in pericentromeric regions. (Capilla-Pérez et al., 2021; Joiselle Blanche Fernandes, Séguéla-Arnaud, et al., 2018; Rowan et al., 2019; Serra et al., 2018a) *The left Y axis, the number of CO formed per Mb and the Y axis in the right, the methylation along the chromosomes. Grey vertical columns represent the centromeres, flanked by the light blue vertical columns representing pericentromeric regions.*

7.4 ADDITIONAL ANTI-CO FACTORS

To contribute to the finding of other antiCO factors regardless of the location in the chromosome of their targets. We used mutant plants that recovered fertility from a forward screen in *hei10* background. Similar to the identification of anti-crossover (antiCO) factors in *zmm* mutant backgrounds through genetic forward screens and mapping of plants with restored fertility, such as FANCM, RECQ4, and FIGL1 (Crismani & Mercier, 2012; Joiselle Blanche Fernandes, Séguéla-Arnaud, et al., 2018), a mutant known as H342 emerged from a genetic forward screen in the *hei10-2* mutant line and was subsequently recovered following EMS mutagenesis.

This approach involved selfing a population of mutant *hei10* (-/-) h342 (+/-) plants. From this population of 352 plants, only 43 individuals (12.21%) exhibited restored fertility and displayed a higher frequency of bivalents (2.3) compared to the single mutant hei10 (-/-) (1.7). Although the bivalent formation was not fully restored, it was sufficient to achieve overall evident fertility (exact seed count per silique was not recorded).

To identify the causal mutation involved in the restoration fertility of the screened candidate, the 43 plants with restored fertility were sequenced and analysed, based on the SHOREmapping tool (James et al., 2013). We found that chromosome 3 showed a higher frequency of mutant alleles with a frequency of 0.7 to 0.9 in a wide region, almost covering the long arm (Figure 15-A); however, we did not observe a very large peak with a frequency close to 1, as it would be expected with efficient selection of a recessive causal mutation. Note also that the parental plant was *hei10-/-* and that the recombination is expected to be low (Ziolkowski et al., 2017), while in the other chromosomes the frequency remained mostly stable lower than 0.7. This means that this whole region in chromosome 3 could be involved with the mutation because it represents a high frequency in common between the sequenced individuals. However, more analysis was necessary to clarify the fluctuation in the frequency of this region.

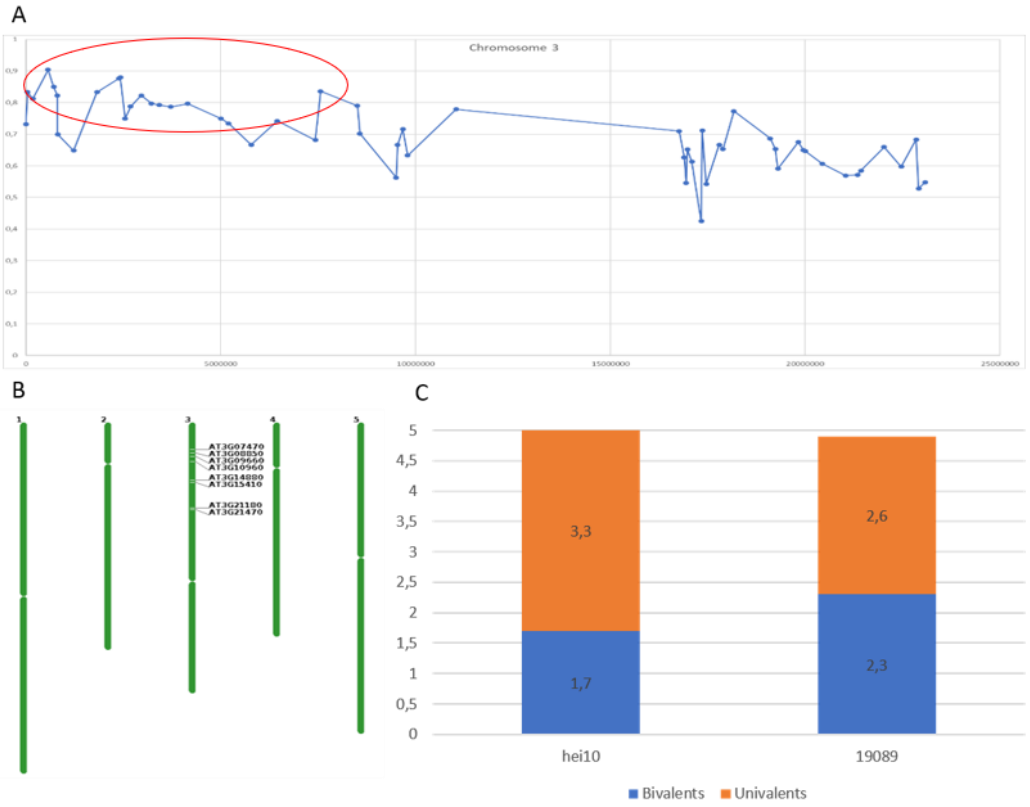

Figure 26 Mapping of causal mutation in Chromosome 3 showing a wider region than expected

We narrowed down the analysis, to identify the genes present in this region of chromosome 3 (Figure 26-B) that were also previously identified with the use of markers by Dipesh Singh in our laboratory. We decided to test three genes by genotyping: AT3G07470, AT3G14880, and AT3G15410, which are still not identified.

We designed primers for amplification of each of these candidate genes to confirm their absence in this population, their segregation and/or penetrance in the population. Remarkably, three plants were heterozygous for the three genes, one plant was wild type for the tree genes and two plants were heterozygous for AT3G07470 but wild type for AT3G14880 and AT3G15410. To find a differential phenotype that could lead us to the responsible gene, further cytological analysis was performed in the plants with different genotypes; however, finding metaphase I stages was not possible in the plants with different genotypes for all the genes. Metaphases were only recovered in completely homozygous plants; where they show that the number of bivalents increases from 1,7 (in control *hei10*) to 2,3 (Figure 26-C) but it was not possible to separate the effect of each of the mutants and the phenotype was not as dramatic as expected to find the causal mutation; therefore, this project was put on a side.

7.5 THE FANCC–FANCE–FANCF COMPLEX IS EVOLUTIONARILY CONSERVED AND REGULATES MEIOTIC RECOMBINATION

7.5.1 Summary

There are two pathways for the formation of crossovers (CO): Class I and Class II. The more common Class I (ZMM) is regulated by interference, while Class II COs are a minority and are restricted by three anti-CO pathways, namely the Fanconi Anemia (FA) pathway, RECQ4/RMI1/TOP3a, and FIGL1/FLIP1. The FA pathway has been studied due to the rare human disease, Fanconi anaemia. Its proteins are conserved and can be classified by their molecular roles: the FA complex, which localizes at replication forks; MHF1-MHF2, which promotes FANCM recruitment at damaged locations; and the FA core complex, which mono-ubiquitinates each promoter of the FANCI-FANCD2 (ID2) heterodimer to close the ID2 clamp on DNA. The FA/HR complex proteins are downstream partners independent of the other groups. The core complex has seven subunits and two FA-associated proteins that form three subcomplexes: FANCB-FANCL-FAAP100, FANCC-FANCE-FANCF (CEF), and FANCA-FANCG-FAAP20. FANCM interacts with the core complex via FANCF, indicating the importance of the substrate-recognition module. Our study shows that the CEF complex is a novel meiotic anti-CO factor and is evolutionarily conserved from mammals, adding to the results already collected by the same forward genetic screen.

The causal mutation, FANCC ortholog was identified by the fertility restoration of the *msh4* mutant from 4.5 to more than 24 seeds per silique, through the Forward genetic screen. It was necessary to use HHpred remote homology detection server to detect the only 16% of shared homology between mammals and plants, before this, homology was not found with standard sequence similarity analysis. In addition, using the prediction method Alphafold2, it was predicted that the three proteins AtFANCC, AtFANCE, AtFANCF were forming a complex, which was also observed in the human complex. A pull-down protein purification coupled with mass spectrometry and a yeast-two-hybrid confirmed the complex formation of FANC with FANCE, FANCL, FANCM and MHF2 and their interaction. It was also observed that FANCC was conserved among several species but not in fungi or in *Drosophila.*

To explore the potential meiotic role of these genes in Arabidopsis, meiotic chromosome spreads and fertility tests were performed in single and triple mutants. Only single *Atfance* and *Atfancf* were showing univalent at low frequencies but the triple *fancc, fance, fancf* did not show any meiotic defects or in sterility, suggesting these three genes act together at meiosis. However, after combining *fancc, fance, fancf* in *msh4* background*,* it slightly restored the bivalent formation with 2.8 bivalents/cell of single *msh4* with 1.4 bivalents/cell and increased fertility, suggesting that FANCC-FENCE-FANCF limit CO in a partially redundant state. But when the double mutant *mhf1 msh4*was combined to *fancc*, there was no more bivalent

restoration, suggesting that FANCC acts in the same anti-CO pathway as MHF1, a partner of FANCM protein.

Interestingly, the increase in bivalent number affected more female than male gametes, suggesting that the limitation of COs is more critical in female rather than male meiosis. To confirm the CO contribution differently in both gametes, we used a Fluorescent marker (FTL420) flanking 5-Mb interval of subtelomeric region of chromosome 3 and measured recombination in the F1 offspring of reciprocal crosses. Recombination was significantly increased in single *fancc* and triple *fancc, fance, fancf,* when comparing to Wild type, contrary to the male counterpart where it was even slightly reduced. When plants are selfed each single mutant and triple are slightly increase in comparison to wild-type recombination, suggesting that the three proteins work together in limiting COs but having a predominant function in females, being able to restore fertility in *zmm* mutants.

Finally, when either *fancc, fance or fancf* single mutants are combined to *mus81* we observed a strong fertility reduction and chromosome fragmentation but not recovered fertility. Demonstrating the importance of FANCC FANCE and FANCF for efficient DSB repair, specially the intermediates that can be repaired by MUS81.

One of the most important contribution of this article, is the evidence that supports the hypothesis that such an important and conserved event like DNA repair can be different between humans and plants. Where in humans the somatic FANC-E-F facilitates the crossover limiting with FANCD2-FANCI mono-ubiquitination in inter-strand crosslink repair; however, in Arabidopsis there is no detectable role to limit COs of any of the orthologue components of the human core complex and its substrate; in addition, the well-described functions of FANC-E-F complex are more inclined to stabilize or support of FANCM in molecule dissolution during meiosis DSB repair, rather than limiting COs like in Arabidopsis.

7.5.2 Author´s contribution

This project was started in Raphael Mercier´s Lab with a forward genetic screen that restores fertility of *zmm* mutants (*zyp4)*. With this powerful screen it was possible to identify the three main players of class II CO limiting. The Fanconi Anemia Complementation group M (FANCM) (Crismani et al., 2012; Joiselle Blanche Fernandes, Séguéla-Arnaud, et al., 2018), FIDGETIN-LIKE-1 (FIGL1) (Joiselle Blanche Fernandes, Duhamel, et al., 2018; Girard et al., 2015) and RECQ4 (RECQ4A/RECQ4B), together with some other players acting in a complex FIDGETIN-LIKE-1 INTERACTING PROTEIN (FLIP), as regulator Breast Cancer Susceptibility 2 (BRCA2) or as mild enhancers that could backup the main function of FANCM interacting histone-fold protein (MHF1, MHF2).

Another gene found in the same screen done mainly by Dipesh Singh, Raphael Mercier and Wayne Crismani who designed the experiments, wrote, revised and edited the manuscript. Together with Imran Siddiqi. Dipesh Singh performed most of the experiments and drafted the manuscript.

My contribution to this article was to measure recombination with the FTLs tools implemented in the lab of single and triple *fancc fance fancf* mutants, together with the male and female contribution, after reciprocal crosses.

7.5.3 Manuscript

The FANCC–FANCE–FANCF complex is evolutionarily conserved and regulates meiotic recombination

Dipesh Kumar Singh1, Rigel Salinas Gamboa1, Avinash Kumar Singh2, Birgit Walkemeier1, Jelle Van Leene3,4, Geert De Jaeger 3,4, Imran Siddiqi2, Raphael Guerois 5, Wayne Crismani 6,7 and Raphael Mercier 1,*

1Department of Chromosome Biology, Max Planck Institute for Plant Breeding Research, Carl-von-Linn´e-Weg 10, 50829 Cologne, Germany,
2CSIR-Centre for Cellular & Molecular Biology, Uppal Road, Hyderabad 500007, India,
3Department of Plant Biotechnology and Bioinformatics, Ghent University, Ghent B-9052, Belgium,
4Center for Plant Systems Biology, VIB, Ghent B-9052, Belgium,
5Institute for Integrative Biology of the Cell (I2BC), Commissariat `a l'Energie Atomique, CNRS, Universit ´e Paris-Sud, Universit ´e Paris-Saclay, Gif-sur-Yvette 91190, France, 6The DNA Repair and Recombination Laboratory, St Vincent's Institute of Medical Research, Melbourne 3065, Australia and 7The Faculty of Medicine, Dentistry and Health Science, The University of Melbourne, Parkville, Victoria, Australia

Received July 07, 2022; Revised November 29, 2022; Editorial Decision December 01, 2022; Accepted December 14, 2022

ABSTRACT

At meiosis, programmed meiotic DNA double-strand breaks are repaired via homologous recombination, resulting in crossovers (COs). From a large excess of DNA double-strand breaks that are formed, only a small proportion gets converted into COs because of active mechanisms that restrict CO formation. The Fanconi anemia (FA) complex proteins AtFANCM, MHF1 and MHF2 were previously identified in a genetic screen as anti-CO factors that function during meiosis in Arabidopsis thaliana. Here, pursuing the same screen, we identify FANCC as a new anti-CO gene. FANCC was previously only identified in mammals because of lowprimary sequence conservation. We show that FANCC, and its physical interaction with FANCE–FANCF, is conserved from vertebrates to plants. Further, we show that FANCC, together with its subcomplex partners FANCE and FANCF, regulates meiotic recombination. Mutations of any of these three genes partially rescues CO-defective mutants, which is particularlymarked in female meiosis. Functional loss of FANCC, FANCE, or FANCF results in synthetic meiotic catastrophe with the pro-CO factor MUS81. This work reveals that FANCC is conserved outside mammals and has an anti-CO role during meiosis together with FANCE and FANCF.

INTRODUCTION

Large-scale exchange of genetic material between homologous chromosomes in the form of meiotic crossovers (COs) generates new allelic combinations in the sexual progeny of eukaryotes. COs are also required for the correct segregation of chromosomes at the first meiotic division in most species. This is likely why a mechanism exists to ensure an 'obligate' crossover per chromosome pair, per meiosis. Meiotic recombination is initiated by the formation of a large number of programmed DNA double-stranded breaks (DSBs), a minority of which are repaired as COs. Two pathways contribute to CO formation, defining two classes of COs. Class I COs depend on a group of proteins called ZMMs, an acronym derived from seven proteins initially described in *Saccharomyces cerevisiae* (Zip1–Zip4,Msh4–5, Mer3) (1,2), and account for most of the COs. Class II COs, which account for a minority of COs in most eukaryotes including mammals and plants, involve notably the MUS81 nuclease (3,4). In *Arabidopsis thaliana*, a mutation in any member of the *ZMMs* causes a drastic decrease in CO number, and notably the loss of the obligate crossover, with only a few

residual COs formed by the class II pathway, leading to chromosome mis-segregation and quasi-sterility. A forward genetic screen for restoration of fertility of *zmm* mutants identified a series of genes that actively limit CO formation in Arabidopsis. These factors specifically limit class II COs and act through three mechanisms. The first anti-CO pathway involves proteins from the Fanconi anaemia (FA) pathway, FANCM (5), MHF1 and MHF2 (6). These three proteins have been shown to physically interact in humans, along with FAAP24, which has not been identified in Arabidopsis (7,8). The second anti-CO mechanism involves RECQ4, RMI1 and TOP3a (9), and the third, the proteins FIGL1 and FLIP (10–12). These three mechanisms contribute in parallel to limiting class II COs (13). The FA pathway is comprised of at least 23 protein subunits in human cells and some, but not all, of them are widely conserved in eukaryotes, including plants. It is traditionally known for its role in inter-strand crosslink repair in somatic cells in humans, with emerging roles in replication fork protection (14). The FA pathway is heavily studied because its proper function is required to prevent serious human disease: FA functions as a tumor suppressor and mutation of FA pathway factors causes the rare condition Fanconi anemia. FA pathway proteins can be classified into three groups on the basis of their molecular roles: (i) the FA core complex localizes to DNA inter-strand crosslink or stalled replication forks, with FANCM acting as an anchor. MHF1–MHF2, a heterotetrameric protein complex, promotes FANCM recruitment at the site of DNA damage (7,15). (ii) The FA core complex mono-ubiquitinates each protomer of the FANCI-FANCD2 (ID2) heterodimer. The post-translational modification results in the closing of the ID2 clamp on DNA (16–21). (iii) FA/HR complex proteins are downstream partners that are considered to function independently of the above two groups (22,23). Structural studies (24–26) have demonstrated that seven subunits of the core complex (FANCA, FANCB, FANCC, FANCE, FANCF, FANCG, FANCL), and two FAassociated proteins (FAAP20 and FAAP100) form three different subcomplexes: (i) FANCB–FANCL–FAAP100 (BL100), (ii) FANCC–FANCE–FANCF (CEF) and (iii) FANCA–FANCG–FAAP20 (AG20) (26,27). The ring finger domain of FANCL acts as an E3 ubiquitin ligase and its two associated proteins FANCB and FAAP100 are organized as a catalytic module (24,26). It has been proposed that FANCA and FANCG form a chromatin-targeting module, while FANCC, FANCE and FANCF organize to establish a substrate-recognition module (24). FANCF acts as a bridge between FANCCand FANCE(24,28). FANCM interacts with the core complex through FANCF (26,29), demonstrating that the substrate-recognition module is an important component of the FA core complex. In this study, extending a previously described forward genetic *zmm* suppressor screen (5,6,9–11) augmented by complementary approaches, we demonstrate that the CEF complex is evolutionarily conserved from mammals and show that it is a novel meiotic anti-CO factor.

MATERIALS AND METHODS

Genetic material

The following Arabidopsis lines were used in this study: *fancc-2* (N542341), *fancc-3*(N1007952), *fancc-4* (N626745), *fance* (N553587) (6) *fancf* (N457070) msh4 (N636296)(30), *msh5-2* (N526553) (30), *mus81-2* (N607515) (31) and *mhf1-3*(N576310) (6). All the T-DNA mutants were obtained from the NASC. Plants were grown under a controlled environment with a photoperiod of 16 h per day and 8 h per night, at a temperature of 20◦C, and 70% humidity.

Genetic analysis

The *msh4* suppressor *Atfancc* was sequenced using Illumina technology at TheGenome Analysis Centre, Norwich, UK, and mutations were identified using ler 1 assembly as reported for the MutDetect pipeline (6,32). The identified causal mutation in *fancc-1* was a G to A substitution at position chr3: 21918909 (Ler-0) equivalent to position chr3: 22288888 in the Columbia (TAIR10) genome. The primers used for genotyping are listed in Supplementary Table S1. Siliques were fixed in 70% ethanol for at least two days and scanned for seed counting manually on images. Fertility was assessed by counting seeds per fruit on a minimum of five plants and ten fruits from each plant.

Sequence analyses

Sequences of *A. thaliana* At3g60310/AtFANCC, FANCE (Q9SU89 ARATH) and FANCF (F4K7F0 ARATH) were used as input for the HHpred remote homology detection server against different eukaryotic profile databases (33,34) and as queries of PSI-BLAST searches (35) against the nr database. Full-length sequences of FANCC orthologs were retrieved and re-aligned with mafft (36) and the multiple sequence alignment was represented using JalView (37). The phylogenetic tree of the FANCC orthologs in plants was generated using the FANCC MSA as a query of the PhyML 3.0 server (38) with standard estimated options, an approximate likelihood-ratio test to estimate the bootstrap values (SH-like), and the Jones–Taylor–Thornton substitution model with four substitution rate categories. The calculated tree was represented using the iTOL server (39).

Structural modelling

Sequences of *A. thaliana* At3g60310/AtFANCC, FANCE (Q9SU89 ARATH) and FANCF (F4K7F0 ARATH) were used as input for the MMseqs2 homology search program (40) to generate a multiple sequence alignment (MSA)against the UniRef30 clustered database for each of the FANC complex subunits (41). The calculated full-length sequences of the orthologs were retrieved and re-aligned with mafft (36). MSAs of FANCC, FANCE and FANCF were then concatenated, matching the sequences of the same species resulting in paired alignments, which were combined with the unpaired sequences for those species that could have not been matched. The resulting paired plus unpaired concatenated MSA was used as input to generate five structural models of the FANCC–FANCE–FANCF complex using a local version of the ColabFold interface (42) running three iterations of the Alphafold2 algorithm (43) trained on the multimer dataset (44) on a local HPC equipped with NVIDIA Ampere A100 80Go GPU cards. The five models converged toward similar conformations and obtained high confidence and quality scores with pLDDTs in the range [79.1, 85] and [72.6, 80.2] and pTMscore in the range [0.64, 0.662]. The model with highest pTMscore was relaxed using rosetta relax protocols to remove steric clashes constrained by the starting structure using the -relax:constrain relax to start coords option (45), and the model with the lowest rosetta global energy was used for structural analysis. Conservation analysis mapped at the structure of the model were performed using the ConSurf server (46).

Cytological techniques

Meiotic chromosome spreads on anthers were performed as previously described (47). For female meiotic chromosome spreads, floral buds of 0.7–1.4 mm in size (buds with

yellow anther) were selected and pistils were isolated. Stigma were removed and the isolated pistil were digested in 0.3% (w/v) cellulase, 0.3% (w/v) pectolyase Y23, 0.3% (w/v) driselase in citrate buffer for 1 h at 37◦C. Ovules were isolated from pistils and macerated in minimum amount of water. Further processing was carried out in the same manner as with the male (47). However, the frequency of meiotic cells per slide was substantially lower in females than in males. Chromosomes were stained with DAPI (1 _g/ml) Images were acquired and processed using a ZEISS microscope (AXIO-Imager.Z2) under a 100× oil immersion objective with ZEN software and figures were prepared using Adobe Photoshop.

Yeast two-hybrid and pull down

Clones were generated using the Gateway cloning system (Thermo Fisher Scientific); the desired inserts were cloned into pDONR221 as pENTR clones and then into different destination vectors using the LR clonase recombination method (Thermo Fisher Scientific).We generated full length ORF pENTR clones for AtFANCC, AtFANCE, and AtMHF2 from an inflorescence cDNA library of Arabidopsis. One additional ORF pENTR of AtFANCC was cloned without a stop codon for in-frame C-terminal fusion and both ORF pENTR clones ofAtFANCCwere used for GSrhino-tagged pulldown. In yeast two-hybrid assays, we used two destination vectors, pGADT7-GW as bait and pGBKT7-GW as prey. The ORF pENTR clones of At-FANCC, AtFANCE and AtMHF2 were cloned into both destination vectors by LRreaction. The ORF of AtFANCF was cloned into the pGBKT7 and PACT2 ADconventional vector using theNCO1, Sal1, and NCO1, XHO1 restriction enzymes, respectively. All pENTR clones and final clones were verified thoroughly by Sanger sequencing to ensure mutation-free cloning and in-frame fusion. Plasmids of bait and prey clones were transformed into the haploid yeast strains AH109 and Y187, and then yeast two-hybrid assays were performed in a Gal4-based system from Clontech in a diploid strain by mating as previously described (9,48). Arabidopsis cell suspension cultures expressing Nterminal GSrhino-tagged FANCC and for C-terminal GSrhino-tagged FANCC were used for pull-down as previously described (49,50). Co-purified proteins were identified using standard protocols utilizing on bead-digested sample evaluated on a Q Exactive mass spectrometer (Thermo Fisher Scientific) (51). After identification, the protein list was filtered for false-positives using a list of non-specific proteins, which was assembled as previously reported (51). Semi-quantitative analysis using the average normalized spectral abundance factors (NSAF) of the discovered proteins in the FANCC pull-downs was used to identify true interactors that may have been filtered out due to their classification in the list of nonspecific proteins. Chosen proteins were identified with at least two peptides in at least two experiments and showed high (at least 10-fold) and significant [log10(*P* value (*t* test)) enrichment relative to estimated average NSAF values from a large dataset of pull-downs with nonrelated bait proteins.

FTL analysis

To measure recombination, we used fluorescent transgenic lines (FTL) (420) generated in a Col background. The used lines harbor seed coat expressing GFP (Chr 3:256 516-GFP) and dsRed (Chr 3:5 361 637-dsRed2) fluorescent protein markers in cis (52,53). We quantified the fluorescence of the seeds using the Fiji image analysis software (54), which identifies seeds and quantifies fluorescence intensity for each seed in all pictures. The output was analysed using a pipeline that was created to normalize the data, plot the frequency of objects with each fluorescent colour, plot the fluorescence intensity, and quantify the number of seeds with only one fluorescent

color, allowing selection of the number of recombinant seeds. For F2, recombination was measured using the formula below, as reported in (52).

$$cM = 100 * (1 - [1 - \frac{2(N_G + N_R)}{N_T}]^{1/2}$$

For male and female backcrosses, recombination was measured as

$$cM = 100 * \frac{(N_G + N_R)}{N_T}$$

where *NG* is the number of green-only fluorescent seeds, *NR* is the number of red-only fluorescent seeds and *NT* is the total number of seeds counted. We generated a segregating population (F2) from which we selected plants heterozygous for the markers in cis with the desired mutants and wild-type control. For each genotype, we used at least three biological replicates (independent plants) with at least three technical replicates, each of them containing a minimum of 400 seeds. To measure CO frequency independently in males and females, reciprocal crosses were made with wild-type Columbia (0). Differences between genotypes were tested by Chi2 on the proportion of recombined seeds (Ng + Nr) among total seeds.

RESULTS

Identification of a novel *zmm* suppressor

CO-deficient *zmm* mutants display a >90% reduced seed set in Arabidopsis, which correlates with shorter fruit, due to random segregation of chromosomes in meiosis. Therefore, inactivating anti-CO genes in a *zmm* mutant leads to an increase in CO number, resulting in improved chromosome segregation, restored fertility and longer fruits. Here, we extended a forward genetic screen for *zmm* mutants exhibiting increase in fruit length following EMS mutagenesis. The screen was previously performed on five *zmm* mutants (*hei10, zip4, shoc1, msh5* and *msh4*), in a total of ~7,000 lines and identified 59 mutants with restored fertility, among which 58 are mutated in one of the previously identified anti-CO genes (Table 1, Supplementary Table S2). (5,6,9–11). In this study, we focused on the last *zmm* suppressor mutation that increased the fertility of a *msh4*mutant (cshl GT14269, L*er* genetic background).Genetic mapping delimited the causal mutation to a 0.47MB region on chromosome 3 (21452882–21919909 in the Ler assembly) (55), and whole genome sequencing identified a candidate mutation in the fourth exon donor splicing site of the At3g60310 gene (G > A 3 21918909 in the Ler assembly, corresponding to 3 22288888 in Col TAIR10). We show below that At3g60310 encodes the Arabidopsis FANCC ortholog. Three independent T-DNA alleles (*fancc-2 N542341*, *fancc-3 N1007952* and *fancc-4 N626745*, Col background) were able to enhance the fertility of *msh4*, from 4.5 to > 24 seeds per fruit (Figure 1 and Supplementary Figures S1, S2), confirming the identification of thecausal mutation in At3g60310.

FANCC is conserved in plants

Standard sequence similarity analysis failed to find any homology of the protein encoded by At3g60310 outside of plants, or with proteins of known function (56). Using the HHpred remote homology detection server (33,34), it was possible to identify a

potential match with human FANCC (XP 011516668) despite both proteins sharing only 16% primary sequence identity (HHpred probability of 94%). To test the hypothesis that At3g60310 is an ortholog of FANCC, we analyzed the physical contacts between human FANCC and the human FANC complex, the cryoEM structure of which was recently determined at 3.1 ˚A (57). Figure 2A illustrates that human FANCC (pale green subunit) is in direct physical contact with three subunits of human FA core complex, FANCE (light pink), FANCF(light blue) together with the ubiquitin E3 ligase FANCL (yellow). Given that FANCC, FANCE, and FANCF are known to constitute a stable sub-complex in humans, we tested the possibility that At3g60310 was a dedicated partner of *A. thaliana* FANCE (6) (Q9SU89 ARATH) and FANCF (F4K7F0 ARATH) using the Alphafold2 prediction method (43). Alphafold2 was recently shown to perform well when predicting structures of proteins and whether two proteins interact with each other (44). Using the AlphaFold2 method trained on multimers (44), we obtained a model of the complex with the three *A. thaliana* subunits with reliability scores above the confidence threshold of 50 and 0.5 for pLDDT and ptmscore, respectively (pLDDT of 72.6 and ptmscore of 0.67) (Supplementary Figure S3). Interestingly, At3g60310 was predicted to form a complex with AtFANCE and AtFANCF with a similar arrangement to that observed for the corresponding orthologs in the human FANC complex (Figure 2B). As a support for the reliability of the model, the surface patches 1 and 2 of At3g60310 (circled in Figure 2C) are involved in the interaction with AtFANCF and At-FANCE respectively and are among the most conserved regions of At3g60310/FANCC (Figure 2C, Supplementary Figure S4). The N-terminal domain of FANCE is found well anchored in the central region of At3g60310/FANCC with low predicted error for the accuracy of the interface modelling (Supplementary Figure S3C). When Al phaFold2 is executed, five models are typically generated whose structural similarity accounts for the robustness of the prediction. In the N-terminal region of FANCE, the five models superimpose very well confirming that the interface between this domain and At3g60310/FANCC is strongly constrained (Supplementary Figure S3B). In contrast, the C-terminal domain of FANCE does not exhibit a strong co-evolutionary signal in the region where it binds to At3g60310/FANCC. The predicted error associated with FANCE C-terminal binding to At3g60310/FANCC is much higher than for the N-terminal domain (Supplementary Figure S3C) and the five models generated for FANCE adopt variable orientations in the C-terminal region (Supplementary Figure S3B). Therefore the relative position of FANCE C-terminal with respect to At3g60310/FANCC should be seen as loosely constrained. Next, we performed an unbiased search for interacting partners of At3g60310 using pull-down protein purification coupled with mass spectrometry. We used overexpressed GSrhino-taggedAt3g60310 as a bait inArabidopsis suspension cell culture (49). After filtering co-purified proteins for false positives, we recovered peptides from At3g60310 itself and a series of additional proteins in three replicate experiments (Table 2). Strikingly, all four co-purified identified proteins were Arabidopsis homologs of members of the FA complex, FANCE, FANCL, FANCM and MHF2 (Table 2). Further, a yeast two-hybrid assay confirmed direct interactions of At3g60310 with FANCE and MHF2. FANCE, FANCF and MHF2 also interacted with each other in yeast two-hybrid (Supplementary Figure S5). Altogether, this demonstrates that At3g60310 encodes the FANCC protein in Arabidopsis, which we term AtFANCC.

FANCC is conserved in distant eukaryotic lineages

Using PSI-BLAST searches, AtFANCC orthologs could be detected in most plants (Supplementary Figures S4 and S6). In-depth analyses using either PSI-BLAST or HHpred failed to detect any homolog in more distantly related green algae such as *Chlamydomonas*, although a FANCE homolog can be detected in *Chlamydomonas reinhardtii*. In metazoans, a previous bioinformatics analysis performed on model species for all the genes of the FANC core complex, noted that several species were missing a FANCC homolog although having a FANCE ortholog (56). We revisited this study using the most recent sequence databases and PSI-BLAST searches starting from human FANCC. Interestingly, five iterations of PSI-BLAST were required to retrieve the first plant ortholog (in the monocot *Spirodela intermedia*), which enabled the retrieval of all the same plant orthologs identified from AtFANCC. After 15 iterations, the search nearly converged with about 2,100 FANCC homologs, highlighting the existence of FANCCs in early branching metazoans such as *Nematostella vectensis* (XP 032241565) and *Ciona intestinalis* (XP 002129616) that were not found previously. In insects, orthologs could also be detected in Hymenoptera (ants and bees) but neither in Diptera (Drosophila) nor in Lepidoptera (Bombyx). Consistently, repeating the PSI BLAST search with human FANCE or FANCF as queries, a similar distribution of homologs was found in insects. Homologs of FANCE and FANCCcould be detected in specific fungal lineages such as *Rhizopus azygosporus* (corresponding to hypothetical proteins RCH90546.1 and RCH79564.1, respectively). A reciprocal HHpred analysis comparing these genes against the human database confirmed they were remote homologs of FANCE and FANCC (HHpred probability score of 100% and sequence identities of 21% and 15%, respectively), suggesting that certain fungal lineages did not lose these FANC complex subunits.

***Atfancc, atfance*, and *atfancf* mutations increase fertility and bivalent formation of crossover-deficient *zmm* mutants**

As the mammalian FANCC was shown to form a structural and functional module with FANCE and FANCF (24,25,57), we explored their potential meiotic roles in parallel. A FANCE homolog was previously described in Arabidopsis (AT4G29560) (6), and the AT5G44010 gene was annotated as *AtFANCF* in Araport11 because of sequence similarity with themammalian *FANCF* (58). TheArabidopsis *FANCC*, *FANCE* and *FANCF* genes are expressed both in somatic and reproductive tissues (59). Single mutants in each of these genes did not show growth or developmental defects but had a slight decrease in fertility (Figure 1A–C, Supplementary Figure S2). Meiotic chromosome spreads in *Atfance* and *Atfancf* single mutants revealed the presence of univalents at low frequencies, showing that some chromosome pairs lack COs (Supplementary Figure S7, Figure 3C–D, G). Combination of *fancc, fance* and *fancf*mutations did not reveal any developmental defects or enhanced sterility and meiotic defects (Figures 1A and 3G). This suggests that, consistent with the pull-down and Y2H data, FANCC, FANCE and FANCF act together at meiosis, playing a role in ensuring the obligate CO. Mutation of *FANCC*, or *FANCE*, or *FANCF* significantly restored the fertility of the *zmm* mutants *msh4* and *msh5*, increasing the seed set more than fourfold (Sidak test, $P < 10{-}6$) (Figure 1A, D, E. Supplementary Figure S2). In the Ler background, chromosome spreads of male meiosis showed an increase of bivalent frequency in *fancc-1 msh4* compared to *msh4* ($P < 0.001$) (Figure 3G). In comparable experiments in the Col background, *fancc*, *fance* or *fancf* individual mutations barely increased bivalents in *msh4* ($P = 0.12$, 0.12 and 0.0002, respectively) (Figure 3G). This mild effect could explain why the anti-CO effect of *FANCE* was missed in previous studies (6). Combining Col *fancc, fance* and *fancf* mutations in *msh4* further restored

bivalent formation to reach an average of 2.8 bivalents/cell compared to 1.4 in *msh4* ($P < 0.0001$) and led to a slightly higher fertility increase compared to *fanccmsh4* ($P = 0.04$). Altogether, this suggests that FANCC, FANCE and FANCF limit CO formation in a partially redundant manner. Note that this restoration of bivalent formation is lesser than that obtained through mutation of *FANCM* (5 bivalents) (5), MHF1 or MHF2 (3.6 bivalents) (Figure 3G) (6), suggesting that the FANCC–FANCE–FANCF module has a supporting role in limiting a portion of the COs prevented by FANCM-MHF1-MHF2. The *fancc*mutation did not further restore bivalent formation in *mhf1 msh4* (*t*-test $P=0.56$), suggesting that FANCCacts in the same anti-CO pathway as MHF1 (Figure 3G).

FANCC, FANCE and FANCF regulate meiotic crossover formation

Intriguingly, in the above experiments, we found that *fancc*, *fance* and *fancf* increased the fertility of *zmm* mutants (*msh4* and *msh5*), but that the increase of bivalent number in male meiotic cells was less robust than the seed set suggested. As fertility in the self-pollinating plant Arabidopsis depends on both male and female meiosis, this may suggest that the role of FANCC, FANCE and FANCF in limiting COs is more critical in female meiosis than in male meiosis. Supporting this suggestion, the average number of bivalents at metaphase I of female meiosis was increased from 1.3 in *msh4* to 3.7 in *fancc-1 msh4* ($n = 9$ and $n = 7$, respectively, *t*-test $P = 0.0005$. Figure 4). Further, we used a test line for recombination (FTL420), which contains two transgenes conferring expression of GFP and RFP in the seed coat and defining a 5-Mb interval of the sub-telomeric region on chromosome 3 (52,53). Crossover frequency was measured for males and females separately, through reciprocal crosses with wild-type plants, and in selfing (Figure 5, Supplementary Table S3). In females, recombination was significantly increased (Fisher test, $P<0.0001$) in *fancc* and *fancc fance fancf* compared to wild type, confirming the anti-CO function of *FANCC* (Figure 5A). In males, crossover frequency was not increased, but slightly reduced ($P = 0.17$ for *fancc* and 0.015 for *fancc fance fancf*). In selfing, which combines male and female meiosis products, recombination was modestly increased in *fancc* compared to wild type ($P = 0.003$). A similar recombination picture was observed in *fance*, *fancf* and the triple mutant *fancc fance fancf*, suggesting that the three proteins act together in limiting meiotic crossovers (Figure 5A).

***fancc, fance*, and *fancf* exhibit chromosome fragmentation in the *mus81* background**

Because of the roles of FANCM, MHF1 andMHF2 in preventing class II COs, combining mutation in these genes with mutation of *MUS81* that catalyses class II COs, leads to chromosome fragmentation at meiosis, resulting in sterility. In addition, the *fancm mus81* double mutant shows a strong developmental defect, demonstrating the role of these two genes in somaticDNA repair (5,6)When we combined *fancc*, *fance*, or *fancf* with the *mus81* mutation, we did not observe developmental defects. However, in double mutants with *mus81* and either *fanc-c*, *-e* or *-f* we observed a strong reduction in fertility, measured by seed per fruit, compared to the respective single mutants (Figure 6A, Supplementary Figure S8). Meiotic chromosome spreads revealed the presence of chromosome fragments at anaphase I and subsequent stages in ~40% of the cells of the double mutants (Figure 6B–J, Supplementary Figure S9 A–D and F–I). This demonstrates that FANCC, FANCE, and FANCF are important for efficient DSB repair in a *mus81* background and suggests that they regulate class II CO formation but with a less critical role than FANCM and MHF1/2. The removal of all four genes—*mus81 fancc fance fancf*—did not drastically enhanced fertility defects or chromosome

fragmentation compared to the double *mus81 fancc* combinations. These results support the hypothesis that all three genes, *FANCC, FANCE* and *FANCF*, are required at meiosis to repair a subset of intermediates that can also be repaired by MUS81.

DISCUSSION

FANCC–FANCE–FANCF constitute a stable subcomplex within the FA core complex. Based on sequence conservation, FANCE and FANCF homologs have been identified in evolutionarily distant eukaryotes such as plants (6,58). However, despite multiple studies that systematically catalogued FA pathway protein conservation across diverse taxa, homologs of FANCC have not been identified beyond vertebrates (6,60), suggesting that FANCC may not be conserved over large evolutionary scales. Here, combining genetics, *in vivo* pull-downs, direct protein-protein interaction studies, and structural modeling, we unambiguously identified the FANCC protein in Arabidopsis. In addition, interaction and modeling studies strongly suggest that FANCC, FANCE and FANCF form a sub-complex in Arabidopsis as they do in vertebrates. Homologs of FANCC can also be readily identified in most other plants. As the plant and animal branches diverged very early in the eukaryotic tree of life (61), this suggests that the FA complex and notably the FANCC–E–F subcomplex was already present in the common ancestor of all living eukaryotes. The algorithm we used to detect divergent homologs succeeded in detecting the link between plant and vertebrate FANCC but failed to detect homologs in fungal lineages, except for a few species. As fungi are more closely related to animals than plants, this suggests that most of the fungal lineages have lost FANCC, or that the FANCC sequence has diverged beyond what we can recognize with current tools. Similarly, FANCC was detected in diverse animal lineages including some insects, but not in Drosophila, which can be attributed either to gene loss or to extreme divergence. We initially identified *FANCC* because its mutation can partially restore the fertility of CO-defective *zmm* mutants, in a similar manner to previously identified anti-CO factors and notably the FA complex components FANCM, MHF1, and MHF2 (5,6). We also found that mutation in either of the two other subunits of the FA CEF subcomplex, *fance* and *fancf*, improves the fertility of *zmm* mutants. Mutations in the three genes individually restored fertility of *zmm* to similar levels, but to a much lower level than previously obtained with *mhf1*, *mhf2* or *fancm*. Further, restoration of *zmm* fertility upon cumulative mutations in *fancc, fance* and *fancf* remained limited. This suggests that FANCC, FANCE and FANCF together regulate meiotic recombination, but with a less critical role than FANCM, MHF1, and MHF2. We observed an increased number of bivalents at male meiosis when mutating *fancc*, *fance* and *fancf* in *zmm* mutants, consistent with an anti-CO function. However, the increase in bivalents in males was limited compared to the observed increase in fertility, suggesting that male and female meiosis could be differently affected. Indeed, chromosome spreads of female meiosis revealed a large increase of bivalents numbers in *msh4 fancc* compared to *msh4*. We also observed a slight decrease in fertility and a low frequency of univalents in male meiocytes in single *fancc*, *fance* or *fancf*mutants, suggesting a pro-CO function. However, when assessing recombination by a genetic assay in *fancc* and *fancc fance fancf*, we observed a large increase in recombination in females and a small decrease in males. Altogether,we propose that FANCC–E–F regulatesmeiotic recombination, with a predominant anti-CO function in females, explaining the capacity of their mutation to restore the fertility of *zmm* mutants. Similar to FANCM and MHF1/MH2, we propose that FANCC–E–F prevents the formation of class II COs that are catalyzed by MUS81. Indeed, combining any of *fancc*, *fance* or *fancf* with the *mus81* mutation led to chromosome fragmentation at meiosis and reduced fertility (Figure 6). Combining the three mutations (*fancc fance fancf*) together had only a slightly increased effect compared to single mutants in the

capacity to increase fertility and bivalents of *zmm* mutants (Figures 1 and 3) or for synthetic meiotic catastrophe and reduced fertility when combined with *mus81* (Figure 6). Further, the recombination assay did not detect differences between the single *fancc* and the triple *fancc fance fancf* (Figure 5), suggesting that FANCC–FANCE–FANCF act together in regulating recombination. The capacity of the *fancc fance fancf* mutations to restore bivalent and fertility of the *zmm* mutants and to increase crossover frequencies is weaker than observed with mutation of MHF1⁄2 or FANCM(5,6). Further, the *fancc-2* has no additive effect with *mhf1* (Figure 3). Altogether, this shows that FANCC–FANCE–FANCF acts in the same anti-CO pathway as FANCM-MHF1⁄2, as also supported by the fact that they form a stable complex *in vivo* (Table 2). We propose that FANCC–FANCE– FANCF supports FANCM activity, which unwinds recombination intermediates and directs them to non-crossover repair. We favor the hypothesis that the meiotic crossoverlimiting role of Arabidopsis FANCC–E–F is distinct from the well-described somatic role of human FANC–C–E–F where it facilitates FANCD2–FANCI mono-ubiquitination in inter-strand crosslink repair. It is unclear if the crossoverlimiting role can be uncouple from the canonical role of the FA core complex as no other core complex components appear to exist in Arabidopsis, which would permit assessing this question. This hypothesis is supported by the following lines of evidence: (i) there is no detectable crossover-limiting role of neither of the Arabidopsis orthologues of the catalytic component of the human FA core complex—the E3 RING ligase, FANCL—and its substrate FANCD2-FANCI (6,62); (ii) human FANCM has well-described functions distinct from the FA core complex (29,63,64) that are associated with remodeling branched DNA structures. The FANCC–E–F complex may act to stabilize or support the activity of FANCM in performing its function of branched molecule dissolution during meiotic DSB repair. Finally, this work shows the value of model organisms to advance knowledge and stimulate new research questions in non-model species such as humans. While *Arabidopsis thaliana* may be a long way from humans, we feel these findings and others (60) create a compelling case that DNA repair functions of FANC genes predate vertebrates, and that there have likely multiple types of DNA repair, both somatic and meiotic.

DATA AVAILABILITY

The data underlying this article are available in the article and in its online supplementary material.

SUPPLEMENTARY DATA

Supplementary Data are available at NAR Online.

ACKNOWLEDGEMENTS

We thank Virginie Portemer for her help in *fancc-1* mapping; Piotr A. Ziolkowski for kindly providing the 420 FTL line; Peter Huijser andMiguel Vallebueno-Estrada for supporting with the FTL image analysis setup; VIB proteomics core facility for performing the Q Exactive analysis of the pull down samples and Neysan Donnelly for proofreading the manuscript.

FUNDING

Max Planck Society (to R.M.); Depart of Biotechnology Centre of Excellence grant (to I.S.); CEFIPRA project SMOKI(to R.M. and I.S.). Funding for open access charge: Max Planck Society. *Conflict of interest statement.* None declared.

REFERENCES

1. Borner,G.V., Kleckner,N. and Hunter,N. (2004) Crossover/noncrossover differentiation, synaptonemal complex formation, and regulatory surveillance at the leptotene/zygotene transition of meiosis. *Cell*, **117**, 29–45.
2. Pyatnitskaya,A., Borde,V. and De Muyt,A. (2019) Crossing and zipping: molecular duties of the ZMM proteins in meiosis. *Chromosoma*, **128**, 181–198.
3. Youds,J.L. and Boulton,S.J. (2011) The choice in meiosis – defining the factors that influence crossover or non-crossover formation. *J. Cell Sci.*, **124**, 501–513.
4. de los Santos,T., Hunter,N., Lee,C., Larkin,B., Loidl,J. and Hollingsworth,N.M. (2003) The Mus81/Mms4 endonuclease acts independently of double-Holliday junction resolution to promote a distinct subset of crossovers during meiosis in budding yeast. *Genetics*, **164**, 81–94.
5. Crismani,W., Girard,C., Froger,N., Pradillo,M., Santos,J.L., Chelysheva,L., Copenhaver,G.P., Horlow,C. and Mercier,R. (2012) FANCM limits meiotic crossovers. *Science*, **336**, 1588–1590.
6. Girard,C., Crismani,W., Froger,N., Mazel,J., Lemhemdi,A., Horlow,C. and Mercier,R. (2014) FANCM-associated proteins MHF1 and MHF2, but not the other Fanconi anemia factors, limit meiotic crossovers. *Nucleic Acids Res.*, **42**, 9087–9095.
7. Singh,T.R., Saro,D., Ali,A.M., Zheng,X.F., Du,C.H., Killen,M.W., Sachpatzidis,A., Wahengbam,K., Pierce,A.J., Xiong,Y. *et al.* (2010) MHF1-MHF2, a histone-fold-containing protein complex, participates in the Fanconi anemia pathway via FANCM. *Mol. Cell*, **37**, 879–886.
8. Tao,Y., Jin,C., Li,X., Qi,S., Chu,L., Niu,L., Yao,X. and Teng,M. (2012) The structure of the FANCM-MHF complex reveals physical features for functional assembly. *Nat. Commun.*, **3**, 782.
9. Seguela-Arnaud,M., Choinard,S., Larcheveque,C., Girard,C., Froger,N., Crismani,W. and Mercier,R. (2017) RMI1 and TOP3alpha limit meiotic CO formation through their C-terminal domains. *Nucleic Acids Res.*, **45**, 1860–1871.
10. Girard,C., Chelysheva,L., Choinard,S., Froger,N., Macaisne,N., Lemhemdi,A., Mazel,J., Crismani,W. and Mercier,R. (2015) AAA-ATPase FIDGETIN-LIKE 1 and helicase FANCM antagonize meiotic crossovers by distinct mechanisms. *PLoS Genet.*, **11**, e1005369.
11. Fernandes,J.B., Duhamel,M., Seguela-Arnaud,M., Froger,N., Girard,C., Choinard,S., Solier,V., De Winne,N., De Jaeger,G., Gevaert,K. *et al.* (2018) FIGL1 and its novel partner FLIP form a conserved complex that regulates homologous recombination. *PLoS Genet.*, **14**, e1007317.
12. Kumar,R., Duhamel,M., Coutant,E., Ben-Nahia,E. and Mercier,R. (2019) Antagonism between BRCA2 and FIGL1 regulates homologous recombination. *Nucleic Acids Res.*, **47**, 5170–5180.
13. Fernandes,J.B., Seguela-Arnaud,M., Larcheveque,C., Lloyd,A.H. and Mercier,R. (2018) Unleashing meiotic crossovers in hybrid plants. *Proc. Natl. Acad. Sci. U.S.A.*, **115**, 2431–2436.
14. Kolinjivadi,A.M., Crismani,W. and Ngeow,J. (2020) Emerging functions of Fanconi anemia genes in replication fork protection pathways. *Hum. Mol. Genet.*, **29**, R158–R164.
15. Yan,Z., Delannoy,M., Ling,C., Daee,D., Osman,F., Muniandy,P.A., Shen,X., Oostra,A.B., Du,H., Steltenpool,J. *et al.* (2010) A histone-fold complex and

FANCM form a conserved DNA-remodeling complex to maintain genome stability. *Mol. Cell*, **37**, 865–878.
16. Smogorzewska,A., Matsuoka,S., Vinciguerra,P.,McDonald,E.R. 3rd, Hurov,K.E., Luo,J., Ballif,B.A., Gygi,S.P., Hofmann,K., D'Andrea,A.D. *et al.* (2007) Identification of the FANCI protein, a monoubiquitinated FANCD2 paralog required for DNA repair. *Cell*, **129**, 289–301.
17. Wang,R., Wang,S., Dhar,A., Peralta,C. and Pavletich,N.P. (2020) DNA clamp function of the monoubiquitinated Fanconi anaemia ID complex. *Nature*, **580**, 278–282.
18. Alcon,P., Shakeel,S., Chen,Z.A., Rappsilber,J., Patel,K.J. and Passmore,L.A. (2020) FANCD2-FANCI is a clamp stabilized on DNA by monoubiquitination of FANCD2 during DNA repair. *Nat. Struct. Mol. Biol.*, **27**, 240–248.
19. Tan,W., van Twest,S., Leis,A., Bythell-Douglas,R., Murphy,V.J., Sharp,M., Parker,M.W., Crismani,W. and Deans,A.J. (2020) Monoubiquitination by the human Fanconi anemia core complex clamps FANCI:FANCD2 on DNA in filamentous arrays. *Elife*, **9**, e54128.
20. Rennie,M.L., Lemonidis,K., Arkinson,C., Chaugule,V.K., Clarke,M., Streetley,J., Spagnolo,L. and Walden,H. (2020) Differential functions of FANCI and FANCD2 ubiquitination stabilize ID2 complex on DNA. *EMBO Rep.*, **21**, e50133.
21. Lopez-Martinez,D., Kupculak,M., Yang,D., Yoshikawa,Y., Liang,C.C., Wu,R., Gygi,S.P. and Cohn,M.A. (2019) Phosphorylation of FANCD2 Inhibits the FANCD2/FANCI complex and suppresses the Fanconi anemia pathway in the absence of DNA damage. *Cell Rep.*, **27**, 2990–3005.
22. Kottemann,M.C. and Smogorzewska,A. (2013) Fanconi anaemia and the repair of Watson and Crick DNA crosslinks. *Nature*, **493**, 356–363.
23. Deakyne,J.S. and Mazin,A.V. (2011) Fanconi anemia: at the crossroads of DNA repair. *Biochemistry (Mosc)*, **76**, 36–48.
24. Shakeel,S., Rajendra,E., Alcon,P., O'Reilly,F., Chorev,D.S., Maslen,S., Degliesposti,G., Russo,C.J., He,S., Hill,C.H. *et al.* (2019) Structure of the Fanconi anaemia monoubiquitin ligase complex. *Nature*, **575**, 234–237.
25. Swuec,P., Renault,L., Borg,A., Shah,F., Murphy,V.J., van Twest,S., Snijders,A.P., Deans,A.J. and Costa,A. (2017) The FA core complex contains a homo-dimeric catalytic module for the symmetric mono-ubiquitination of FANCI-FANCD2. *Cell Rep.*, **18**, 611–623.
26. Huang,Y., Leung,J.W., Lowery,M., Matsushita,N.,Wang,Y., Shen,X., Huong,D., Takata,M., Chen,J. and Li,L. (2014) Modularized functions of the Fanconi anemia core complex. *Cell Rep.*, **7**, 1849–1857.
27. Rajendra,E., Oestergaard,V.H., Langevin,F.,Wang,M., Dornan,G.L., Patel,K.J. and Passmore,L.A. (2014) The genetic and biochemical basis of FANCD2 monoubiquitination. *Mol. Cell*, **54**, 858–869.
28. Leveille,F., Blom,E., Medhurst,A.L., Bier,P., Laghmani el,H., Johnson,M., Rooimans,M.A., Sobeck,A., Waisfisz,Q., Arwert,F. *et al.* (2004) The Fanconi anemia gene product FANCF is a flexible adaptor protein. *J. Biol. Chem.*, **279**, 39421–39430.
29. Deans,A.J. and West,S.C. (2009) FANCM connects the genome instability disorders Bloom's syndrome and Fanconi Anemia. *Mol. Cell*, **36**, 943–953.
30. Higgins,J.D., Vignard,J., Mercier,R., Pugh,A.G., Franklin,F.C. and Jones,G.H. (2008) AtMSH5 partners AtMSH4 in the class I meiotic crossover pathway in *Arabidopsis thaliana*, but is not required for synapsis. *Plant J.*, **55**, 28–39.

31. Berchowitz,L.E., Francis,K.E., Bey,A.L. and Copenhaver,G.P. (2007) The role of AtMUS81 in interference-insensitive crossovers in A. thaliana. *PLos Genet.*, **3**, e132.
32. Schneeberger,K., Ossowski,S., Ott,F., Klein,J.D., Wang,X., Lanz,C., Smith,L.M., Cao,J., Fitz,J., Warthmann,N. *et al.* (2011) Reference-guided assembly of four diverse Arabidopsis thaliana genomes. *Proc. Natl. Acad. Sci. U.S.A.*, **108**, 10249–10254.
33. Zimmermann,L., Stephens,A., Nam,S.Z., Rau,D., Kubler,J., Lozajic,M., Gabler,F., Soding,J., Lupas,A.N. and Alva,V. (2018) A completely reimplemented MPI bioinformatics toolkit with a new HHpred server at its core. *J. Mol. Biol.*, **430**, 2237–2243.
34. Soding,J. (2005) Protein homology detection by HMM-HMM comparison. *Bioinformatics*, **21**, 951–960.
35. Altschul,S.F., Madden,T.L., Schaffer,A.A., Zhang,J., Zhang,Z., Miller,W. and Lipman,D.J. (1997) Gapped BLAST and PSI-BLAST: a new generation of protein database search programs. *Nucleic Acids Res.*, **25**, 3389–3402.
36. Katoh,K. and Standley,D.M. (2013) MAFFT multiple sequence alignment software version 7: improvements in performance and usability. *Mol. Biol. Evol.*, **30**, 772–780.
37. Waterhouse,A.M., Procter,J.B., Martin,D.M., Clamp,M. and Barton,G.J. (2009) Jalview Version 2–a multiple sequence alignment editor and analysis workbench. *Bioinformatics*, **25**, 1189–1191.
38. Dereeper,A., Guignon,V., Blanc,G., Audic,S., Buffet,S., Chevenet,F., Dufayard,J.F., Guindon,S., Lefort,V., Lescot,M. *et al.* (2008) Phylogeny.fr: robust phylogenetic analysis for the non-specialist. *Nucleic Acids Res.*, **36**, W465–W469.
39. Letunic,I. and Bork,P. (2021) Interactive Tree Of Life (iTOL) v5: an online tool for phylogenetic tree display and annotation. *Nucleic Acids Res.*, **49**, W293–W296.
40. Steinegger,M. and Soding,J. (2017) MMseqs2 enables sensitive protein sequence searching for the analysis of massive data sets. *Nat. Biotechnol.*, **35**, 1026–1028.
41. Mirdita,M., von den Driesch,L., Galiez,C., Martin,M.J., Soding,J. and Steinegger,M. (2017) Uniclust databases of clustered and deeply annotated protein sequences and alignments. *Nucleic Acids Res.*, **45**, D170–D176.
42. Mirdita,M., Sch¨utze,K., Moriwaki,Y., Heo,L., Ovchinnikov,S. and Steinegger,M. (2022) ColabFold: making protein folding accessible to all. *Nat. Methods*, **19**, 679–682.
43. Jumper,J., Evans,R., Pritzel,A., Green,T., Figurnov,M., Ronneberger,O., Tunyasuvunakool,K., Bates,R., Zidek,A., Potapenko,A. *et al.* (2021) Highly accurate protein structure prediction with AlphaFold. *Nature*, **596**, 583–589.
44. Evans,R., O'Neill,M., Pritzel,A., Antropova,N., Senior,A., Green,T., ˇZ´ıdek,A., Bates,R., Blackwell,S., Yim,J. *et al.* (2021) Protein complex prediction with AlphaFold-Multimer. bioRxiv doi: https://doi.org/10.1101/2021.10.04.463034, 10 March 2022, preprint: not peer reviewed.
45. Leman,J.K., Weitzner,B.D., Lewis,S.M., Adolf-Bryfogle,J., Alam,N., Alford,R.F., Aprahamian,M., Baker,D., Barlow,K.A., Barth,P. *et al.* (2020) Macromolecular modeling and design in Rosetta: recent methods and frameworks. *Nat. Methods*, **17**, 665–680.

46. Ashkenazy, H., Abadi, S., Martz, E., Chay, O., Mayrose, I., Pupko, T. and Ben-Tal, N. (2016) ConSurf 2016: an improved methodology to estimate and visualize evolutionary conservation in macromolecules. *Nucleic. Acids. Res.*, **44**, W344–W350.
47. Ross, K.J., Fransz, P. and Jones, G.H. (1996) A light microscopic atlas of meiosis in Arabidopsis thaliana. *Chromosome Res.*, **4**, 507–516.
48. Rossignol, P., Collier, S., Bush, M., Shaw, P. and Doonan, J.H. (2007) Arabidopsis POT1A interacts with TERT-V(I8), an N-terminal splicing variant of telomerase. *J. Cell Sci.*, **120**, 3678–3687.
49. Van Leene,J., Han,C., Gadeyne,A., Eeckhout,D., Matthijs,C., Cannoot,B., De Winne,N., Persiau,G., Van De Slijke,E., Van de Cotte,B. *et al.* (2019) Capturing the phosphorylation and protein interaction landscape of the plant TOR kinase. *Nat Plants*, **5**, 316–327.
50. Cromer,L., Jolivet,S., Singh,D.K., Berthier,F., De Winne,N., De Jaeger,G., Komaki,S., Prusicki,M.A., Schnittger,A., Guerois,R. *et al.* (2019) Patronus is the elusive plant securin, preventing chromosome separation by antagonizing separase. *Proc. Natl. Acad. Sci. U.S.A.*,**116**, 16018–16027.
51. Van Leene,J., Eeckhout,D., Cannoot,B., De Winne,N., Persiau,G., Van De Slijke,E., Vercruysse,L., Dedecker,M., Verkest,A., Vandepoele,K. *et al.* (2015) An improved toolbox to Unravel the Plant cellular machinery by tandem affinity purification of Arabidopsis protein complexes. *Nat. Protoc.*, **10**, 169–187.
52. Ziolkowski,P.A., Berchowitz,L.E., Lambing,C., Yelina,N.E., Zhao,X., Kelly,K.A., Choi,K., Ziolkowska,L., June,V., Sanchez-Moran,E. *et al.* (2015) Juxtaposition of heterozygous and homozygous regions causes reciprocal crossover remodelling via interference during Arabidopsis meiosis. *Elife*, **4**, e03708.
53. Melamed-Bessudo, C., Yehuda, E., Stuitje, A.R. and Levy, A.A. (2005) A new seed-based assay for meiotic recombination in Arabidopsis thaliana. *Plant J.*, **43**, 458–466.
54. Schindelin,J., Arganda-Carreras,I., Frise,E., Kaynig,V., Longair,M., Pietzsch,T., Preibisch,S., Rueden,C., Saalfeld,S., Schmid,B. *et al.* (2012) Fiji: an open-source platform for biological-image analysis. *Nat. Methods*, **9**, 676–682.
55. Zapata,L., Ding,J., Willing,E.M., Hartwig,B., Bezdan,D., Jiao,W.B., Patel,V., Velikkakam James,G., Koornneef,M., Ossowski,S. *et al.* (2016) Chromosome-level assembly of Arabidopsis thaliana Ler reveals the extent of translocation and inversion polymorphisms. *Proc. Natl. Acad. Sci. U.S.A.*, **113**, E4052–E4060.
56. Stanley, E.C., Azzinaro, P.A., Vierra, D.A., Howlett, N.G. and Irvine, S.Q. (2016) The Simple Chordate Ciona intestinalis Has a Reduced Complement of Genes Associated with Fanconi Anemia. *Evol. Bioinform. Online*, **12**, 133–148.
57. Wang, S., Wang, R., Peralta, C., Yaseen, A. and Pavletich, N.P. (2021) Structure of the FA core ubiquitin ligase closing the ID clamp on DNA. *Nat. Struct. Mol. Biol.*, **28**, 300–309.
58. Cheng, C.Y., Krishnakumar, V., Chan, A.P., Thibaud-Nissen, F., Schobel, S. and Town, C.D. (2017) Araport11: a complete reannotation of the *Arabidopsis thaliana* reference genome. *Plant J.*, **89**, 789–804.
59. Klepikova, A.V., Kasianov, A.S., Gerasimov, E.S., Logacheva, M.D. and Penin, A.A. (2016) A high resolution map of the *Arabidopsis thaliana* developmental transcriptome based on RNA-seq profiling. *Plant J.*, **88**, 1058–1070.

60. Zhang,X.Y., Langenick,J., Traynor,D., Babu,M.M., Kay,R.R. and Patel,K.J. (2009) Xpf and not the Fanconi anaemia proteins or Rev3 accounts for the extreme resistance to cisplatin in Dictyostelium discoideum. *PLoS Genet.*, **5**, e1000645.
61. . Burki,F., Roger,A.J., Brown,M.W. and Simpson,A.G.B. (2020) The new tree of eukaryotes. *Trends Ecol. Evol.*, **35**, 43–55.
62. Kurzbauer,M.T., Pradillo,M., Kerzendorfer,C., Sims,J., Ladurner,R., Oliver,C., Janisiw,M.P., Mosiolek,M., Schweizer,D., Copenhaver,G.P. *et al.* (2018) *Arabidopsis thaliana* FANCD2 promotes meiotic crossover formation. *Plant Cell*, **30**, 415–428.
63. Walden,H. and Deans,A.J. (2014) The Fanconi anemia DNA repair pathway: structural and functional insights into a complex disorder. *Annu. Rev. Biophys.*, **43**, 257–278.
64. Ito,S. and Nishino,T. (2021) Structural analysis of the chicken FANCM-MHF complex and its stability. *Acta Crystallogr. F Struct. Biol. Commun.*, **77**, 1–7.

Figure 1. Analysis of fertility of *zmm* suppressor mutants. (**A**) Each dot indicates the fertility of an individual plant, measured as the number of seeds per fruit averaged on 10 fruits. The mean fertility for each genotype is shown by a red bar. Each mutant was compared to sibling controls grown together, and the data of independent experiments are shown in Supplementary Figure S2. Some genotypes were represented in several experiments and their data were pooled for this figure. Stars summarize the one-way ANOVA followed by Sidak test shown in Supplementary Figure S2. (**B**–**E**) Representative fruits of *wild type, fancc-2, msh4*, and *fancc-2 msh4*, cleared with 70% ethanol.

Figure 2. Structural analysis of the experimental human and modeled A. *thaliana* FANCC-FANCE–FANCF complexes. (**A**) Structural representation of the human FANC core complex (PDB:7KZP) (57) Most of the subunits are shown in gray with the exception of those in direct contact with the human FANCC (light green), namely hFANCE (light pink), hFANCL (yellow) and hFANCF (light blue). A zoomed-in view of the four subunits is shown in the inset on the right with the contact region between hFANCL and hFANCC highlighted by a dotted rectangle. (**B**) AlphaFold2 structural model of the AtFANCC-AtFANCE-AtFANCF complex represented as a cartoon in two orientations with a dotted square indicating the C-terminal domain of FANCE located in a region of FANCC that directly binds to the FANCL subunit in the human FANC core complex structure. (**C**) Same view as (B) with AtFANCC shown as a surface and colored according to conservation from white to red for the least to most conserved positions. Pymol software was used to draw the different structures (The PyMOL Molecular Graphics System, Version 2.0 Schr¨odinger, LLC).

Figure 3. Metaphase I chromosome spreads of malemeiocytes. (**A**)Wild type with five bivalents, (**B**) *msh4* with one bivalent, (**C**) *fancc-2* with four bivalents and one pair of univalents. (**D**) *fancc-2* with five bivalents. (**E**) *fancc-2 msh4* with two bivalents. (**F**) *fancc-2 fance fancf msh4* with two bivalents. Scale bar, 10 _m. (**G**) Quantification of bivalents at metaphase I. The proportion of cells with 0–5 bivalents is shown with a color code. The number of analyzed cells and the average bivalent number per cell is shown for each genotype. All the genotypes are in the Col background, except when Ler is mentioned.

Figure 4. Metaphase I chromosome spreads of female meiocytes. (**A**) Quantification of bivalents at female metaphase I. Each dot indicates the bivalent number of individual meiotic cells. The mean bivalent number for each genotype is shown by a red bar. (**B**) Female *msh4* meiocyte with one bivalent. (**C**) Female *fancc-2 msh4* meiocyte with four bivalents. Scale bar, 10 _m.

Figure 5. Recombination in *fancc*, *fance* and *fancf*mutant. (**A**)Recombination was measured in seeds produced by crosses with wild type (female and male) or after selfing. Each dot represents the recombination frequency measured in an individual plant, and the red lines show the mean. *P* values are from two-sided Fisher's exact test on the proportion of recombined seeds. Raw data are shown in Supplementary Table S3 (**B**–**E**). Representative image of seeds from a 420/++ hemizygote imaged under bright-field, red fluorescence channel, green fluorescence channel, and merged fluorescence.

Figure 6. Combining *fanc* and *mus81* mutations lead to reduced fertility and chromosome fragmentation at meiosis. (**A**) Each dot indicates the fertility of an individual plant, measured as the number of seeds per fruit averaged on ten fruits. The means for each genotype are shown by red bars. Each double mutant was compared to sibling controls grown together; the independent experiments are shown in Supplementary Figure S8. Wild type and *mus81* control were represented in several experiments and their data are pooled in this plot. (**B**) Quantification of cells with and without chromosome fragments. N = number of cells analyzed for each genotype. Stars summarize the one-way ANOVA followed by Sidak test shown in Supplementary Figure S8. (C–J) Chromosome spreads of male meiocytes (Scale bar, 10 _m). Arrow heads indicate chromosome fragments. (**C**, **G**) *mus81*. (**D**,**H**) *fancc-2 mus81.* (**E**, **I**) *fancemus81* (**F**, **J**) *fancf mus81.*

Table 1. Summary of the *zmm* suppressor screen results

		Number of alleles identified in each screen					
	Number of M2 populations screened	total ~7000	*zip4* ~2000	*hei10* ~2000	*msh5* ~1000	*shoc1* ~1000	*msh4 (Ler)* ~1000
identified gene	*FANCC*	**1**					1
	FANCM	**29**	5	5	4	8	7
	MHF2	**4**	1	2			1
	TOP3	**4**		3			1
	RECQ4	**3**					3
	RMI1	**2**				1	1
	FIGL1	**15**	2	5	3	3	2
	FLIP	**1**		1			
	total	**59**	8	16	7	12	16

A suppressor screen was performed in five *zmm* mutants (*zip4, hei10, msh5, shoc1* and *msh4*). One to two thousand independent M2 populations were screened for each *zmm*. At total of 59 causal mutations falling in eight genes were identified and we report the number of alleles identified per gene and per screen. The colors represent three distinct pathways (FA blue, BTR green, FIGL1 red). Note that *msh4* is in the Ler background while others are in Col. As *RECQ4* is duplicated in Col but not in Ler, it could be found only in the *msh4* screen. The list of mutant alleles is shown in Supplementary Table S2.

Table 2. Pull-down protein purification using AT3G60310/FANCC as bait

Gene Id	Protein name	CGSrhino PD1	CGSrhino PD2	CGSrhino PD3
AT3G60310	FANCC	19	18	15
AT4G29560	FANCE	6	4	5
AT5G65740	FANCL	5	4	4
AT1G78790	MHF2	2	-	3
AT1G35530	FANCM*	2	-	-

Three replicates of pull-down purifications (PD1, PD2 and PD3) followed by mass spectrometry were performed using FANCC as a bait. After filtering (see material and methods), the number of specific peptides is reported for each identified protein. *Only identified in one experiment. MS data are shown in Supplementary Table S4.

Graphical abstract

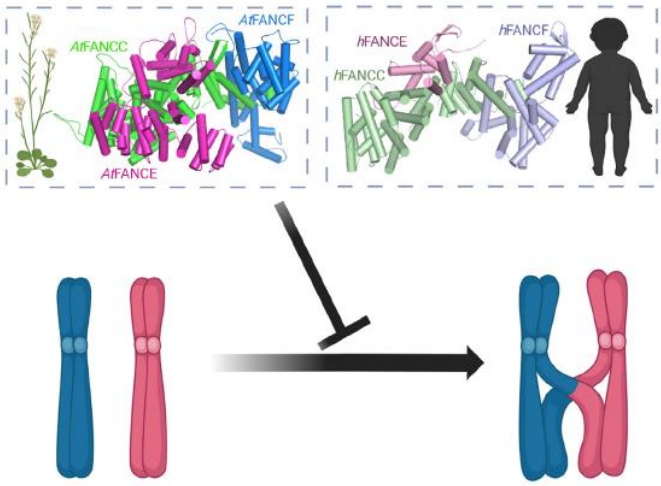

Figure 1

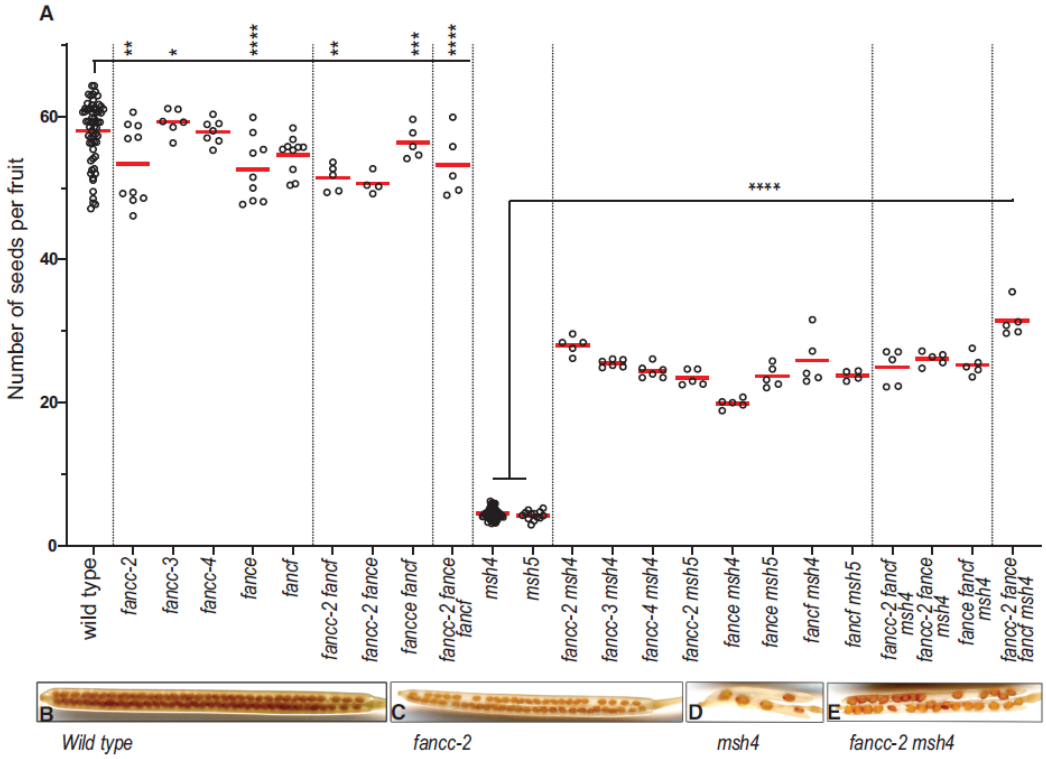

Figure 2

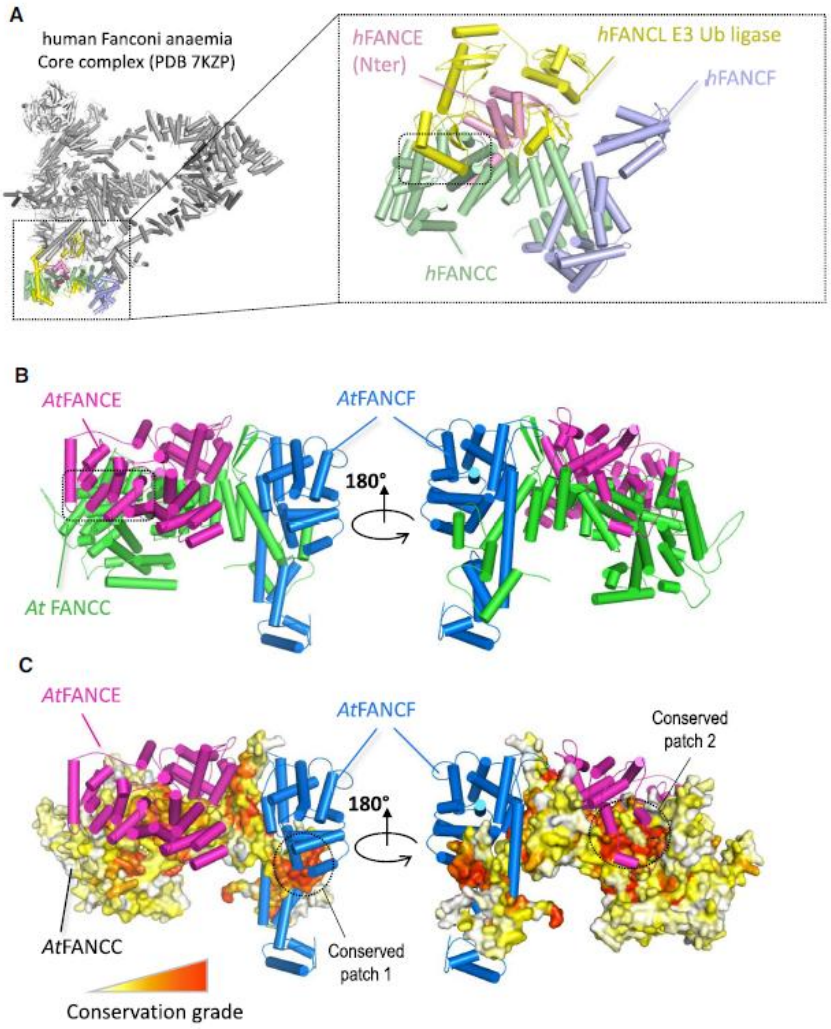
A
human Fanconi anaemia
Core complex (PDB 7KZP)
hFANCE
(Nter)
hFANCL E3 Ub ligase
hFANCF
hFANCC
B
AtFANCE
AtFANCF
180°
At FANCC
C
AtFANCE
AtFANCF
Conserved
patch 2
180°
AtFANCC
Conserved
patch 1
Conservation grade

Figure 3

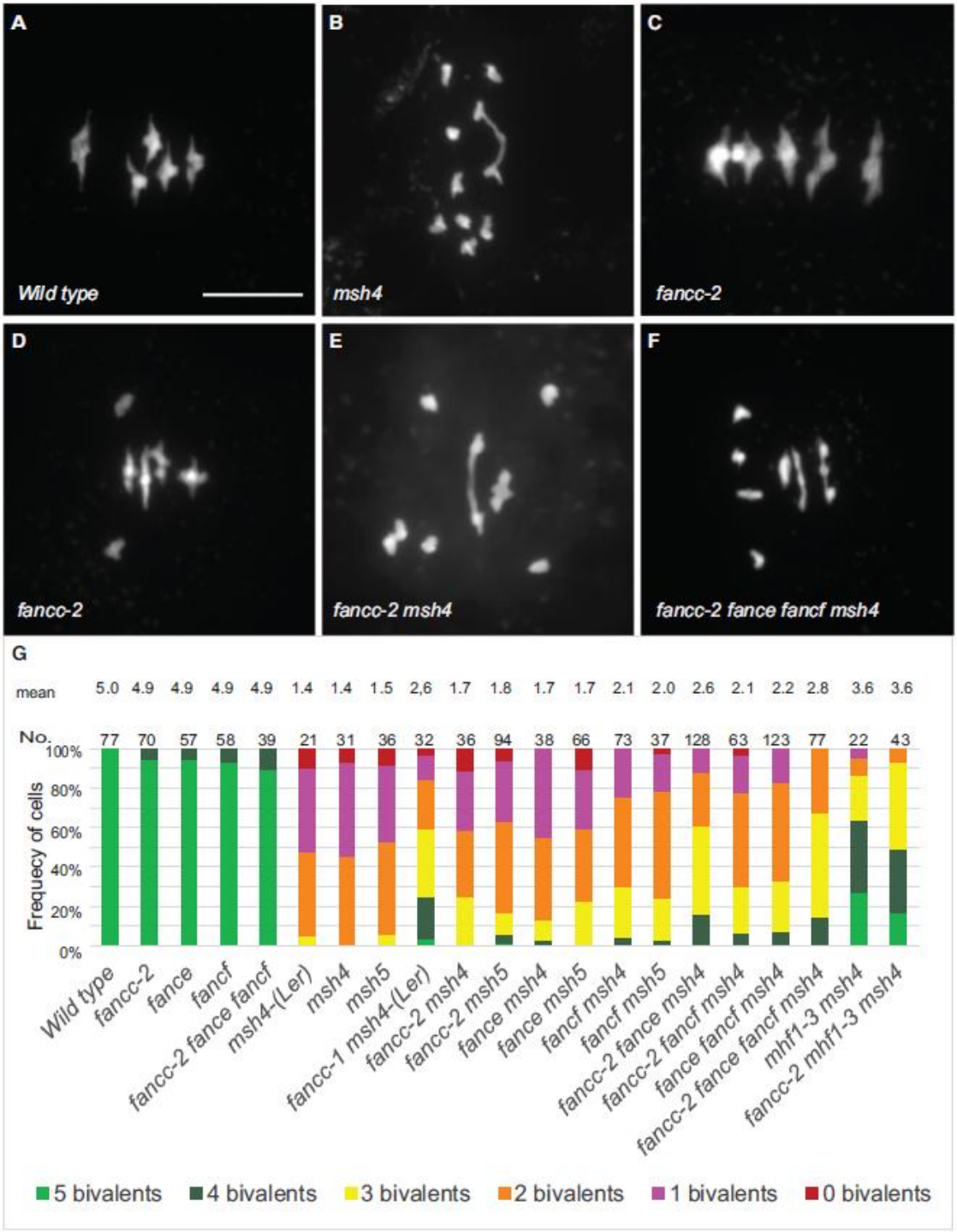
A
Wild type
B
msh4
C
fancc-2
D
fancc-2
E
fancc-2 msh4
F
fancc-2 fance fancf msh4
G
mean 5.0 4.9 4.9 4.9 4.9 1.4 1.4 1.5 2,6 1.7 1.8 1.7 1.7 2.1 2.0 2.6 2.1 2.2 2.8 3.6 3.6
No. 77 70 57 58 39 21 31 36 32 36 94 38 66 73 37 128 63 123 77 22 43
Frequecy of cells
100%
80%
60%
40%
20%
0%
Wild type
fancc-2
fance
fancf
fancc-2 fance fancf
msh4-(Ler)
msh4
msh5
fancc-1 msh4-(Ler)
fancc-2 msh4
fancc-2 msh5
fance msh4
fance msh5
fancf msh4
fancf msh5
fancc-2 fance msh4
fancc-2 fancf msh4
fance fancf msh4
fancc-2 fance fancf msh4
mhf1-3 msh4
fancc-2 mhf1-3 msh4
5 bivalents
4 bivalents
3 bivalents
2 bivalents
1 bivalents
0 bivalents

Figure 4

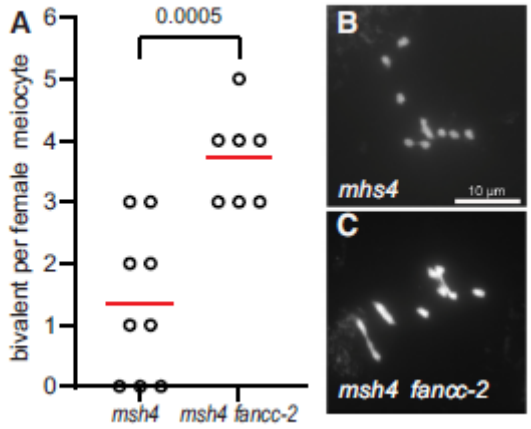
A
0.0005
bivalent per female meiocyte
0
1
2
3
4
5
6
msh4
msh4 fancc-2
B
mhs4
10 µm
C
msh4 fancc-2

Figure 5

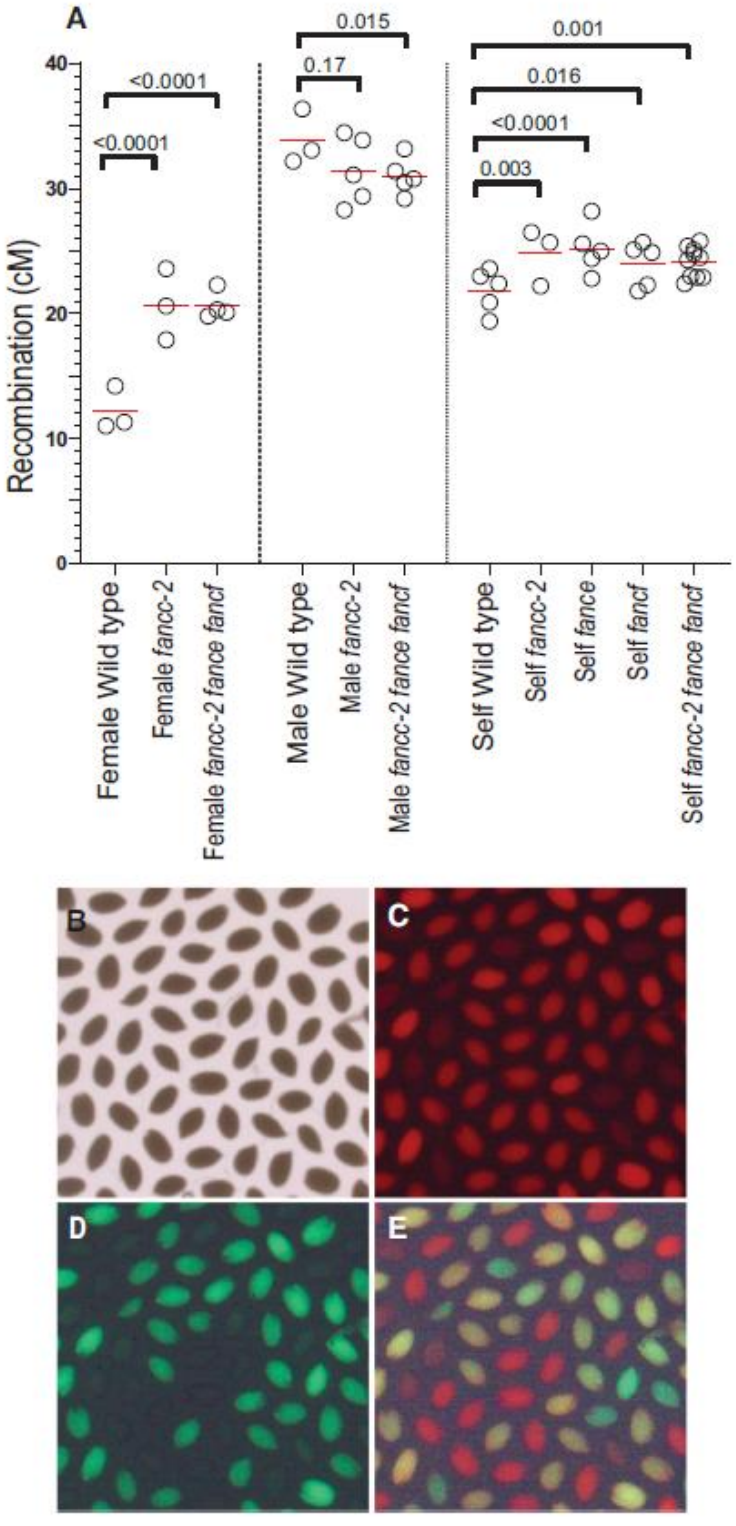
A
Recombination (cM)
40
30
20
10
0
<0.0001
<0.0001
0.015
0.17
0.001
0.016
<0.0001
0.003
Female Wild type
Female fancc-2
Female fancc-2 fance fancf
Male Wild type
Male fancc-2
Male fancc-2 fance fancf
Self Wild type
Self fancc-2
Self fance
Self fancf
Self fancc-2 fance fancf
B
C
D
E

Figure 6

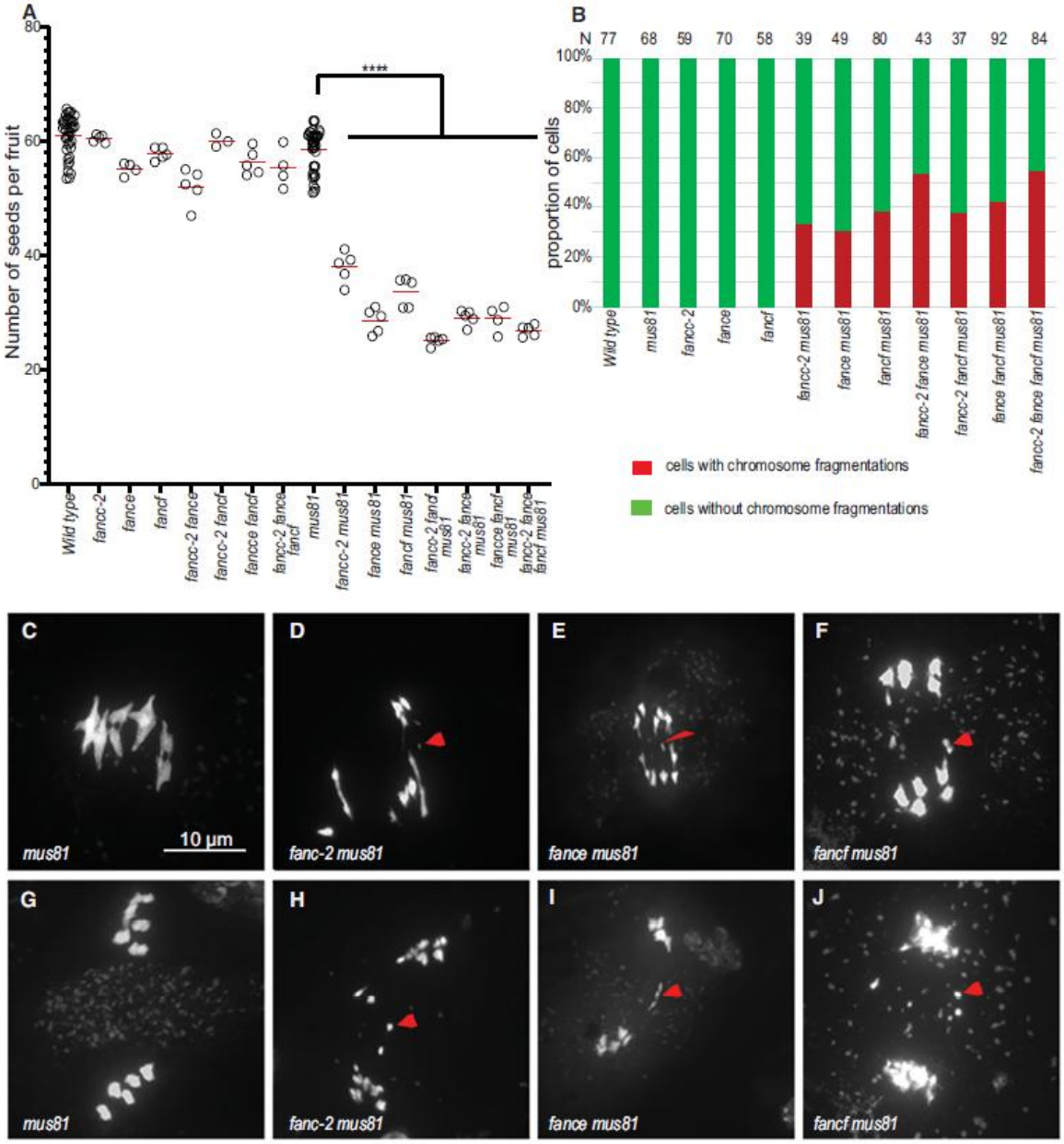
A
Number of seeds per fruit
****
Wild type
fancc-2
fance
fancf
fancc-2 fance
fancc-2 fancf
fancce fancf
fancc-2 fance fancf
mus81
fancc-2 mus81
fance mus81
fancf mus81
fancc-2 fancf mus81
fancc-2 fance mus81
fancce fancf mus81
fancc-2 fance fancf mus81
B
N 77 68 59 70 58 39 49 80 43 37 92 84
proportion of cells
cells with chromosome fragmentations
cells without chromosome fragmentations
C
mus81
10 µm
D
fanc-2 mus81
E
fance mus81
F
fancf mus81
G
mus81
H
fanc-2 mus81
I
fance mus81
J
fancf mus81

Agnès Bergerat, Bernard de Massy, Danielle Gadelle, Paul-Christophe Varoutas, Alain Nicolas, & Patrick Forterre. (1997). An atypical topoisomerase II from archaea with implications for meiotic recombination. *Nature*, *386*(MARCH), 414–417.

Ahmed, H. I., Heuberger, M., Schoen, A., Koo, D., Quiroz-chavez, J., Adhikari, L., … Krattinger, S. G. (2023). *Einkorn genomics sheds light on history of the oldest domesticated wheat*. https://doi.org/10.1038/s41586-023-06389-7

Alexander, M. P. (1969). Differential staining of aborted and nonaborted pollen. *Biotechnic and Histochemistry*, *44*(3), 117–122. https://doi.org/10.3109/10520296909063335

Altemose, N., Logsdon, G. A., Bzikadze, A. V., Sidhwani, P., Langley, S. A., Caldas, G. V., … Miga, K. H. (2022). Complete genomic and epigenetic maps of human centromeres. *Science*, *376*(6588), 1–30. https://doi.org/10.1126/science.abl4178

Anderson, L. K., Lohmiller, L. D., Tang, X., Hammond, D. B., Javernick, L., Shearer, L., … Falque, M. (2014). Combined fluorescent and electron microscopic imaging unveils the specific properties of two classes of meiotic crossovers. *Proceedings of the National Academy of Sciences of the United States of America*, *111*(37), 13415–13420. https://doi.org/10.1073/pnas.1406846111

Armstrong, S. J., Caryl, A. P., Jones, G. H., & Franklin, F. C. H. (2002). ASY1, a protein required for meiotic chromosome synapsis, localizes to axis-associated chromatin in Arabidopsis and Brassica. *Journal of Cell Science*, *115*(Pt 18), 3645–3655. https://doi.org/10.1242/jcs.00048

Börner, G. V., Kleckner, N., & Hunter, N. (2004). Crossover/Noncrossover Differentiation, Synaptonemal Complex Formation, and Regulatory Surveillance at the Leptotene/Zygotene Transition of Meiosis. *Cell*, *117*, 29–45. Retrieved from https://doi.org/10.1016/S0092-8674(04)00292-2

Buonomo, S. B. C., Clyne, R. K., Fuchs, J., Loidl, J., Uhlmann, F., & Nasmyth, K. (2000). Disjunction of homologous chromosomes in meiosis I depends on proteolytic cleavage of the meiotic cohesin Rec8 by separin. *Cell*, *103*(3), 387–398. https://doi.org/10.1016/S0092-8674(00)00131-8

Cai, X., Dong, F., Edelmann, R. E., & Makaroff, C. a. (2003). The Arabidopsis SYN1 cohesin protein is required for sister chromatid arm cohesion and homologous chromosome pairing. *Journal of Cell Science*, *116*(Pt 14), 2999–3007. https://doi.org/10.1242/jcs.00601

Capilla-Pérez, L., Durand, S., Hurel, A., Lian, Q., Chambon, A., Taochy, C., … Mercier, R. (2021). The synaptonemal complex imposes crossover interference and heterochiasmy in Arabidopsis. *Proceedings of the National Academy of Sciences of the United States of America*, *118*(12), 1–11. https://doi.org/10.1073/pnas.2023613118

Chan, G. K., Liu, S. T., & Yen, T. J. (2005). Kinetochore structure and function. *Trends in Cell Biology*, *15*(11), 589–598. https://doi.org/10.1016/j.tcb.2005.09.010

Chelysheva, L., Diallo, S., Vezon, D., Gendrot, G., Vrielynck, N., Belcram, K., … Grelon, M. (2005). AtREC8 and AtSCC3 are essential to the monopolar

orientation of the kinetochores during meiosis. *Journal of Cell Science*, *118*(20), 4621–4632. https://doi.org/10.1242/jcs.02583

Chelysheva, L., Vezon, D., Chambon, A., Gendrot, G., Pereira, L., Lemhemdi, A., … Grelon, M. (2012). The Arabidopsis HEI10 is a new ZMM protein related to Zip3. *PLoS Genetics*, *8*(7). https://doi.org/10.1371/journal.pgen.1002799

Chen, J., Wang, Z., Tan, K., Huang, W., Shi, J., Li, T., … Lai, J. (2023). A complete telomere-to-telomere assembly of the maize genome. *Nature Genetics*, *55*(July). https://doi.org/10.1038/s41588-023-01419-6

Cheng, C. H., Lo, Y. H., Liang, S. S., Ti, S. C., Lin, F. M., Yeh, C. H., … Wang, T. F. (2006). SUMO modifications control assembly of synaptonemal complex and polycomplex in meiosis of Saccharomyces cerevisiae. *Genes and Development*, *20*(15), 2067–2081. https://doi.org/10.1101/gad.1430406

Cheng, C. Y., Krishnakumar, V., Chan, A. P., Thibaud-Nissen, F., Schobel, S., & Town, C. D. (2017). Araport11: a complete reannotation of the Arabidopsis thaliana reference genome. *Plant Journal*, *89*(4), 789–804. https://doi.org/10.1111/tpj.13415

Choi, K., & Henderson, I. R. (2015). Meiotic recombination hotspots - A comparative view. *Plant Journal*, *83*(1), 52–61. https://doi.org/10.1111/tpj.12870

Choi, K., Reinhard, C., Serra, H., Ziolkowski, P. A., Underwood, C. J., Zhao, X., … Henderson, I. R. (2016). Recombination Rate Heterogeneity within Arabidopsis Disease Resistance Genes. *PLoS Genetics*, *12*(7), 1–30. https://doi.org/10.1371/journal.pgen.1006179

Choi, K., Zhao, X., Tock, A. J., Lambing, C., Underwood, C. J., Hardcastle, T. J., … Henderson, I. R. (2018). Nucleosomes and DNA methylation shape meiotic DSB frequency in Arabidopsis thaliana transposons and gene regulatory regions. *Genome Research*, 1–16. https://doi.org/10.1101/gr.225599.117.28

Choulet et al., 2014. (2014). Structural and functional partitioning of bread wheat chromosome 3B. *Science (New York, N.Y.)*, *345*(6194), 1250092.

Copenhaver, G. P., Nickel, K., Kuromori, T., Benito, M. I., Kaul, S., Lin, X., … Preuss, D. (1999). Genetic definition and sequence analysis of Arabidopsis centromeres. *Science*, *286*(5449), 2468–2474. https://doi.org/10.1126/science.286.5449.2468

Crismani, W., Girard, C., Froger, N., Pradillo, M., Santos, J. L., Chelysheva, L., … Mercier, R. (2012). FANCM limits meiotic crossovers. *Science*, *336*(6088), 1588–1590. https://doi.org/10.1126/science.1220381

Crismani, W., & Mercier, R. (2012). What limits meiotic crossovers. *Cell Cycle*, 3527–3528. https://doi.org/10.4161/cc.21963

Cromer, L., Jolivet, S., Singh, D. K., Berthier, F., De Winne, N., De Jaeger, G., … Mercier, R. (2019). Patronus is the elusive plant securin, preventing chromosome separation by antagonizing separase. *Proceedings of the National Academy of Sciences of the United States of America*, *116*(32), 16018–16027. https://doi.org/10.1073/pnas.1906237116

Cromie, G. A., & Smith, G. R. (2007). Branching out: meiotic recombination and its

regulation. *Trends in Cell Biology*, *17*(9), 448–455. https://doi.org/10.1016/j.tcb.2007.07.007

De Muyt, A., Pereira, L., Vezon, D., Chelysheva, L., Gendrot, G., Chambon, A., … Grelon, M. (2009). A high throughput genetic screen identifies new early meiotic recombination functions in Arabidopsis thaliana. *PLoS Genetics*, *5*(9). https://doi.org/10.1371/journal.pgen.1000654

Dreissig, S., Maurer, A., Sharma, R., Milne, L., Flavell, A. J., Schmutzer, T., & Pillen, K. (2020). Natural variation in meiotic recombination rate shapes introgression patterns in intraspecific hybrids between wild and domesticated barley. *New Phytologist*, *228*(6), 1852–1863. https://doi.org/10.1111/nph.16810

Eijpe, M., Heyting, C., Gross, B., & Jessberger, R. (2000). Association of mammalian SMC1 and SMC3 proteins with meiotic chromosomes and synaptonemal complexes. *Journal of Cell Science*, *113*(4), 673–682. https://doi.org/10.1242/jcs.113.4.673

Fernandes, Joiselle B., Wlodzimierz, P., & Henderson, I. R. (2019a). Meiotic recombination within plant centromeres. *Current Opinion in Plant Biology*, *48*, 26–35. https://doi.org/10.1016/j.pbi.2019.02.008

Fernandes, Joiselle B., Wlodzimierz, P., & Henderson, I. R. (2019b). Meiotic recombination within plant centromeres. *Current Opinion in Plant Biology*, *48*, 26–35. https://doi.org/10.1016/j.pbi.2019.02.008

Fernandes, Joiselle B, Naish, M., Lian, Q., Burns, R., Tock, A. J., Rabanal, F. A., … Henderson, I. R. (2023). Structural variation and DNA methylation shape the centromere-proximal meiotic crossover landscape in Arabidopsis. *BioRxiv*, 1–64.

Fernandes, Joiselle Blanche, Duhamel, M., Seguéla-Arnaud, M., Froger, N., Girard, C., Choinard, S., … Mercier, R. (2018). FIGL1 and its novel partner FLIP form a conserved complex that regulates homologous recombination. *Electronic Publishing*, *23*, 1–22.

Fernandes, Joiselle Blanche, Séguéla-Arnaud, M., Larchevêque, C., Lloyd, A. H., & Mercier, R. (2018). Unleashing meiotic crossovers in hybrid plants. *Proceedings of the National Academy of Sciences of the United States of America*, *115*(10), 2431–2436. https://doi.org/10.1073/pnas.1713078114

Francis, K. E., Lam, S. Y., Harrison, B. D., Bey, A. L., Berchowitz, L. E., & Copenhaver, G. P. (2007). Pollen tetrad-based visual assay for meiotic recombination in Arabidopsis. *Proceedings of the National Academy of Sciences of the United States of America*, *104*(10), 3913–3918. https://doi.org/10.1073/pnas.0608936104

Fransz, P. F., Armstrong, S., De Jong, J. H., Parnell, L. D., Van Drunen, C., Dean, C., … Jones, G. H. (2000). Integrated cytogenetic map of chromosome arm 4S of A. thaliana: Structural organization of heterochromatic knob and centromere region. *Cell*, *100*(3), 367–376. https://doi.org/10.1016/S0092-8674(00)80672-8

Frédéric Choulet, Adriana Alberti, Sébastien Theil, Natasha Glover, Valérie Barbe, Josquin Daron, Lise Pingault, Pierre Sourdille, Arnaud Couloux, Etienne Paux, Philippe Leroy, Sophie Mangenot, Nicolas Guilhot, Jacques Le Gouis, Francois Balfourier, Micha, C. F. (2014). Structural and functional partitioning of bread

wheat chromosome 3B. *Science (New York, N.Y.)*, *345*(6194), 1250092. Retrieved from http://www.sciencemag.org/content/345/6194/1250092.abstract

Galander, S., & Marston, A. L. (2020). Meiosis I Kinase Regulators: Conserved Orchestrators of Reductional Chromosome Segregation. *BioEssays*, *42*(10), 1–13. https://doi.org/10.1002/bies.202000018

Girard, C., Chelysheva, L., Choinard, S., Froger, N., Macaisne, N., Lehmemdi, A., … Mercier, R. (2015). AAA-ATPase FIDGETIN-LIKE 1 and Helicase FANCM Antagonize Meiotic Crossovers by Distinct Mechanisms. *PLoS Genetics*, *11*(7), 1–22. https://doi.org/10.1371/journal.pgen.1005369

Girard, C., Zwicker, D., & Mercier, R. (2023). The regulation of meiotic crossover distribution: a coarse solution to a century-old mystery? *Biochemical Society Transactions*, *51*(3), 1179–1190. https://doi.org/10.1042/bst20221329

Giraut, L., Falque, M., Drouaud, J., Pereira, L., Martin, O. C., & Mézard, C. (2011). Genome-wide crossover distribution in Arabidopsis thaliana meiosis reveals sex-specific patterns along chromosomes. *PLoS Genetics*, *7*(11). https://doi.org/10.1371/journal.pgen.1002354

Gloria A. Brar, A. H., Ly-sha S. Ee, and A. A., & *David. (2009). The Multiple Roles of Cohesin in Meiotic Chromosome Morphogenesis and Pairing. *Molecular Biology of the Cell*, *20*, 2673–2683. https://doi.org/10.1091/mbc.E08

Grelon, M., Vezon, D., Gendrot, G., & Pelletier, G. (2001). AtSPO11-1 is necessary for efficient meiotic recombination in plants. *EMBO Journal*, *20*(3), 589–600. https://doi.org/10.1093/emboj/20.3.589

Grishaeva, T. M., & Bogdanov, Y. F. (2000). Genetic control of meiosis in Drosophila. In *Genetika* (Vol. 36).

Grützner, R., Martin, P., Horn, C., Mortensen, S., Cram, E. J., Lee-Parsons, C. W. T., … Marillonnet, S. (2020). Addition of multiple introns to a Cas9 gene results in dramatic improvement in efficiency for generation of gene knockouts in plants. *BioRxiv*, 1–32. https://doi.org/10.1101/2020.04.03.023036

Grützner, R., Martin, P., Horn, C., Mortensen, S., Cram, E. J., Lee-Parsons, C. W. T., … Marillonnet, S. (2021). High-efficiency genome editing in plants mediated by a Cas9 gene containing multiple introns. *Plant Communications*, *2*(2), 1–15. https://doi.org/10.1016/j.xplc.2020.100135

Haber, J. E. (2014). *Genome stability. DNA repair and recombination*. Routledge.

Hartung, F., Wurz-Wildersinn, R., Fuchs, J., Schubert, I., Suer, S., & Puchta, H. (2007). The catalytically active tyrosine residues of both SPO11-1 and SPO11-2 are required for meiotic double-strand break induction in Arabidopsis. *Plant Cell*, *19*(10), 3090–3099. https://doi.org/10.1105/tpc.107.054817

He, Y., Wang, M., Dukowic-Schulze, S., Zhou, A., Tiang, C. L., Shilo, S., … Pawlowski, W. P. (2017). Genomic features shaping the landscape of meiotic double-strand-break hotspots in maize. *Proceedings of the National Academy of Sciences of the United States of America*, *114*(46), 12231–12236. https://doi.org/10.1073/pnas.1713225114

Higgins, J. D., Sanchez-Moran, E., Armstrong, S. J., Jones, G. H., & Franklin, F. C. H. (2005). The Arabidopsis synaptonemal complex protein ZYP1 is required for chromosome synapsis and normal fidelity of crossing over. *Genes and Development*, *19*(20), 2488–2500. https://doi.org/10.1101/gad.354705

Hörandl, E. (2009). A combinational theory for maintenance of sex. *Heredity*, *103*(6), 445–457. https://doi.org/10.1038/hdy.2009.85

Hunter, N. (2015). Meiotic recombination: The essence of heredity. *Cold Spring Harbor Perspectives in Biology*, *7*(12). https://doi.org/10.1101/cshperspect.a016618

Initiative, A. G. (2000). Analysis of the genome sequence of the Flowering plant Arabidopsis thaliana. *Nature*. Retrieved from https://www.nature.com/articles/35048692

James, G. V., Patel, V., Nordström, K. J. V., Klasen, J. R., Salomé, P. A., Weigel, D., & Schneeberger, K. (2013). User guide for mapping-by-sequencing in Arabidopsis. *Genome Biology*, *14*(6). https://doi.org/10.1186/gb-2013-14-6-r61

Jiang, J., Birchler, J. A., Parrott, W. A., & Dawe, R. K. (2003). A molecular view of plant centromeres. *Trends in Plant Science*, *8*(12), 570–575. https://doi.org/10.1016/j.tplants.2003.10.011

Johnson, E. S. (2004). Protein modification by SUMO. *Annual Review of Biochemistry*, *73*, 355–382. https://doi.org/10.1146/annurev.biochem.73.011303.074118

Joly-Lopez, Z., & Bureau, T. E. (2014). Diversity and evolution of transposable elements in Arabidopsis. *Chromosome Research*, *22*(2), 203–216. https://doi.org/10.1007/s10577-014-9418-8

Katis, V. L., Galova, M., Rabitsch, K. P., Gregan, J., & Nasmyth, K. (2004). Maintenance of Cohesin at Centromeres after Meiosis I in Budding Yeast Requires a Kinetochore-Associated Protein Related to MEI-S332. *Current Biology*, *14*, 560–572. https://doi.org/DOI 10.1016/j.cub.2004.03.001

Keeney, S., & Neale, M. J. (2006). Initiation of meiotic recombination by formation of DNA double-strand breaks: Mechanism and regulation. *Biochemical Society Transactions*, *34*(4), 523–525. https://doi.org/10.1042/BST0340523

Keeney, Scott, Giroux, C. N., & Kleckner, N. (1997). Meiosis-specific DNA double-strand breaks are catalyzed by Spo11, a member of a widely conserved protein family. *Cell*, *88*(3), 375–384. https://doi.org/10.1016/S0092-8674(00)81876-0

Kerrebrock, A. W., Moore, D. P., Wu, J. S., & Orr-Weaver, T. L. (1995). Mei-S332, a drosophila protein required for sister-chromatid cohesion, can localize to meiotic centromere regions. *Cell*, *83*(2), 247–256. https://doi.org/10.1016/0092-8674(95)90166-3

Kianian, P. M. A., Wang, M., Simons, K., Ghavami, F., He, Y., Dukowic-Schulze, S., … Pawlowski, W. P. (2018). High-resolution crossover mapping reveals similarities and differences of male and female recombination in maize. *Nature Communications*, *9*(1). https://doi.org/10.1038/s41467-018-04562-5

Kim, J., Park, J., Kim, H., Son, N., Kim, E., Kim, J., … Choi, K. (2022). Arabidopsis HEAT SHOCK FACTOR BINDING PROTEIN is required to limit meiotic crossovers and HEI10 transcription . *The EMBO Journal*, *41*(14), 1–19. https://doi.org/10.15252/embj.2021109958

Klein, F., Mahr, P., Galova, M., Buonomo, S. B. C., Michaelis, C., Nairz, K., & Nasmyth, K. (1999). A Central Role for Cohesins in Sister Chromatid Cohesion, Formation of Axial Elements, and Recombination during Yeast Meiosis Genetic and biochemical analyses have identified. *Cell*, *98*, 91–103.

Kong, X., Luo, X., Qu, G. P., Liu, P., & Jin, J. B. (2017). Arabidopsis SUMO protease ASP1 positively regulates flowering time partially through regulating FLC stability. *Journal of Integrative Plant Biology*, *59*(1), 15–29. https://doi.org/10.1111/jipb.12509

Kumar, R., Duhamel, M., Coutant, E., Ben-Nahia, E., & Mercier, R. (2019). Antagonism between BRCA2 and FIGL1 regulates homologous recombination. *Nucleic Acids Research*, *47*(10), 5170–5180. https://doi.org/10.1093/nar/gkz225

Kurzbauer, M. T., Uanschou, C., Chen, D., & Schlögelhofer, P. (2012). The recombinases DMC1 and RAD51 are functionally and spatially separated during meiosis in Arabidopsis. *Plant Cell*, *24*(5), 2058–2070. https://doi.org/10.1105/tpc.112.098459

Lam, W. S., Yang, X., & Makaroff, C. A. (2005). Characterization of Arabidopsis thaliana SMC1 and SMC3: Evidence that AtSMC3 may function beyond chromosomes cohesion. *Journal of Cell Science*, *118*(14), 3037–3048. https://doi.org/10.1242/jcs.02443

Lee, J. Y., Hayashi-Hagihara, A., & Orr-Weaver, T. L. (2005). Roles and regulation of the Drosophila centromere cohesion protein MEI-S332 family. *Philosophical Transactions of the Royal Society B: Biological Sciences*, *360*(1455), 543–552. https://doi.org/10.1098/rstb.2005.1619

Lenormand, T., Engelstädter, J., Johnston, S. E., Wijnker, E., & Haag, C. R. (2016). Evolutionary mysteries in meiosis. *Philosophical Transactions of the Royal Society B: Biological Sciences*, *371*(1706). https://doi.org/10.1098/rstb.2016.0001

Lin, T., Zhu, G., Zhang, J., Xu, X., Yu, Q., Zheng, Z., … Huang, S. (2014). Genomic analyses provide insights into the history of tomato breeding. *Nature Genetics*, *46*(11), 1220–1226. https://doi.org/10.1038/ng.3117

Ling, Y. H., & Yuen, K. W. Y. (2019). Point centromere activity requires an optimal level of centromeric noncoding RNA. *Proceedings of the National Academy of Sciences of the United States of America*, *116*(13), 6270–6279. https://doi.org/10.1073/pnas.1821384116

Liu, L., Jiang, Y., Zhang, X., Wang, X., Wang, Y., Han, Y., … Chen, F. (2017). Two SUMO proteases SUMO PROTEASE RELATED TO FERTILITY1 and 2 are required for fertility in arabidopsis. *Plant Physiology*, *175*(4), 1703–1719. https://doi.org/10.1104/pp.17.00021

Liu, S., Yeh, C. T., Ji, T., Ying, K., Wu, H., Tang, H. M., … Schnable, P. S. (2009). Mu transposon insertion sites and meiotic recombination events co-localize with

epigenetic marks for open chromatin across the maize genome. *PLoS Genetics*, *5*(11). https://doi.org/10.1371/journal.pgen.1000733

Lorenz, A., Osman, F., Sun, W., Nandi, S., Steinacher, R., & Whitby, M. C. (2012). The Fission Yeast FANCM Ortholog Directs Non-Crossover Recombination During Meiosis. *Science*, *336*(June), 1585–1588.

Lynn, A., Soucek, R., & Börner, G. V. (2007). ZMM proteins during meiosis: Crossover artists at work. *Chromosome Research*, *15*(5), 591–605. https://doi.org/10.1007/s10577-007-1150-1

Marand, A. P., Jansky, S. H., Zhao, H., Leisner, C. P., Zhu, X., Zeng, Z., … Jiang, J. (2017). Meiotic crossovers are associated with open chromatin and enriched with Stowaway transposons in potato. *Genome Biology*, *18*(1), 1–16. https://doi.org/10.1186/s13059-017-1326-8

McKinley, K. L., & Cheeseman, I. M. (2016). The molecular basis for centromere identity and function. *Nature Reviews Molecular Cell Biology*, *17*(1), 16–29. https://doi.org/10.1038/nrm.2015.5

Melamed-Bessudo, C., Yehuda, E., Stuitje, A. R., & Levy, A. A. (2005). A new seed-based assay for meiotic recombination in Arabidopsis thaliana. *Plant Journal*, *43*(3), 458–466. https://doi.org/10.1111/j.1365-313X.2005.02466.x

Mercier, R., & Grelon, M. (2008). Meiosis in plants: Ten years of gene discovery. *Cytogenetic and Genome Research*, *120*(3–4), 281–290. https://doi.org/10.1159/000121077

Mercier, Raphaël, Mézard, C., Jenczewski, E., Macaisne, N., & Grelon, M. (2015). The molecular biology of meiosis in plants. *Annual Review of Plant Biology*, *66*, 297–327. https://doi.org/10.1146/annurev-arplant-050213-035923

Mieulet, D., Aubert, G., Bres, C., Klein, A., Droc, G., Vieille, E., … Mercier, R. (2018). Unleashing meiotic crossovers in crops. *Nature Plants*, *4*(12), 1010–1016. https://doi.org/10.1038/s41477-018-0311-x

Mitra, S., Bodor, D. L., David, A. F., Abdul-Zani, I., Mata, J. F., Neumann, B., … Jansen, L. E. T. (2020). Genetic screening identifies a SUMO protease dynamically maintaining centromeric chromatin. *Nature Communications*, *11*(1), 1–15. https://doi.org/10.1038/s41467-019-14276-x

Morgan, C., Fozard, J. A., Hartley, M., Henderson, I. R., Bomblies, K., & Howard, M. (2021). Diffusion-mediated HEI10 coarsening can explain meiotic crossover positioning in Arabidopsis. *Nature Communications*, *12*(1). https://doi.org/10.1038/s41467-021-24827-w

Mukhopadhyay, D., & Dasso, M. (2007). Modification in reverse: the SUMO proteases. *Trends in Biochemical Sciences*, *32*(6), 286–295. https://doi.org/10.1016/j.tibs.2007.05.002

Nageswaran, D. C., Kim, J., Lambing, C., Kim, J., Park, J., Kim, E. J., … Henderson, I. R. (2021). HIGH CROSSOVER RATE1 encodes PROTEIN PHOSPHATASE X1 and restricts meiotic crossovers in Arabidopsis. *Nature Plants*, *7*(4), 452–467. https://doi.org/10.1038/s41477-021-00889-y

Naish, M., Alonge, M., Wlodzimierz, P., Tock, A. J., Abramson, B. W., Lambing, C., … Henderson, I. R. (2021a). The genetic and epigenetic landscape of the Arabidopsis centromeres. *Plant Science*, *7489*(November), 2021.05.30.446350. https://doi.org/10.1126/science.abi7489

Naish, M., Alonge, M., Wlodzimierz, P., Tock, A. J., Abramson, B. W., Lambing, C., … Henderson, I. R. (2021b). The genetic and epigenetic landscape of the Arabidopsis centromeres. *Science*, *7489*(November), 2021.05.30.446350. https://doi.org/10.1126/science.abi7489

Nambiar, M., & Smith, G. R. (2016). Repression of harmful meiotic recombination in centromeric regions. *Semin Cell Dev Biol.*, (54), 188–197. https://doi.org/10.1016/j.semcdb.2016.01.042.Repression

O'Malley, R. C., Barragan, C. C., & Ecker, J. R. (2015). HHMI Author Manuscript A User ' s Guide to the Arabidopsis T-DNA Insertional Mutant Collections. *Methods in Molecular Biology*, 323–342.

Petronczki, M., Siomos, Maria, F., & Nasmyth, K. (2003). Un Menage a Quatre: The Molecular Biology of Chromosome Segregation in Meiosis. *Cell*, *112*, 423–440. https://doi.org/10.1016/S1089-3261(05)70234-8

Roberts, E. H. (1972). Storage Environment and the Control of Viability. *Viability of Seeds*, 14–58. https://doi.org/10.1007/978-94-009-5685-8_2

Rowan, B. A., Heavens, D., Feuerborn, T. R., Tock, A. J., Henderson, I. R., & Weigel, D. (2019). An Ultra High-Density Arabidopsis thaliana Crossover. *Genetics*, *213*(November), 771–787.

Saintenac, C., Falque, M., Martin, O. C., Paux, E., Feuillet, C., & Sourdille, P. (2009). Detailed recombination studies along chromosome 3B provide new insights on crossover distribution in wheat (Triticum aestivum L.). *Genetics*, *181*(2), 393–403. https://doi.org/10.1534/genetics.108.097469

Séguéla-Arnaud, M., Crismani, W., Larchevêque, C., Mazel, J., Froger, N., Choinard, S., … Mercier, R. (2015). Multiple mechanisms limit meiotic crossovers: TOP3α and two BLM homologs antagonize crossovers in parallel to FANCM. *Proceedings of the National Academy of Sciences of the United States of America*, *112*(15), 4713–4718. https://doi.org/10.1073/pnas.1423107112

Sen, S., Dodamani, A., & Nambiar, M. (2022). Emerging mechanisms and roles of meiotic crossover repression at centromeres. In *Current Topics in Developmental Biology* (1st ed.). https://doi.org/10.1016/bs.ctdb.2022.06.003

Serra, H., Lambing, C., Griffin, C. H., Topp, S. D., Nageswaran, D. C., Underwood, C. J., … Henderson, I. R. (2018a). Massive crossover elevation via combination of HEI10 and recq4a recq4b during Arabidopsis meiosis. *Proceedings of the National Academy of Sciences of the United States of America*, *115*(10), 2437–2442. https://doi.org/10.1073/pnas.1713071115

Serra, H., Lambing, C., Griffin, C. H., Topp, S. D., Nageswaran, D. C., Underwood, C. J., … Henderson, I. R. (2018b). Massive crossover elevation via combination of *HEI10* and *recq4a recq4b* during *Arabidopsis* meiosis. *Proceedings of the National Academy of Sciences*, 201713071. https://doi.org/10.1073/pnas.1713071115

Sherman, J., & Stack, S. (1995). Two-dimensional spreads of synaptonemal complexes from solanaceous plants. I. The technique. *Biotechnic and Histochemistry*, *57*(5), 265–272. https://doi.org/10.3109/10520298209066722

Shi, J., Wolf, S. E., Burke, J. M., Presting, G. G., Ross-Ibarra, J., & Dawe, R. K. (2010). Widespread gene conversion in centromere cores. *PLoS Biology*, *8*(3). https://doi.org/10.1371/journal.pbio.1000327

Si, W., Yuan, Y., Huang, J., Zhang, X., Zhang, Y., Zhang, Y., … Yang, S. (2015). Widely distributed hot and cold spots in meiotic recombination as shown by the sequencing of rice F2 plants. *New Phytologist*, *206*(4), 1491–1502. https://doi.org/10.1111/nph.13319

Simon, L., Voisin, M., Tatout, C., & Probst, A. V. (2015). Structure and function of centromeric and pericentromeric heterochromatin in arabidopsis thaliana. *Frontiers in Plant Science*, *6*(NOVEMBER), 1–8. https://doi.org/10.3389/fpls.2015.01049

Sims, J., Schlögelhofer, P., & Kurzbauer, M. T. (2021). From Microscopy to Nanoscopy: Defining an Arabidopsis thaliana Meiotic Atlas at the Nanometer Scale. *Frontiers in Plant Science*, *12*(May). https://doi.org/10.3389/fpls.2021.672914

Singh, D. K., Salinas Gamboa, R., Singh, A. K., Walkemeier, B., Van Leene, J., De Jaeger, G., … Mercier, R. (2023). The FANCC–FANCE–FANCF complex is evolutionarily conserved and regulates meiotic recombination. *Nucleic Acids Research*, *51*(6), 2516–2528. https://doi.org/10.1093/nar/gkac1244

Srivastava, M., Srivastava, A. K., Roy, D., Mansi, M., Gough, C., Bhagat, P. K., … Sadanandom, A. (2022). The conjugation of SUMO to the transcription factor MYC2 functions in blue light-mediated seedling development in Arabidopsis. *Plant Cell*, *34*(8), 2892–2906. https://doi.org/10.1093/plcell/koac142

Stuitje, A. R., Verbree, E. C., Van Der Linden, K. H., Mietkiewska, E. M., Nap, J.-P., & Kneppers, T. J. A. (2003). Seed-expressed fluorescent proteins as versatile tools for easy (co)transformation and high-throughput functional genomics in Arabidopsis. *Plant Biotechnology Journal*, *1*(4), 301–309. https://doi.org/10.1046/j.1467-7652.2003.00028.x

Su, X. B., Wang, M., Schaffner, C., Nerusheva, O., Clift, D., Spanos, C., … Marston, A. L. (2021). Sumoylation stabilizes sister kinetochore biorientation to allow timely anaphase. *Journal of Cell Biology*, *220*(7). https://doi.org/10.1083/jcb.202005130

Su, X., Wang, B., Geng, X., Du, Y., Yang, Q., Liang, B., … Lin, T. (2021). A high-continuity and annotated tomato reference genome. *BMC Genomics*, *22*(1), 1–12. https://doi.org/10.1186/s12864-021-08212-x

Takahashi, N., Quimbaya, M., Schubert, V., Lammens, T., Vandepoele, K., Schubert, I., … De Veylder, L. (2010). The MCM-binding protein ETG1 aids sister chromatid cohesion required for postreplicative homologous recombination repair. *PLoS Genetics*, *6*(1). https://doi.org/10.1371/journal.pgen.1000817

Talbert, P. B., & Henikoff, S. (2010). Centromeres convert but don't cross. *PLoS Biology*, *8*(3), 1–5. https://doi.org/10.1371/journal.pbio.1000326

Tock, A. J., Holland, D. M., Jiang, W., Osman, K., Sanchez-Moran, E., Higgins, J. D., … Henderson, I. R. (2021). Crossover-active regions of the wheat genome are distinguished by DMC1, the chromosome axis, H3K27me3, and signatures of adaptation. *Genome Research*, *31*(9), 1614–1628. https://doi.org/10.1101/gr.273672.120

Tóth, A., Rabitsch, K. P., Gálová, M., Schleiffer, A., Buonomo, S. B. C., & Nasmyth, K. (2000). Functional genomics identifies monopolin: A kinetochore protein required for segregation of homologs during meiosis I. *Cell*, *103*(7), 1155–1168. https://doi.org/10.1016/S0092-8674(00)00217-8

Underwood, C. J., Choi, K., Lambing, C., Zhao, X., Serra, H., Borges, F., … Martienssen, R. A. (2018). Epigenetic activation of meiotic recombination near Arabidopsis thaliana centromeres via loss of H3K9me2 and non-CG DNA methylation. *Genome Research*, *28*(4), 519–531. https://doi.org/10.1101/gr.227116.117

Vincenten, N., Kuhl, L. M., Lam, I., Oke, A., Kerr, A. R. W., Hochwagen, A., … Marston, A. L. (2015). The kinetochore prevents centromere-proximal crossover recombination during meiosis. *ELife*, *4*(DECEMBER2015), 1–25. https://doi.org/10.7554/eLife.10850

Wang, N., & Dawe, R. K. (2018). Centromere Size and Its Relationship to Haploid Formation in Plants. *Molecular Plant*, *11*(3), 398–406. https://doi.org/10.1016/j.molp.2017.12.009

Wang, Y., & Copenhaver, G. P. (2018). Meiotic Recombination: Mixing It Up in Plants. *Annual Review of Plant Biology*, *69*(1), 577–609. https://doi.org/10.1146/annurev-arplant-042817-040431

Watanabe, Y. (2004). Modifying sister chromatid cohesion for meiosis. *Journal of Cell Science*, *117*(18), 4017–4023. https://doi.org/10.1242/jcs.01352

Watanabe, Y. (2012). Geometry and force behind kinetochore orientation: Lessons from meiosis. *Nature Reviews Molecular Cell Biology*, *13*(6), 370–382. https://doi.org/10.1038/nrm3349

Wei, W., & Lin, H.-K. (2012). The key role of ubiquitination and sumoylation in signaling and cancer: a research topic. *Frontiers in Oncology*, *2*(December), 1–2. https://doi.org/10.3389/fonc.2012.00187

Wu, G., Rossidivito, G., Hu, T., Berlyand, Y., & Poethig, R. S. (2015). Traffic lines: New tools for genetic analysis in Arabidopsis thaliana. *Genetics*, *200*(1), 35–45. https://doi.org/10.1534/genetics.114.173435

Xue, X., Sung, P., & Zhao, X. (2015). Functions and regulation of the multitasking FANCM family of DNA motor proteins. *Genes and Development*, *29*(17), 1777–1788. https://doi.org/10.1101/gad.266593.115

Yelina, N E, Lambing, C., Hardcastle, T. J., Zhao, X., Santos, B., & Henderson, I. R. (2015). DNA methylation epigenetically silences crossover hot spots and controls chromosomal domains of meiotic recombination in Arabidopsis. *Genes Dev*, *29*(20), 2183–2202. https://doi.org/10.1101/gad.270876.115

Yelina, Nataliya E., Choi, K., Chelysheva, L., Macaulay, M., de Snoo, B., Wijnker, E.,

… Henderson, I. R. (2012). Epigenetic Remodeling of Meiotic Crossover Frequency in Arabidopsis thaliana DNA Methyltransferase Mutants. *PLoS Genetics*, *8*(8). https://doi.org/10.1371/journal.pgen.1002844

Yelina, Nataliya E., Lambing, C., Hardcastle, T. J., Zhao, X., Santos, B., & Henderson, I. R. (2015). DNA methylation epigenetically silences crossover hot spots and controls chromosomal domains of meiotic recombination in Arabidopsis. *Genes and Development*, *29*(20), 2183–2202. https://doi.org/10.1101/gad.270876.115

Yelina, Nataliya E., Ziolkowski, P. A., Miller, N., Zhao, X., Kelly, K. A., Muñoz, D. F., … Henderson, I. R. (2013). High-throughput analysis of meiotic crossover frequency and interference via flow cytometry of fluorescent pollen in Arabidopsis thaliana. *Nature Protocols*, *8*(11), 2119–2134. https://doi.org/10.1038/nprot.2013.131

Yu, H. G., Dawe, R. K., Hiatt, E. N., & Dawe, R. K. (2000). The plant kinetochore. *Trends in Plant Science*, *5*(12), 543–547. https://doi.org/10.1016/S1360-1385(00)01789-1

Zamariola, L., De Storme, N., Tiang, C. L., Armstrong, S. J., Franklin, F. C. H., & Geelen, D. (2013). SGO1 but not SGO2 is required for maintenance of centromere cohesion in Arabidopsis thaliana meiosis. *Plant Reproduction*, *26*(3), 197–208. https://doi.org/10.1007/s00497-013-0231-x

Zhang, H., Lang, Z., & Zhu, J. K. (2018). Dynamics and function of DNA methylation in plants. *Nature Reviews Molecular Cell Biology*, *19*(8), 489–506. https://doi.org/10.1038/s41580-018-0016-z

Zhang, L., Stauffer, W., Zwicker, D., & Dernburg, A. F. (2021). *Crossover patterning through kinase-regulated condensation and coarsening of recombination nodules*.

Zhu, L., Fernández-Jiménez, N., Szymanska-Lejman, M., Pelé, A., Underwood, C. J., Serra, H., … Ziolkowski, P. A. (2021). Natural variation identifies SNI1, the SMC5/6 component, as a modifier of meiotic crossover in Arabidopsis. *Proceedings of the National Academy of Sciences of the United States of America*, *118*(33), 1–12. https://doi.org/10.1073/pnas.2021970118

Ziolkowski, P. A., Berchowitz, L. E., Lambing, C., Yelina, N. E., Zhao, X., Kelly, K. A., … Henderson, I. R. (2015a). Juxtaposition of heterozygous and homozygous regions causes reciprocal crossover remodelling via interference during Arabidopsis meiosis. *ELife*, *4*, 1–29. https://doi.org/10.7554/eLife.03708

Ziolkowski, P. A., Berchowitz, L. E., Lambing, C., Yelina, N. E., Zhao, X., Kelly, K. A., … Henderson, I. R. (2015b). Juxtaposition of heterozygous and homozygous regions causes reciprocal crossover remodelling via interference during Arabidopsis meiosis. *ELife*, *4*, 1–29. https://doi.org/10.7554/eLife.03708

Ziolkowski, P. A., Underwood, C. J., Lambing, C., Martinez-Garcia, M., Lawrence, E. J., Ziolkowska, L., … Henderson, I. R. (2017). Natural variation and dosage of the HEI10 meiotic E3 ligase control Arabidopsis crossover recombination. *Genes and Development*, *31*(3), 306–317. https://doi.org/10.1101/gad.295501.116

8 DISCUSSION AND PERSPECTIVES

8.1 NOVEL CENTROMERIC -SPECIFIC ANTI-CO FACTORS

Limitation of the Fluorescent Transgenic Lines (FTLs) in Col-o background: During the construction of the mutant background, in Col-0 accession, we observed that the segregation specifically of the mutant *recq4b* and *fancm* when combined with the FTLs (intervals CTL3.437.55 and CTL4.15.909) was not Mendelian, even though the genes were not linked. The source of the skewed segregation was not found but we hypothesised that some structural rearrangement might give us a hint. Likely, if a mutant with more than one T-DNA insertion and has a structural rearrangement as a defect, it can disturb the segregation even more. Additionally, some other structural organization can enhance the defects in segregation, like the one observed on chromosome 4, where the heterochromatic knob inversion located in the arm of the chromosome shows a recombination coldspot (Fransz et al., 2000; Serra et al., 2018b). Since the FTLs recombination measurements rely only on the segregation of the genes, this skewed segregation is a source of artefact for the screen, therefore we decided not to use the markers in the Col-0 background for the screen.

Instead of using the *recq4ab* mutant in Col-0 for the screen, we decided to test the segregation of *recq4, fancm* and FTLs (chromosome 5) in Landsberg background. Ler accession lacks the Recq4b gene, simplifying the segregation analysis of this mutant but in plants carrying *fancm* mutation we observed slightly skewed segregation; this might be due to structural defects of the *fancm-10* line, although cannot rule out defects in the FTL itself. Therefore, the *recq4* mutant in Ler turned out to be the best

We showed that different Traffic Lines can have different fluorescence intensities and segregation. It has been observed that insertional T-DNA lines can show distorted segregation, sometimes by reducing transmission of some genes or alleles, or in extreme cases increasing lethality, mostly due to structural rearrangements that were carried together with the transformation induction procedure (O'Malley, Barragan, & Ecker, 2015). In addition, the FTLs are located in the pericentromeric regions, especially where the DNA methylation in CG and non-CG contexts (CHG) is highly abundant in comparison to the rest of the chromosome as observed in Figure 27. In contrast, line 420 that is located in the arms of chromosome 3 show a constantly bright fluorescence and Mendelian recombination even when combined with other mutants (Singh et al., 2023), suggesting that the methylation in heterochromatin regions might affect the expression of the fluorescent markers.

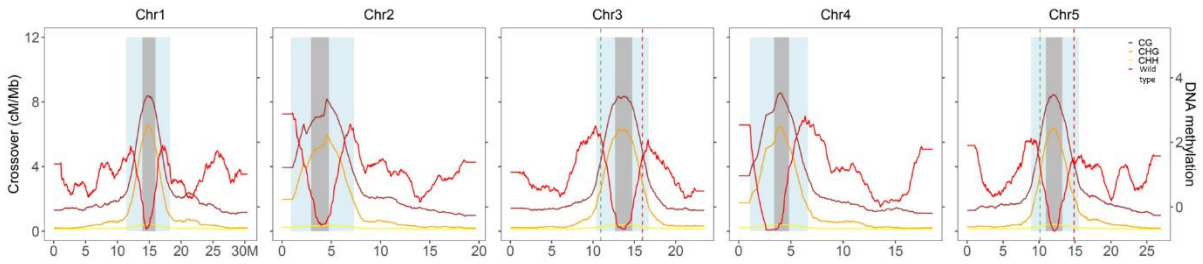

Figure 27. Location of FTLs in chromosome 3 in Col-0 and in Chromosome 5 in Ler respective to the methylation in CG, CHG and CHH context. Each plot represents each chromosome of Arabidopsis; they are depicted in 5Mb windows in the X axis. The left Y axis, the number of CO formed per Mb and the Y axis in the right, the methylation along the chromosomes. Grey vertical columns represent the centromeres, flanked by the light blue vertical columns representing pericentromeric regions. FTLs (green and red vertical dotted lines) in chromosome 3 in Col-0 and in Chromosome 5 in Ler. Picture credits Dr. Qichao Lian with data from (Serra et al., 2018b)

In both the Forward and Reverse screens, notable alterations in the fluorescence intensities of the Fluorescent Traffic Lines (FTL) were evident upon exposure to elevated temperatures. Given that these lines incorporate a NAP promoter with specific expression in the seed coat, it is conceivable that the observed fluorescence variations might serve as an indicator of seed viability. This trend has been documented across diverse seed types, including wheat, rice, peas, tomatoes, and others. Following a only two-week exposure to elevated temperatures, with conditions reaching up to 45°C, the viability of such seeds can decrease, presenting an approximate 50% likelihood of survival, even under conditions of elevated moisture content (18%) (Roberts, 1972). These observations strongly imply a probable reduction in the viability of the mentioned seeds.

8.1.1 Perspectives

The mutants of *recq4* in Ler background with the FTLs (LTL5.43.179) were treated with EMS reagent, both the fluorescence and segregation of the mentioned markers are stable and the system to analyse the seeds has been already successfully implemented in the lab. To find new anti-CO factors in a near future, the following step would be to complete the forward genetic screen with this plant material. The method with more accurate results was the Plate method and the recommended to follow in this material. Higher recombination could reveal factors limiting recombination specifically in centromeres.

Many of the results are showing that the mutant plants specially *recq4ab,* when preselected for the FTLs, homozygous/heterozygous colours are also counter selecting for *recq4b*, observed as a skewed segregation and similar observations in *recq4* context were identified independently in two different labs. To find the potential cause of skewed segregation, further analysis of the FTLs lines looking for structural rearrangement could be done.

8.2 THREE PATHWAY LIMIT PERI-CENTROMERIC RECOMBINATION LIMITATION OF PERICENTROMERIC RECOMBINATION

Eight mutants that were potentially affected in recombination at centromeres were tested to look for the responsible genes that limit recombination: *zyp1* mutant that has shown to increase recombination in centromeric regions in *S. cerevisiae* (Vincenten et al., 2015), *cmt3* that showed the same phenotype in Arabidopsis (Underwood et al., 2018) and six mutants with affected kinetochores coming from an independent screen performed in the lab (*ctf18, cenpc, smc1, smc3, sgo2, asp2*); in *S. cerevisiae,* kinetochores were proposed to be involved in pericentromeric recombination limiting as it was proposed for kinetochores through the modulation of cohesion density. At least three different pathways: Asp2/Sgo2, Ctf18 and Cmt3 were found to be related with the centromeric recombination limitation.

It was observed that several genes could potentially contribute to understanding the kinetochore orientation (*ctf18, cenpc, smc1, smc3, sgo2, asp2*). Although, normally null mutants can be highly informative in some contexts, in some others where the mutants are essential leaky mutants are more useful. In this project, it was possible to obtain several leaky alleles for important mutants and observe their roles in the recombination limiting in centromere. Particularly, the knockout mutants *cenpc, smc1 and smc3* that are embryo lethal, but the leaky mutants were still viable. *cenpc* and *smc3* didn´t show any obvious defects on fertility; but *smc1* mutant was still showing an important decrease in fertility being only possible to analyse the heterozygous mutant, which was only partially fertile. While for *ctf18,* the point mutation was the allele showing significantly more recombination. Even if the different alleles were not showing the same result within the same mutants, the tendency of showing more recombination was still present in both alleles.

8.2.1 Cohesion complex

The cohesion complex including cohesion proteins Smc1 and Smc3 prevents premature separation of sister chromatids, they work as a heterodimer and are present also in mitotic cells. We observed that *smc1* had high rate of fertility loss*,* in comparison to *smc3* which didn´t have any, this might be explained by an allelic difference since both genes are essential. Since *smc1* and *smc3* are essential members of the cohesion complex and have a very important role in keeping the chromosome cohesion during segregation, it was expected to have an important role in blocking recombination at centromeric regions as well, notably, an allele with not a strong effect that is not viable, is necessary. However, we observed that our *smc3* allele has not a significant increased recombination, therefore probably it would be necessary to use another more informative allele. On the other hand, *smc1* has less recombination suggesting that *smc1* has a role in promoting recombination in the pericentromeric region but not limiting it. It would be necessary to explore recombination in the rest of the chromosome to confirm the possibility of its specificity to the pericentromeric regions.

8.2.2 Cohesion loading

In Arabidopsis, CTF18 expression was found at the shoot apical and root meristems and to be important for loss of sister centromere cohesion. The single mutant showed sister chromatid

separation in vegetative leaf cells, suggesting Ctf18 is important for cohesion establishment (Takahashi et al., 2010).

Our recombination results showed that in the single *ctf18* mutant background with the FTL lines in Col-0, in around 10,000 seeds we observed there is a significant recombination; suggesting that is also involved in limiting centromeric CO formation. We confirmed this significant recombination with PCR amplification of the same FTLs markers in 200 plants. However, in hybrid (Col/Ler) context, the increased recombination -measured with genetic markers- is not significant not in; putting all these results together is suggesting that Ctf18 gene does have an impact on centromeric recombination.

Further, we wanted to know if the recombination increase is specific to the centromeric region or if there is a genome wide recombination effect, so observed the genome wide recombination landscape of the F2s in the hybrid (Col/Ler) context and we observed no significant differences in the overall chromosomes when we include arms of the chromosomes; however, when we isolate recombination in the same interval as the genetic markers we recover the significance already observed previously. Notably, the wild type genotype mapping was not showing a good resolution, likely because of the number of samples sequenced was less (95 plants) than the *ctf18* mutant (190 plants) but we could still confirm a slight increase of recombination in pericentromeric regions. All these data need to be reconfirmed with the additional wild type data; however, the current evidence strongly suggest that Ctf18 has a role in limiting CO formation in the pericentromeric region.

In yeast, it has been suggested that Ctf18 may not be a necessary part of the replisome. Studies have shown that even in mutant strains with different versions of the gene, there was only a minor increase in recombination in the centromeric regions (Takahashi et al., 2010). This suggests that while Ctf18 may play a secondary role, there could be other proteins working together that have a greater impact.

Based on the genetic interaction data, it was observed that when *ctf18* was combined with either *asp2, sgo2, or cmt3*, there was a significant increase in recombination in double mutants. This indicates that Ctf18 is not the primary factor in the CO regulation in centromeric region. It is more likely that Cmt3 might regulate the cohesion loading, and with Sgo2 and Asp2 in a different pathway to ensure sister chromatid cohesion. This helps to limit crossover formation in the pericentromeric regions and maintain cohesion along the chromosomes to restrict CO formation.

8.2.3 Centromeric protection

SGO2 is a centromeric protein that protects Rec8 from cleavage of sister chromatids at metaphase I, which is crucial for keeping the monopolar orientation and proper homologous segregation. SGO2 also controls the localization of the CPC, a protein complex that senses lack of tension between kinetochores and microtubules (Zamariola et al., 2013). Therefore, it was predicted to have a potential importance also in limiting recombination specifically in centromeres. We found that the *sgo2* mutant showed indeed increased recombination in the pericentromeric regions. Confirming the importance on the influence of the cohesins and the

recombination in pericentromeric regions, something already observed in *S. cerevisae* where they found that the kinetochore complex mutants and cohesion disruption showed increased recombination (Vincenten et al., 2015). The whole genome sequencing of the F2 *sgo2* mutant hybrids will explore if this increased recombination effect is specific of the centromeric region or is it is also affecting other regions. If the recombination in the rest of the chromosome were also increased, it could mean that Sgo2 influences the overall recombination including the centromeric region, maybe on top of regulating the cohesion protection of centromeres or also by allowing the transcription machinery to enter the centromeric region. If, however, the recombination in the rest of the chromosome were decreased significantly more than the centromeric region, it would mean that Sgo2 is important for recombination overall but with a special importance in centromeric region probably by allowing the recombination machinery to access the DNA strand during prophase I. The alternative would be if recombination is only increased in pericentromeric region, then it would mean that Sgo2 would be modifying recombination specifically in the centromeric regions.

8.2.4 Kinetochore protein

The CENP-C protein creates a bridge between kinetochores and CENH3, and colocalizes with them. In yeast it has been observed that one of the inner kinetochore complexes, known as the Constitutive Centromere-Associated Network (CCAN) or Ctf19 has an important role in suppression of CO formation in the pericentromeres, through both cohesion-independent suppression of DSB formation and cohesin-dependent repair pathway (Vincenten et al., 2015). However, in our results we didn´t see any increase in recombination in the kinetochore protein CENP-C, likely because of the allele. However, it doesn´t discard the possibility of another allele that might have a different effect.

8.2.5 DNA methylation by Chromomethylase 3 (CMT3)

The CHROMOMETHYLASE 3 recognizes heterochromatic H3K9me2 marks via BAH and both H3K9me2 and non-CG DNA methylation and they showed to activate CO frequency in proximity to centromeres (Underwood et al., 2018). In our results we confirmed that the single *cmt3* mutant showed significantly more recombination than Wild type, without affecting the fertility.

8.2.6 SUMOylation

ASP2 is a SUMOylase protein that regulates various nuclear processes similarly as ubiquitination, it was proved to be essential for fertility in Arabidopsis (Kong et al., 2017; Srivastava et al., 2022) and presumed to have a role in centromeric identity in humans (Mitra et al., 2020) but it has never been described any Asp2 role specifically during meiosis, although other processes have been proposed to be regulated by SUMOylation; for example, in yeast, Siz1/Siz2 that disrupt SGOs interaction to moderate the pericentromeric signalling pathway to promote metaphase-anaphase transition (X. B. Su et al., 2021), or in mammals, yeast and Arabidopsis that HEI10 has been linked to SUMO a E3 ligase activity (Chelysheva et al., 2012). We observed that single *asp2* shows higher recombination in pericentromeric regions without affecting fertility.

8.2.7 Interaction of genetic pathways

Single mutant results indicate that *asp2, sgo2* and *ctf18* showed more recombination, suggesting to play a role in recombination limiting in centromeric regions. To determine whether these genes act in the same or different pathways we combined mutants with higher centromeric recombination (*asp2, sgo2, ctf18* and *cmt3)*. We analysed a total of six populations of around 10,000 seeds each and we found that in Arabidopsis there are at least three different pathways that are regulating recombination in the centromeric region: ASP2/SGO2, CTF18 and CMT3.

Most of the double mutants revealed notable cumulative effects in recombination, except for the *asp2 sgo2* combination, which displayed similar recombination levels to the single *asp2* mutant, suggesting that these two genes act in the same pathway.

In humans SUMO E3 ligases and SUMO-protease SENP6 were found to be important to deconjugate Synaptonemal Complex (SC) formation (C. H. Cheng et al., 2006), they are also important to control the localization of human centromere proteins and they are required to stabilize CENP-A chromatin throughout the cell cycle (Mitra et al., 2020). In yeast, it has been proposed SUMOylation to ensure the loss of centromeric protection, targeting SGO2 and to ensure proper segregation during Meiosis II (X. B. Su et al., 2021). In Arabidopsis, Hei10 (Zyp3 in *S.cerevisiae*) is (small ubiquitin-related modifier) a E3 ligase that has showed to control meiotic recombination; both by dosage (Ziolkowski et al., 2017) and indirectly by temperature dependent by heat shock factor binding protein (HSBP) (Kim et al., 2022). Additionally, it has been proposed to be the main driver of CO interference (Morgan et al., 2021; L. Zhang et al., 2021) through coarsening foci. Therefore, we could state from our data that ASP2 SUMOylase protein may target SGO2 to ensure centromeric loss protection and to regulate CO formation; it can also play a role in regulating SC formation and CO designation, specifically at centromeric regions. Additionally, it might also be playing a centromere stabilization role, as observed in humans. However, further studies are necessary to confirm this.

Cmt3 is identified to act in a pathway independent from Asp2/Sgo2 and Ctf18. Cmt3 has been shown to be implicated in many different process especially to adaptation to different environments under stress conditions (H. Zhang, Lang, & Zhu, 2018) usually interacting directly with the DNA molecules. As already discussed in Choi et al., 2018 probably the loss of nucleosome occupancy, gain of euchromatic marks (H3K4me3) transcription in the repetitive regions allowing recombination machinery to act where usually is blocked.

Ctf18 was also proofed to be in a different genetic pathway, as the double mutants showed more recombination than the correspondent single mutants. In Arabidopsis, the knockout mutation of CTF18 when combined to *E2F TARGET GENE 1* (*etg1)* showed loss of sister centromere cohesion, but the single *ctf18* showed separation in 40% of homologous chromosomes (Takahashi et al., 2010).

In terms of fertility, the double mutant *asp2sgo2* has shown to be affected by 20%, inspite of having essentially the same increase in recombination than single *asp2*. Here we see that

fertility might be affected either because of 1) a cohesion problem independently of recombination or 2) by CO formation in pericentromeric regions. We would expect for the single *asp2* -that show the same recombination levels- to have equally affected fertility. Since it is not the case, we favoured the first hypothesis where we proposed that the fertility loss might be independent of recombination, something previously proposed (Choi et al., 2018). On the other hand, we observed a similar effect on the fertility of the double mutant *asp2ctf18* where fertility is affected by 40%, in spite of showing one of the highest recombination rates (17,1 cM). Since we observed that cohesion was affected in at least 67% of the times and although the effect was quite subtle, it seems to be enough to affect fertility so much. Probably, the female side might be affected as well. We also observed that *asp2cmt3* shows a subtle effect in cohesion but a more dramatic effect in pollen viability where we see that in the same plant some of the anthers are almost completely sterile, suggesting that likely the female side is not as affected, or not enough to be able to compensate and generate a big number of seeds. These results reinforce the hypothesis that this defect is independent of recombination and because both *ctf18* and *asp2* seem to have a role on cohesion, the fertility drop might be caused by the loss of centromeric cohesion and premature sister chromatid segregation carried by the mutations can lead to aneuploidy as observed in the proposed model (Fig.3), also observed in double mutant *sgo1sgo2* (Cromer et al., 2019); notably, affecting differently male and female gametes

In contrast to previous publications where it has been found that mutations in anti-CO factors are enough to increase recombination in chromosome arms (Serra et al., 2018b), the control of pericentromeric recombination seems to have a more constrained regulation not only by anti-CO factors but also by structural factors; similarly as it was described in yeast that the kinetochore assembly has an impact in centromeric recombination (Vincenten et al., 2015).

These results are confirming that the centromere CO suppression is caused by several factors interplaying. Some of them, previously mentioned in 2018, as CG and non-CG DNA methylation inhibiting the formation of DSB precursors in centromeric regions and that only non-CG methylation and /or H3K9me2 inhibit crossovers (Choi et al., 2018) but also the protein dynamic between the chromosome cohesion loading (CTF18), cohesion centromeric protection, and their post transcriptional regulations through methylation and SUMOylation. Specifically, we observed that there are two main mechanisms limiting CO in pericentromeres: 1) Closed chromatin regulated by the loss of nucleosome occupancy and DNA methylation in CG and non-CG contexts by CMT3 and 2) Cohesion protection regulation in the centromeres by ASP2/SGO2 and cohesion loading in the arms of the chromosomes by CTF18.

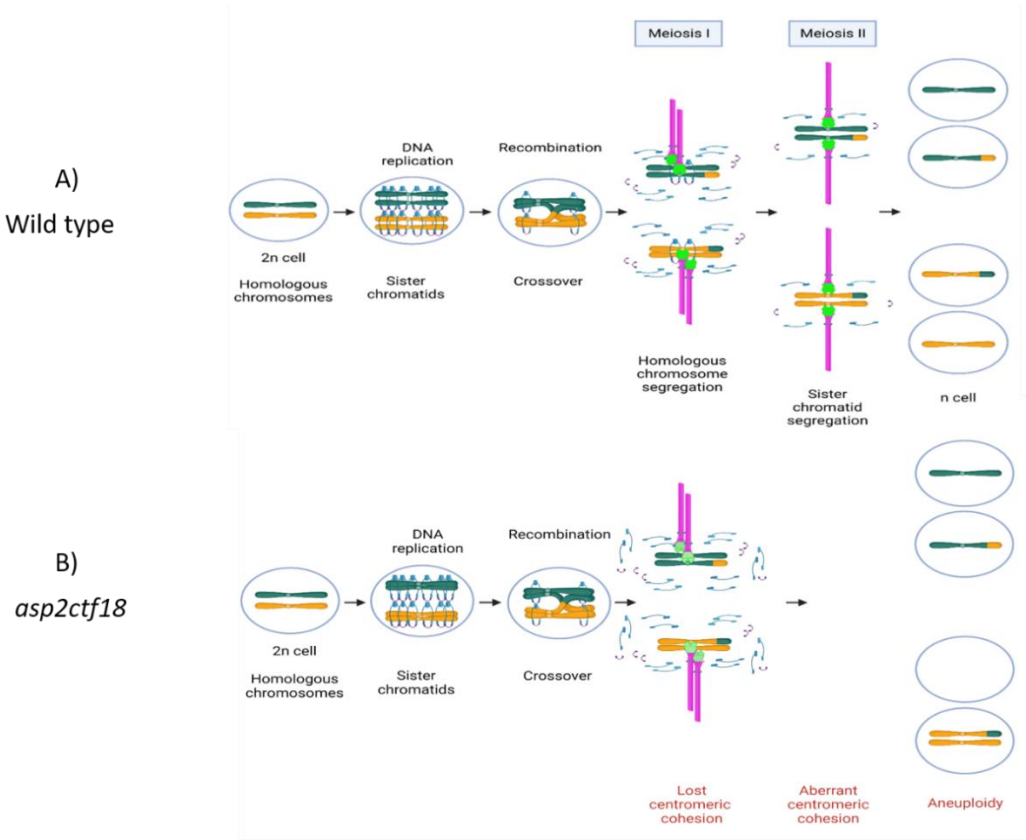

Figure 29. Dynamic model of loss of fertility, likely recovering aneuploid cells in double mutant asp2ctf18

8.2.8 Perspectives

After finding genes having a role in pericentromeric recombination, further questions remain to be answered; for example, to know if the recombination increase is specific to the centromeric region or if there is a genome wide recombination effect. For this, we are still in the process of observing genome-wide recombination in the two main mutants *asp2* and *sgo2* with higher recombination in hybrid context.

As mentioned before, it has been suggested that the CG and non-CG DNA methylation inhibit the formation of DSB precursors in centromeric regions and that only non-CG methylation and /or H3K9me2 inhibit crossovers (Choi et al., 2018). To investigate whether the amount of DSB and H3K9me2 accumulation is increased in the centromeric regions of our mutants with increased recombination; cytological analysis can be done. This can help to determine if the recombination precursors are behaving differently in wild type than in the mutant. Localisation of RAD51, DMC1, and other precursors could help to check if DSB are increased within this region in mutant, compared to wild type, differently in centromere and arms of the chromosomes.

Additionally, we wondered if the structure of the pericentromeres are different in the mutants with higher recombination in comparison to wild type plants. Immunocytological approaches can be helpful to examine REC8 cohesion changes: its density in centromeres, in comparison to chromosome arms. The amount of H3K9me2 heterochromatin marks which could probably

be related to the fluorescence intensity accumulated. Preliminary data (not-shown) showed to be possible to combine the required cytological markers (H3K9me2, MLH1, CENP-C, etc).

Downstream of the recombination process, we wondered if other factors of recombination were acting differently in the mutants with higher recombination. Additional cytological assays will be necessary to localise and quantify the procrossover factors HEI10 and MLH1. Likely these two proteins would be increased in pericentromeres of the mutants, compared to wild type. These two CO markers would also be helpful to know if the CO pathway is regulating recombination by Class I CO pathway in our mutants, and if it is affected by interference. To address if the increased COs are formed by Class II CO pathway, further genetic interactions would have to be done by combining *asp2, sgo2* or *ctf18* with *mus81* procrossover mutant and check in double mutants if there are chromosome fragmentation or not.

To understand why *asp2cmt3, asp2ctf18* have fertility defects despite having similar recombination. More DAPI spreads need to be done to look for meiotic defects mainly in metaphase II in both male and female gametes. As mentioned before, it might be due to premature loss of cohesion differently in each gamete but his would need to be confirmed.

In the search of recombination increase specifically in centromeric regions, combining all the four mutants *asp2, sgo2, cmt3* and *ctf18* would be interesting to observe; probably also the genome wide recombination of the combined mutants. This increase could be potentiated along the chromosome if the mutants with higher centromeric increase would be combined also with *recq4*. All this material has been already created: the quadruple mutants and the double mutants combined with *recq4*.

To obtain more candidates that regulate centromeric recombination, it would be very interesting to carry out the forward genetic screen in *recq4* background in Ler accession, which the material has also been created.

Finally, to decipher in more detail the mechanism of these proteins and other interacting proteins and/or targets (like the potential SGO2 target of ASP2 (X. B. Su et al., 2021)), a pull down experiment would be very interesting to perform.

Some of the mutants with modified kinetochore were used in the beginning but no longer because did not show increased recombination; however, we observed that some of the double mutants potentiate the recombination effect in the centromeric region when they are in combination with other mutants with an important role in centromeric recombination, such as *asp2* and *sgo2*. To discard a possible effect of the essential proteins for cohesion SMC1 and SMC3 and kinetochore protein CENP-C in the pericentromeric region, it would be interesting to perform double mutants of *smc1, smc3* or *cenp-c*, with *asp2* and *sgo2.* It might had happened that a bigger effect was not observed because of the nature of the alleles but a more significant impact could be seen in the double mutants.

8.3 CONTRIBUTION TO CROP DEVELOPMENT

Improved new plant varieties are essential for the breeding industry to address challenges posed by a growing human population and limited resources. Increasing recombination tools in plant breeding is a promising one; however, low recombination at centromeres can limit the power of plant breeding to cover the necessary production. Anti-CO factors have brought new insight to the field, enhancing recombination and plant improvement efficiency. Mutating orthologue gene Recq4 in crops like rice, pea and tomato has been proven to increase recombination by about three-fold (Mieulet et al., 2018).

It was shown in barley, after crossing 25 wild accessions, that long introgression regions (600Mb) were observed in pericentromeric regions but low recombination fixed the genetic material reducing genetic variation in that region for several generations (Dreissig et al., 2020). In tomato, genes important for virus (Tm-2^2 and Ty-1) and nematode resistance (Mi-1) and are known to be within a large introgression located in low recombining centromeric regions but are usually not recombining (Lin et al., 2014). Similarly, discovering new genes that increase recombination in low recombining regions of chromosomes especially in repetitive sequences, could further expand the plant improvement field and increase crop varieties. Understanding the mechanisms of the centromere effect can be useful for not only plant species, but also for mammals, insects, fungi, etc. The discovery of three genes in Arabidopsis that (Asp2, Ctf18 and Sgo2) contribute to the knowledge of the recombination limitation in centromeric regions and the centromere effect could be potentially useful for enhancing genetic gain and also for increasing powerful tools like gene mapping construction during in plant breeding.

9 REFERENCES

Agnès Bergerat, Bernard de Massy, Danielle Gadelle, Paul-Christophe Varoutas, Alain Nicolas, & Patrick Forterre. (1997). An atypical topoisomerase II from archaea with implications for meiotic recombination. *Nature*, *386*(MARCH), 414–417.

Ahmed, H. I., Heuberger, M., Schoen, A., Koo, D., Quiroz-chavez, J., Adhikari, L., … Krattinger, S. G. (2023). *Einkorn genomics sheds light on history of the oldest domesticated wheat*. https://doi.org/10.1038/s41586-023-06389-7

Alexander, M. P. (1969). Differential staining of aborted and nonaborted pollen. *Biotechnic and Histochemistry*, *44*(3), 117–122. https://doi.org/10.3109/10520296909063335

Altemose, N., Logsdon, G. A., Bzikadze, A. V., Sidhwani, P., Langley, S. A., Caldas, G. V., … Miga, K. H. (2022). Complete genomic and epigenetic maps of human centromeres. *Science*, *376*(6588), 1–30. https://doi.org/10.1126/science.abl4178

Anderson, L. K., Lohmiller, L. D., Tang, X., Hammond, D. B., Javernick, L., Shearer, L., … Falque, M. (2014). Combined fluorescent and electron microscopic imaging unveils the specific properties of two classes of meiotic crossovers. *Proceedings of the National Academy of Sciences of the United States of America*, *111*(37), 13415–13420. https://doi.org/10.1073/pnas.1406846111

Armstrong, S. J., Caryl, A. P., Jones, G. H., & Franklin, F. C. H. (2002). ASY1, a protein required for meiotic chromosome synapsis, localizes to axis-associated chromatin in Arabidopsis and Brassica. *Journal of Cell Science*, *115*(Pt 18), 3645–3655. https://doi.org/10.1242/jcs.00048

Börner, G. V., Kleckner, N., & Hunter, N. (2004). Crossover/Noncrossover Differentiation, Synaptonemal Complex Formation, and Regulatory Surveillance at the Leptotene/Zygotene Transition of Meiosis. *Cell*, *117*, 29–45. Retrieved from https://doi.org/10.1016/S0092-8674(04)00292-2

Buonomo, S. B. C., Clyne, R. K., Fuchs, J., Loidl, J., Uhlmann, F., & Nasmyth, K. (2000). Disjunction of homologous chromosomes in meiosis I depends on proteolytic cleavage of the meiotic cohesin Rec8 by separin. *Cell*, *103*(3), 387–398. https://doi.org/10.1016/S0092-8674(00)00131-8

Cai, X., Dong, F., Edelmann, R. E., & Makaroff, C. a. (2003). The Arabidopsis SYN1 cohesin protein is required for sister chromatid arm cohesion and homologous chromosome pairing. *Journal of Cell Science*, *116*(Pt 14), 2999–3007. https://doi.org/10.1242/jcs.00601

Capilla-Pérez, L., Durand, S., Hurel, A., Lian, Q., Chambon, A., Taochy, C., … Mercier, R. (2021). The synaptonemal complex imposes crossover interference and heterochiasmy in Arabidopsis. *Proceedings of the National Academy of Sciences of the United States of America*, *118*(12), 1–11. https://doi.org/10.1073/pnas.2023613118

Chan, G. K., Liu, S. T., & Yen, T. J. (2005). Kinetochore structure and function. *Trends in Cell Biology*, *15*(11), 589–598. https://doi.org/10.1016/j.tcb.2005.09.010

Chelysheva, L., Diallo, S., Vezon, D., Gendrot, G., Vrielynck, N., Belcram, K., … Grelon, M. (2005). AtREC8 and AtSCC3 are essential to the monopolar orientation of the kinetochores during meiosis. *Journal of Cell Science*, *118*(20), 4621–4632. https://doi.org/10.1242/jcs.02583

Chelysheva, L., Vezon, D., Chambon, A., Gendrot, G., Pereira, L., Lemhemdi, A., … Grelon, M. (2012). The Arabidopsis HEI10 is a new ZMM protein related to Zip3. *PLoS Genetics*, *8*(7). https://doi.org/10.1371/journal.pgen.1002799

Chen, J., Wang, Z., Tan, K., Huang, W., Shi, J., Li, T., … Lai, J. (2023). A complete telomere-to-telomere

assembly of the maize genome. *Nature Genetics*, *55*(July). https://doi.org/10.1038/s41588-023-01419-6

Cheng, C. H., Lo, Y. H., Liang, S. S., Ti, S. C., Lin, F. M., Yeh, C. H., … Wang, T. F. (2006). SUMO modifications control assembly of synaptonemal complex and polycomplex in meiosis of Saccharomyces cerevisiae. *Genes and Development*, *20*(15), 2067–2081. https://doi.org/10.1101/gad.1430406

Cheng, C. Y., Krishnakumar, V., Chan, A. P., Thibaud-Nissen, F., Schobel, S., & Town, C. D. (2017). Araport11: a complete reannotation of the Arabidopsis thaliana reference genome. *Plant Journal*, *89*(4), 789–804. https://doi.org/10.1111/tpj.13415

Choi, K., & Henderson, I. R. (2015). Meiotic recombination hotspots - A comparative view. *Plant Journal*, *83*(1), 52–61. https://doi.org/10.1111/tpj.12870

Choi, K., Reinhard, C., Serra, H., Ziolkowski, P. A., Underwood, C. J., Zhao, X., … Henderson, I. R. (2016). Recombination Rate Heterogeneity within Arabidopsis Disease Resistance Genes. *PLoS Genetics*, *12*(7), 1–30. https://doi.org/10.1371/journal.pgen.1006179

Choi, K., Zhao, X., Tock, A. J., Lambing, C., Underwood, C. J., Hardcastle, T. J., … Henderson, I. R. (2018). Nucleosomes and DNA methylation shape meiotic DSB frequency in Arabidopsis thaliana transposons and gene regulatory regions. *Genome Research*, 1–16. https://doi.org/10.1101/gr.225599.117.28

Choulet et al., 2014. (2014). Structural and functional partitioning of bread wheat chromosome 3B. *Science (New York, N.Y.)*, *345*(6194), 1250092.

Copenhaver, G. P., Nickel, K., Kuromori, T., Benito, M. I., Kaul, S., Lin, X., … Preuss, D. (1999). Genetic definition and sequence analysis of Arabidopsis centromeres. *Science*, *286*(5449), 2468–2474. https://doi.org/10.1126/science.286.5449.2468

Crismani, W., Girard, C., Froger, N., Pradillo, M., Santos, J. L., Chelysheva, L., … Mercier, R. (2012). FANCM limits meiotic crossovers. *Science*, *336*(6088), 1588–1590. https://doi.org/10.1126/science.1220381

Crismani, W., & Mercier, R. (2012). What limits meiotic crossovers. *Cell Cycle*, 3527–3528. https://doi.org/10.4161/cc.21963

Cromer, L., Jolivet, S., Singh, D. K., Berthier, F., De Winne, N., De Jaeger, G., … Mercier, R. (2019). Patronus is the elusive plant securin, preventing chromosome separation by antagonizing separase. *Proceedings of the National Academy of Sciences of the United States of America*, *116*(32), 16018–16027. https://doi.org/10.1073/pnas.1906237116

Cromie, G. A., & Smith, G. R. (2007). Branching out: meiotic recombination and its regulation. *Trends in Cell Biology*, *17*(9), 448–455. https://doi.org/10.1016/j.tcb.2007.07.007

De Muyt, A., Pereira, L., Vezon, D., Chelysheva, L., Gendrot, G., Chambon, A., … Grelon, M. (2009). A high throughput genetic screen identifies new early meiotic recombination functions in Arabidopsis thaliana. *PLoS Genetics*, *5*(9). https://doi.org/10.1371/journal.pgen.1000654

Dreissig, S., Maurer, A., Sharma, R., Milne, L., Flavell, A. J., Schmutzer, T., & Pillen, K. (2020). Natural variation in meiotic recombination rate shapes introgression patterns in intraspecific hybrids between wild and domesticated barley. *New Phytologist*, *228*(6), 1852–1863. https://doi.org/10.1111/nph.16810

Eijpe, M., Heyting, C., Gross, B., & Jessberger, R. (2000). Association of mammalian SMC1 and SMC3 proteins with meiotic chromosomes and synaptonemal complexes. *Journal of Cell Science*,

113(4), 673–682. https://doi.org/10.1242/jcs.113.4.673

Fernandes, Joiselle B., Wlodzimierz, P., & Henderson, I. R. (2019a). Meiotic recombination within plant centromeres. *Current Opinion in Plant Biology*, *48*, 26–35. https://doi.org/10.1016/j.pbi.2019.02.008

Fernandes, Joiselle B., Wlodzimierz, P., & Henderson, I. R. (2019b). Meiotic recombination within plant centromeres. *Current Opinion in Plant Biology*, *48*, 26–35. https://doi.org/10.1016/j.pbi.2019.02.008

Fernandes, Joiselle B, Naish, M., Lian, Q., Burns, R., Tock, A. J., Rabanal, F. A., … Henderson, I. R. (2023). Structural variation and DNA methylation shape the centromere-proximal meiotic crossover landscape in Arabidopsis. *BioRxiv*, 1–64.

Fernandes, Joiselle Blanche, Duhamel, M., Seguéla-Arnaud, M., Froger, N., Girard, C., Choinard, S., … Mercier, R. (2018). FIGL1 and its novel partner FLIP form a conserved complex that regulates homologous recombination. *Electronic Publishing*, *23*, 1–22.

Fernandes, Joiselle Blanche, Séguéla-Arnaud, M., Larchevêque, C., Lloyd, A. H., & Mercier, R. (2018). Unleashing meiotic crossovers in hybrid plants. *Proceedings of the National Academy of Sciences of the United States of America*, *115*(10), 2431–2436. https://doi.org/10.1073/pnas.1713078114

Francis, K. E., Lam, S. Y., Harrison, B. D., Bey, A. L., Berchowitz, L. E., & Copenhaver, G. P. (2007). Pollen tetrad-based visual assay for meiotic recombination in Arabidopsis. *Proceedings of the National Academy of Sciences of the United States of America*, *104*(10), 3913–3918. https://doi.org/10.1073/pnas.0608936104

Fransz, P. F., Armstrong, S., De Jong, J. H., Parnell, L. D., Van Drunen, C., Dean, C., … Jones, G. H. (2000). Integrated cytogenetic map of chromosome arm 4S of A. thaliana: Structural organization of heterochromatic knob and centromere region. *Cell*, *100*(3), 367–376. https://doi.org/10.1016/S0092-8674(00)80672-8

Frédéric Choulet, Adriana Alberti, Sébastien Theil, Natasha Glover, Valérie Barbe, Josquin Daron, Lise Pingault, Pierre Sourdille, Arnaud Couloux, Etienne Paux, Philippe Leroy, Sophie Mangenot, Nicolas Guilhot, Jacques Le Gouis, Francois Balfourier, Micha, C. F. (2014). Structural and functional partitioning of bread wheat chromosome 3B. *Science (New York, N.Y.)*, *345*(6194), 1250092. Retrieved from http://www.sciencemag.org/content/345/6194/1250092.abstract

Galander, S., & Marston, A. L. (2020). Meiosis I Kinase Regulators: Conserved Orchestrators of Reductional Chromosome Segregation. *BioEssays*, *42*(10), 1–13. https://doi.org/10.1002/bies.202000018

Girard, C., Chelysheva, L., Choinard, S., Froger, N., Macaisne, N., Lehmemdi, A., … Mercier, R. (2015). AAA-ATPase FIDGETIN-LIKE 1 and Helicase FANCM Antagonize Meiotic Crossovers by Distinct Mechanisms. *PLoS Genetics*, *11*(7), 1–22. https://doi.org/10.1371/journal.pgen.1005369

Girard, C., Zwicker, D., & Mercier, R. (2023). The regulation of meiotic crossover distribution: a coarse solution to a century-old mystery? *Biochemical Society Transactions*, *51*(3), 1179–1190. https://doi.org/10.1042/bst20221329

Giraut, L., Falque, M., Drouaud, J., Pereira, L., Martin, O. C., & Mézard, C. (2011). Genome-wide crossover distribution in Arabidopsis thaliana meiosis reveals sex-specific patterns along chromosomes. *PLoS Genetics*, *7*(11). https://doi.org/10.1371/journal.pgen.1002354

Gloria A. Brar, A. H., Ly-sha S. Ee, and A. A., & *David. (2009). The Multiple Roles of Cohesin in Meiotic Chromosome Morphogenesis and Pairing. *Molecular Biology of the Cell*, *20*, 2673–2683.

https://doi.org/10.1091/mbc.E08

Grelon, M., Vezon, D., Gendrot, G., & Pelletier, G. (2001). AtSPO11-1 is necessary for efficient meiotic recombination in plants. *EMBO Journal*, *20*(3), 589–600. https://doi.org/10.1093/emboj/20.3.589

Grishaeva, T. M., & Bogdanov, Y. F. (2000). Genetic control of meiosis in Drosophila. In *Genetika* (Vol. 36).

Grützner, R., Martin, P., Horn, C., Mortensen, S., Cram, E. J., Lee-Parsons, C. W. T., … Marillonnet, S. (2020). Addition of multiple introns to a Cas9 gene results in dramatic improvement in efficiency for generation of gene knockouts in plants. *BioRxiv*, 1–32. https://doi.org/10.1101/2020.04.03.023036

Grützner, R., Martin, P., Horn, C., Mortensen, S., Cram, E. J., Lee-Parsons, C. W. T., … Marillonnet, S. (2021). High-efficiency genome editing in plants mediated by a Cas9 gene containing multiple introns. *Plant Communications*, *2*(2), 1–15. https://doi.org/10.1016/j.xplc.2020.100135

Haber, J. E. (2014). *Genome stability. DNA repair and recombination*. Routledge.

Hartung, F., Wurz-Wildersinn, R., Fuchs, J., Schubert, I., Suer, S., & Puchta, H. (2007). The catalytically active tyrosine residues of both SPO11-1 and SPO11-2 are required for meiotic double-strand break induction in Arabidopsis. *Plant Cell*, *19*(10), 3090–3099. https://doi.org/10.1105/tpc.107.054817

He, Y., Wang, M., Dukowic-Schulze, S., Zhou, A., Tiang, C. L., Shilo, S., … Pawlowski, W. P. (2017). Genomic features shaping the landscape of meiotic double-strand-break hotspots in maize. *Proceedings of the National Academy of Sciences of the United States of America*, *114*(46), 12231–12236. https://doi.org/10.1073/pnas.1713225114

Higgins, J. D., Sanchez-Moran, E., Armstrong, S. J., Jones, G. H., & Franklin, F. C. H. (2005). The Arabidopsis synaptonemal complex protein ZYP1 is required for chromosome synapsis and normal fidelity of crossing over. *Genes and Development*, *19*(20), 2488–2500. https://doi.org/10.1101/gad.354705

Hörandl, E. (2009). A combinational theory for maintenance of sex. *Heredity*, *103*(6), 445–457. https://doi.org/10.1038/hdy.2009.85

Hunter, N. (2015). Meiotic recombination: The essence of heredity. *Cold Spring Harbor Perspectives in Biology*, *7*(12). https://doi.org/10.1101/cshperspect.a016618

Initiative, A. G. (2000). Analysis of the genome sequence of the Flowering plant Arabidopsis thaliana. *Nature*. Retrieved from https://www.nature.com/articles/35048692

James, G. V., Patel, V., Nordström, K. J. V., Klasen, J. R., Salomé, P. A., Weigel, D., & Schneeberger, K. (2013). User guide for mapping-by-sequencing in Arabidopsis. *Genome Biology*, *14*(6). https://doi.org/10.1186/gb-2013-14-6-r61

Jiang, J., Birchler, J. A., Parrott, W. A., & Dawe, R. K. (2003). A molecular view of plant centromeres. *Trends in Plant Science*, *8*(12), 570–575. https://doi.org/10.1016/j.tplants.2003.10.011

Johnson, E. S. (2004). Protein modification by SUMO. *Annual Review of Biochemistry*, *73*, 355–382. https://doi.org/10.1146/annurev.biochem.73.011303.074118

Joly-Lopez, Z., & Bureau, T. E. (2014). Diversity and evolution of transposable elements in Arabidopsis. *Chromosome Research*, *22*(2), 203–216. https://doi.org/10.1007/s10577-014-9418-8

Katis, V. L., Galova, M., Rabitsch, K. P., Gregan, J., & Nasmyth, K. (2004). Maintenance of Cohesin at Centromeres after Meiosis I in Budding Yeast Requires a Kinetochore-Associated Protein Related to MEI-S332. *Current Biology*, *14*, 560–572. https://doi.org/DOI 10.1016/j.cub.2004.03.001

Keeney, S., & Neale, M. J. (2006). Initiation of meiotic recombination by formation of DNA double-strand breaks: Mechanism and regulation. *Biochemical Society Transactions*, *34*(4), 523–525. https://doi.org/10.1042/BST0340523

Keeney, Scott, Giroux, C. N., & Kleckner, N. (1997). Meiosis-specific DNA double-strand breaks are catalyzed by Spo11, a member of a widely conserved protein family. *Cell*, *88*(3), 375–384. https://doi.org/10.1016/S0092-8674(00)81876-0

Kerrebrock, A. W., Moore, D. P., Wu, J. S., & Orr-Weaver, T. L. (1995). Mei-S332, a drosophila protein required for sister-chromatid cohesion, can localize to meiotic centromere regions. *Cell*, *83*(2), 247–256. https://doi.org/10.1016/0092-8674(95)90166-3

Kianian, P. M. A., Wang, M., Simons, K., Ghavami, F., He, Y., Dukowic-Schulze, S., … Pawlowski, W. P. (2018). High-resolution crossover mapping reveals similarities and differences of male and female recombination in maize. *Nature Communications*, *9*(1). https://doi.org/10.1038/s41467-018-04562-5

Kim, J., Park, J., Kim, H., Son, N., Kim, E., Kim, J., … Choi, K. (2022). Arabidopsis HEAT SHOCK FACTOR BINDING PROTEIN is required to limit meiotic crossovers and HEI10 transcription . *The EMBO Journal*, *41*(14), 1–19. https://doi.org/10.15252/embj.2021109958

Klein, F., Mahr, P., Galova, M., Buonomo, S. B. C., Michaelis, C., Nairz, K., & Nasmyth, K. (1999). A Central Role for Cohesins in Sister Chromatid Cohesion, Formation of Axial Elements, and Recombination during Yeast Meiosis Genetic and biochemical analyses have identified. *Cell*, *98*, 91–103.

Kong, X., Luo, X., Qu, G. P., Liu, P., & Jin, J. B. (2017). Arabidopsis SUMO protease ASP1 positively regulates flowering time partially through regulating FLC stability. *Journal of Integrative Plant Biology*, *59*(1), 15–29. https://doi.org/10.1111/jipb.12509

Kumar, R., Duhamel, M., Coutant, E., Ben-Nahia, E., & Mercier, R. (2019). Antagonism between BRCA2 and FIGL1 regulates homologous recombination. *Nucleic Acids Research*, *47*(10), 5170–5180. https://doi.org/10.1093/nar/gkz225

Kurzbauer, M. T., Uanschou, C., Chen, D., & Schlögelhofer, P. (2012). The recombinases DMC1 and RAD51 are functionally and spatially separated during meiosis in Arabidopsis. *Plant Cell*, *24*(5), 2058–2070. https://doi.org/10.1105/tpc.112.098459

Lam, W. S., Yang, X., & Makaroff, C. A. (2005). Characterization of Arabidopsis thaliana SMC1 and SMC3: Evidence that AtSMC3 may function beyond chromosomes cohesion. *Journal of Cell Science*, *118*(14), 3037–3048. https://doi.org/10.1242/jcs.02443

Lee, J. Y., Hayashi-Hagihara, A., & Orr-Weaver, T. L. (2005). Roles and regulation of the Drosophila centromere cohesion protein MEI-S332 family. *Philosophical Transactions of the Royal Society B: Biological Sciences*, *360*(1455), 543–552. https://doi.org/10.1098/rstb.2005.1619

Lenormand, T., Engelstädter, J., Johnston, S. E., Wijnker, E., & Haag, C. R. (2016). Evolutionary mysteries in meiosis. *Philosophical Transactions of the Royal Society B: Biological Sciences*, *371*(1706). https://doi.org/10.1098/rstb.2016.0001

Lin, T., Zhu, G., Zhang, J., Xu, X., Yu, Q., Zheng, Z., … Huang, S. (2014). Genomic analyses provide insights into the history of tomato breeding. *Nature Genetics*, *46*(11), 1220–1226.

https://doi.org/10.1038/ng.3117

Ling, Y. H., & Yuen, K. W. Y. (2019). Point centromere activity requires an optimal level of centromeric noncoding RNA. *Proceedings of the National Academy of Sciences of the United States of America*, *116*(13), 6270–6279. https://doi.org/10.1073/pnas.1821384116

Liu, L., Jiang, Y., Zhang, X., Wang, X., Wang, Y., Han, Y., … Chen, F. (2017). Two SUMO proteases SUMO PROTEASE RELATED TO FERTILITY1 and 2 are required for fertility in arabidopsis. *Plant Physiology*, *175*(4), 1703–1719. https://doi.org/10.1104/pp.17.00021

Liu, S., Yeh, C. T., Ji, T., Ying, K., Wu, H., Tang, H. M., … Schnable, P. S. (2009). Mu transposon insertion sites and meiotic recombination events co-localize with epigenetic marks for open chromatin across the maize genome. *PLoS Genetics*, *5*(11). https://doi.org/10.1371/journal.pgen.1000733

Lorenz, A., Osman, F., Sun, W., Nandi, S., Steinacher, R., & Whitby, M. C. (2012). The Fission Yeast FANCM Ortholog Directs Non-Crossover Recombination During Meiosis. *Science*, *336*(June), 1585–1588.

Lynn, A., Soucek, R., & Börner, G. V. (2007). ZMM proteins during meiosis: Crossover artists at work. *Chromosome Research*, *15*(5), 591–605. https://doi.org/10.1007/s10577-007-1150-1

Marand, A. P., Jansky, S. H., Zhao, H., Leisner, C. P., Zhu, X., Zeng, Z., … Jiang, J. (2017). Meiotic crossovers are associated with open chromatin and enriched with Stowaway transposons in potato. *Genome Biology*, *18*(1), 1–16. https://doi.org/10.1186/s13059-017-1326-8

McKinley, K. L., & Cheeseman, I. M. (2016). The molecular basis for centromere identity and function. *Nature Reviews Molecular Cell Biology*, *17*(1), 16–29. https://doi.org/10.1038/nrm.2015.5

Melamed-Bessudo, C., Yehuda, E., Stuitje, A. R., & Levy, A. A. (2005). A new seed-based assay for meiotic recombination in Arabidopsis thaliana. *Plant Journal*, *43*(3), 458–466. https://doi.org/10.1111/j.1365-313X.2005.02466.x

Mercier, R., & Grelon, M. (2008). Meiosis in plants: Ten years of gene discovery. *Cytogenetic and Genome Research*, *120*(3–4), 281–290. https://doi.org/10.1159/000121077

Mercier, Raphaël, Mézard, C., Jenczewski, E., Macaisne, N., & Grelon, M. (2015). The molecular biology of meiosis in plants. *Annual Review of Plant Biology*, *66*, 297–327. https://doi.org/10.1146/annurev-arplant-050213-035923

Mieulet, D., Aubert, G., Bres, C., Klein, A., Droc, G., Vieille, E., … Mercier, R. (2018). Unleashing meiotic crossovers in crops. *Nature Plants*, *4*(12), 1010–1016. https://doi.org/10.1038/s41477-018-0311-x

Mitra, S., Bodor, D. L., David, A. F., Abdul-Zani, I., Mata, J. F., Neumann, B., … Jansen, L. E. T. (2020). Genetic screening identifies a SUMO protease dynamically maintaining centromeric chromatin. *Nature Communications*, *11*(1), 1–15. https://doi.org/10.1038/s41467-019-14276-x

Morgan, C., Fozard, J. A., Hartley, M., Henderson, I. R., Bomblies, K., & Howard, M. (2021). Diffusion-mediated HEI10 coarsening can explain meiotic crossover positioning in Arabidopsis. *Nature Communications*, *12*(1). https://doi.org/10.1038/s41467-021-24827-w

Mukhopadhyay, D., & Dasso, M. (2007). Modification in reverse: the SUMO proteases. *Trends in Biochemical Sciences*, *32*(6), 286–295. https://doi.org/10.1016/j.tibs.2007.05.002

Nageswaran, D. C., Kim, J., Lambing, C., Kim, J., Park, J., Kim, E. J., … Henderson, I. R. (2021). HIGH CROSSOVER RATE1 encodes PROTEIN PHOSPHATASE X1 and restricts meiotic crossovers in Arabidopsis. *Nature Plants*, *7*(4), 452–467. https://doi.org/10.1038/s41477-021-00889-y

Naish, M., Alonge, M., Wlodzimierz, P., Tock, A. J., Abramson, B. W., Lambing, C., … Henderson, I. R. (2021a). The genetic and epigenetic landscape of the Arabidopsis centromeres. *Plant Science*, *7489*(November), 2021.05.30.446350. https://doi.org/10.1126/science.abi7489

Naish, M., Alonge, M., Wlodzimierz, P., Tock, A. J., Abramson, B. W., Lambing, C., … Henderson, I. R. (2021b). The genetic and epigenetic landscape of the Arabidopsis centromeres. *Science*, *7489*(November), 2021.05.30.446350. https://doi.org/10.1126/science.abi7489

Nambiar, M., & Smith, G. R. (2016). Repression of harmful meiotic recombination in centromeric regions. *Semin Cell Dev Biol.*, (54), 188–197. https://doi.org/10.1016/j.semcdb.2016.01.042.Repression

O'Malley, R. C., Barragan, C. C., & Ecker, J. R. (2015). HHMI Author Manuscript A User ' s Guide to the Arabidopsis T-DNA Insertional Mutant Collections. *Methods in Molecular Biology*, 323–342.

Petronczki, M., Siomos, Maria, F., & Nasmyth, K. (2003). Un Menage a Quatre: The Molecular Biology of Chromosome Segregation in Meiosis. *Cell*, *112*, 423–440. https://doi.org/10.1016/S1089-3261(05)70234-8

Roberts, E. H. (1972). Storage Environment and the Control of Viability. *Viability of Seeds*, 14–58. https://doi.org/10.1007/978-94-009-5685-8_2

Rowan, B. A., Heavens, D., Feuerborn, T. R., Tock, A. J., Henderson, I. R., & Weigel, D. (2019). An Ultra High-Density Arabidopsis thaliana Crossover. *Genetics*, *213*(November), 771–787.

Saintenac, C., Falque, M., Martin, O. C., Paux, E., Feuillet, C., & Sourdille, P. (2009). Detailed recombination studies along chromosome 3B provide new insights on crossover distribution in wheat (Triticum aestivum L.). *Genetics*, *181*(2), 393–403. https://doi.org/10.1534/genetics.108.097469

Séguéla-Arnaud, M., Crismani, W., Larchevêque, C., Mazel, J., Froger, N., Choinard, S., … Mercier, R. (2015). Multiple mechanisms limit meiotic crossovers: TOP3α and two BLM homologs antagonize crossovers in parallel to FANCM. *Proceedings of the National Academy of Sciences of the United States of America*, *112*(15), 4713–4718. https://doi.org/10.1073/pnas.1423107112

Sen, S., Dodamani, A., & Nambiar, M. (2022). Emerging mechanisms and roles of meiotic crossover repression at centromeres. In *Current Topics in Developmental Biology* (1st ed.). https://doi.org/10.1016/bs.ctdb.2022.06.003

Serra, H., Lambing, C., Griffin, C. H., Topp, S. D., Nageswaran, D. C., Underwood, C. J., … Henderson, I. R. (2018a). Massive crossover elevation via combination of HEI10 and recq4a recq4b during Arabidopsis meiosis. *Proceedings of the National Academy of Sciences of the United States of America*, *115*(10), 2437–2442. https://doi.org/10.1073/pnas.1713071115

Serra, H., Lambing, C., Griffin, C. H., Topp, S. D., Nageswaran, D. C., Underwood, C. J., … Henderson, I. R. (2018b). Massive crossover elevation via combination of *HEI10* and *recq4a recq4b* during *Arabidopsis* meiosis. *Proceedings of the National Academy of Sciences*, 201713071. https://doi.org/10.1073/pnas.1713071115

Sherman, J., & Stack, S. (1995). Two-dimensional spreads of synaptonemal complexes from solanaceous plants. I. The technique. *Biotechnic and Histochemistry*, *57*(5), 265–272. https://doi.org/10.3109/10520298209066722

Shi, J., Wolf, S. E., Burke, J. M., Presting, G. G., Ross-Ibarra, J., & Dawe, R. K. (2010). Widespread gene conversion in centromere cores. *PLoS Biology*, *8*(3). https://doi.org/10.1371/journal.pbio.1000327

Si, W., Yuan, Y., Huang, J., Zhang, X., Zhang, Y., Zhang, Y., … Yang, S. (2015). Widely distributed hot and cold spots in meiotic recombination as shown by the sequencing of rice F2 plants. *New Phytologist*, *206*(4), 1491–1502. https://doi.org/10.1111/nph.13319

Simon, L., Voisin, M., Tatout, C., & Probst, A. V. (2015). Structure and function of centromeric and pericentromeric heterochromatin in arabidopsis thaliana. *Frontiers in Plant Science*, *6*(NOVEMBER), 1–8. https://doi.org/10.3389/fpls.2015.01049

Sims, J., Schlögelhofer, P., & Kurzbauer, M. T. (2021). From Microscopy to Nanoscopy: Defining an Arabidopsis thaliana Meiotic Atlas at the Nanometer Scale. *Frontiers in Plant Science*, *12*(May). https://doi.org/10.3389/fpls.2021.672914

Singh, D. K., Salinas Gamboa, R., Singh, A. K., Walkemeier, B., Van Leene, J., De Jaeger, G., … Mercier, R. (2023). The FANCC–FANCE–FANCF complex is evolutionarily conserved and regulates meiotic recombination. *Nucleic Acids Research*, *51*(6), 2516–2528. https://doi.org/10.1093/nar/gkac1244

Srivastava, M., Srivastava, A. K., Roy, D., Mansi, M., Gough, C., Bhagat, P. K., … Sadanandom, A. (2022). The conjugation of SUMO to the transcription factor MYC2 functions in blue light-mediated seedling development in Arabidopsis. *Plant Cell*, *34*(8), 2892–2906. https://doi.org/10.1093/plcell/koac142

Stuitje, A. R., Verbree, E. C., Van Der Linden, K. H., Mietkiewska, E. M., Nap, J.-P., & Kneppers, T. J. A. (2003). Seed-expressed fluorescent proteins as versatile tools for easy (co)transformation and high-throughput functional genomics in Arabidopsis. *Plant Biotechnology Journal*, *1*(4), 301–309. https://doi.org/10.1046/j.1467-7652.2003.00028.x

Su, X. B., Wang, M., Schaffner, C., Nerusheva, O., Clift, D., Spanos, C., … Marston, A. L. (2021). Sumoylation stabilizes sister kinetochore biorientation to allow timely anaphase. *Journal of Cell Biology*, *220*(7). https://doi.org/10.1083/jcb.202005130

Su, X., Wang, B., Geng, X., Du, Y., Yang, Q., Liang, B., … Lin, T. (2021). A high-continuity and annotated tomato reference genome. *BMC Genomics*, *22*(1), 1–12. https://doi.org/10.1186/s12864-021-08212-x

Takahashi, N., Quimbaya, M., Schubert, V., Lammens, T., Vandepoele, K., Schubert, I., … De Veylder, L. (2010). The MCM-binding protein ETG1 aids sister chromatid cohesion required for postreplicative homologous recombination repair. *PLoS Genetics*, *6*(1). https://doi.org/10.1371/journal.pgen.1000817

Talbert, P. B., & Henikoff, S. (2010). Centromeres convert but don't cross. *PLoS Biology*, *8*(3), 1–5. https://doi.org/10.1371/journal.pbio.1000326

Tock, A. J., Holland, D. M., Jiang, W., Osman, K., Sanchez-Moran, E., Higgins, J. D., … Henderson, I. R. (2021). Crossover-active regions of the wheat genome are distinguished by DMC1, the chromosome axis, H3K27me3, and signatures of adaptation. *Genome Research*, *31*(9), 1614–1628. https://doi.org/10.1101/gr.273672.120

Tóth, A., Rabitsch, K. P., Gálová, M., Schleiffer, A., Buonomo, S. B. C., & Nasmyth, K. (2000). Functional genomics identifies monopolin: A kinetochore protein required for segregation of homologs during meiosis I. *Cell*, *103*(7), 1155–1168. https://doi.org/10.1016/S0092-8674(00)00217-8

Underwood, C. J., Choi, K., Lambing, C., Zhao, X., Serra, H., Borges, F., … Martienssen, R. A. (2018). Epigenetic activation of meiotic recombination near Arabidopsis thaliana centromeres via loss of H3K9me2 and non-CG DNA methylation. *Genome Research*, *28*(4), 519–531.

https://doi.org/10.1101/gr.227116.117

Vincenten, N., Kuhl, L. M., Lam, I., Oke, A., Kerr, A. R. W., Hochwagen, A., … Marston, A. L. (2015). The kinetochore prevents centromere-proximal crossover recombination during meiosis. *ELife*, *4*(DECEMBER2015), 1–25. https://doi.org/10.7554/eLife.10850

Wang, N., & Dawe, R. K. (2018). Centromere Size and Its Relationship to Haploid Formation in Plants. *Molecular Plant*, *11*(3), 398–406. https://doi.org/10.1016/j.molp.2017.12.009

Wang, Y., & Copenhaver, G. P. (2018). Meiotic Recombination: Mixing It Up in Plants. *Annual Review of Plant Biology*, *69*(1), 577–609. https://doi.org/10.1146/annurev-arplant-042817-040431

Watanabe, Y. (2004). Modifying sister chromatid cohesion for meiosis. *Journal of Cell Science*, *117*(18), 4017–4023. https://doi.org/10.1242/jcs.01352

Watanabe, Y. (2012). Geometry and force behind kinetochore orientation: Lessons from meiosis. *Nature Reviews Molecular Cell Biology*, *13*(6), 370–382. https://doi.org/10.1038/nrm3349

Wei, W., & Lin, H.-K. (2012). The key role of ubiquitination and sumoylation in signaling and cancer: a research topic. *Frontiers in Oncology*, *2*(December), 1–2. https://doi.org/10.3389/fonc.2012.00187

Wu, G., Rossidivito, G., Hu, T., Berlyand, Y., & Poethig, R. S. (2015). Traffic lines: New tools for genetic analysis in Arabidopsis thaliana. *Genetics*, *200*(1), 35–45. https://doi.org/10.1534/genetics.114.173435

Xue, X., Sung, P., & Zhao, X. (2015). Functions and regulation of the multitasking FANCM family of DNA motor proteins. *Genes and Development*, *29*(17), 1777–1788. https://doi.org/10.1101/gad.266593.115

Yelina, N E, Lambing, C., Hardcastle, T. J., Zhao, X., Santos, B., & Henderson, I. R. (2015). DNA methylation epigenetically silences crossover hot spots and controls chromosomal domains of meiotic recombination in Arabidopsis. *Genes Dev*, *29*(20), 2183–2202. https://doi.org/10.1101/gad.270876.115

Yelina, Nataliya E., Choi, K., Chelysheva, L., Macaulay, M., de Snoo, B., Wijnker, E., … Henderson, I. R. (2012). Epigenetic Remodeling of Meiotic Crossover Frequency in Arabidopsis thaliana DNA Methyltransferase Mutants. *PLoS Genetics*, *8*(8). https://doi.org/10.1371/journal.pgen.1002844

Yelina, Nataliya E., Lambing, C., Hardcastle, T. J., Zhao, X., Santos, B., & Henderson, I. R. (2015). DNA methylation epigenetically silences crossover hot spots and controls chromosomal domains of meiotic recombination in Arabidopsis. *Genes and Development*, *29*(20), 2183–2202. https://doi.org/10.1101/gad.270876.115

Yelina, Nataliya E., Ziolkowski, P. A., Miller, N., Zhao, X., Kelly, K. A., Muñoz, D. F., … Henderson, I. R. (2013). High-throughput analysis of meiotic crossover frequency and interference via flow cytometry of fluorescent pollen in Arabidopsis thaliana. *Nature Protocols*, *8*(11), 2119–2134. https://doi.org/10.1038/nprot.2013.131

Yu, H. G., Dawe, R. K., Hiatt, E. N., & Dawe, R. K. (2000). The plant kinetochore. *Trends in Plant Science*, *5*(12), 543–547. https://doi.org/10.1016/S1360-1385(00)01789-1

Zamariola, L., De Storme, N., Tiang, C. L., Armstrong, S. J., Franklin, F. C. H., & Geelen, D. (2013). SGO1 but not SGO2 is required for maintenance of centromere cohesion in Arabidopsis thaliana meiosis. *Plant Reproduction*, *26*(3), 197–208. https://doi.org/10.1007/s00497-013-0231-x

Zhang, H., Lang, Z., & Zhu, J. K. (2018). Dynamics and function of DNA methylation in plants. *Nature*

Reviews Molecular Cell Biology, *19*(8), 489–506. https://doi.org/10.1038/s41580-018-0016-z

Zhang, L., Stauffer, W., Zwicker, D., & Dernburg, A. F. (2021). *Crossover patterning through kinase-regulated condensation and coarsening of recombination nodules*.

Zhu, L., Fernández-Jiménez, N., Szymanska-Lejman, M., Pelé, A., Underwood, C. J., Serra, H., … Ziolkowski, P. A. (2021). Natural variation identifies SNI1, the SMC5/6 component, as a modifier of meiotic crossover in Arabidopsis. *Proceedings of the National Academy of Sciences of the United States of America*, *118*(33), 1–12. https://doi.org/10.1073/pnas.2021970118

Ziolkowski, P. A., Berchowitz, L. E., Lambing, C., Yelina, N. E., Zhao, X., Kelly, K. A., … Henderson, I. R. (2015a). Juxtaposition of heterozygous and homozygous regions causes reciprocal crossover remodelling via interference during Arabidopsis meiosis. *ELife*, *4*, 1–29. https://doi.org/10.7554/eLife.03708

Ziolkowski, P. A., Berchowitz, L. E., Lambing, C., Yelina, N. E., Zhao, X., Kelly, K. A., … Henderson, I. R. (2015b). Juxtaposition of heterozygous and homozygous regions causes reciprocal crossover remodelling via interference during Arabidopsis meiosis. *ELife*, *4*, 1–29. https://doi.org/10.7554/eLife.03708

Ziolkowski, P. A., Underwood, C. J., Lambing, C., Martinez-Garcia, M., Lawrence, E. J., Ziolkowska, L., … Henderson, I. R. (2017). Natural variation and dosage of the HEI10 meiotic E3 ligase control Arabidopsis crossover recombination. *Genes and Development*, *31*(3), 306–317. https://doi.org/10.1101/gad.295501.116